

Beauty and charm physics at Belle and Belle II

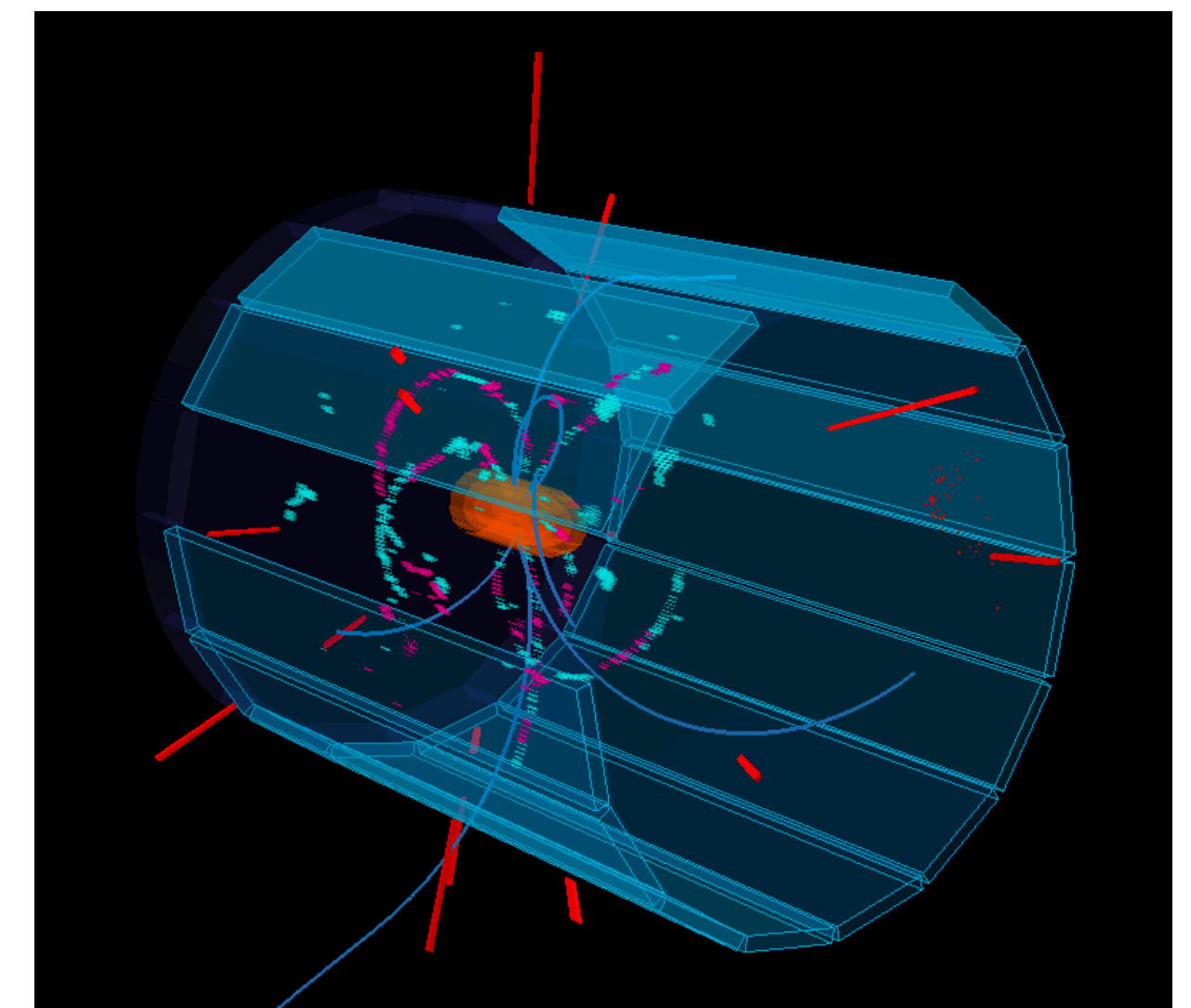
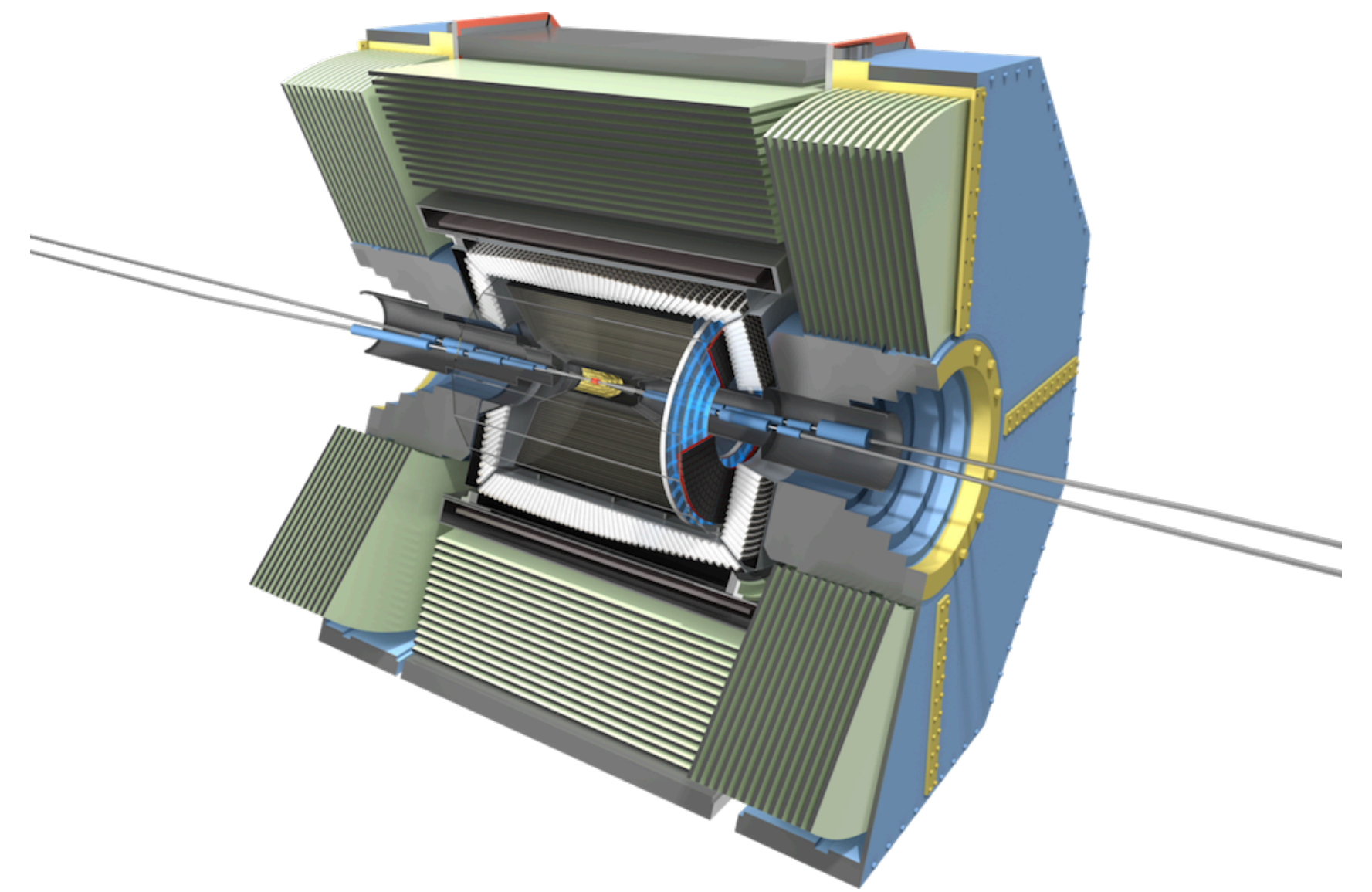
Michele Veronesi
La Thuile 2025

IOWA STATE
UNIVERSITY



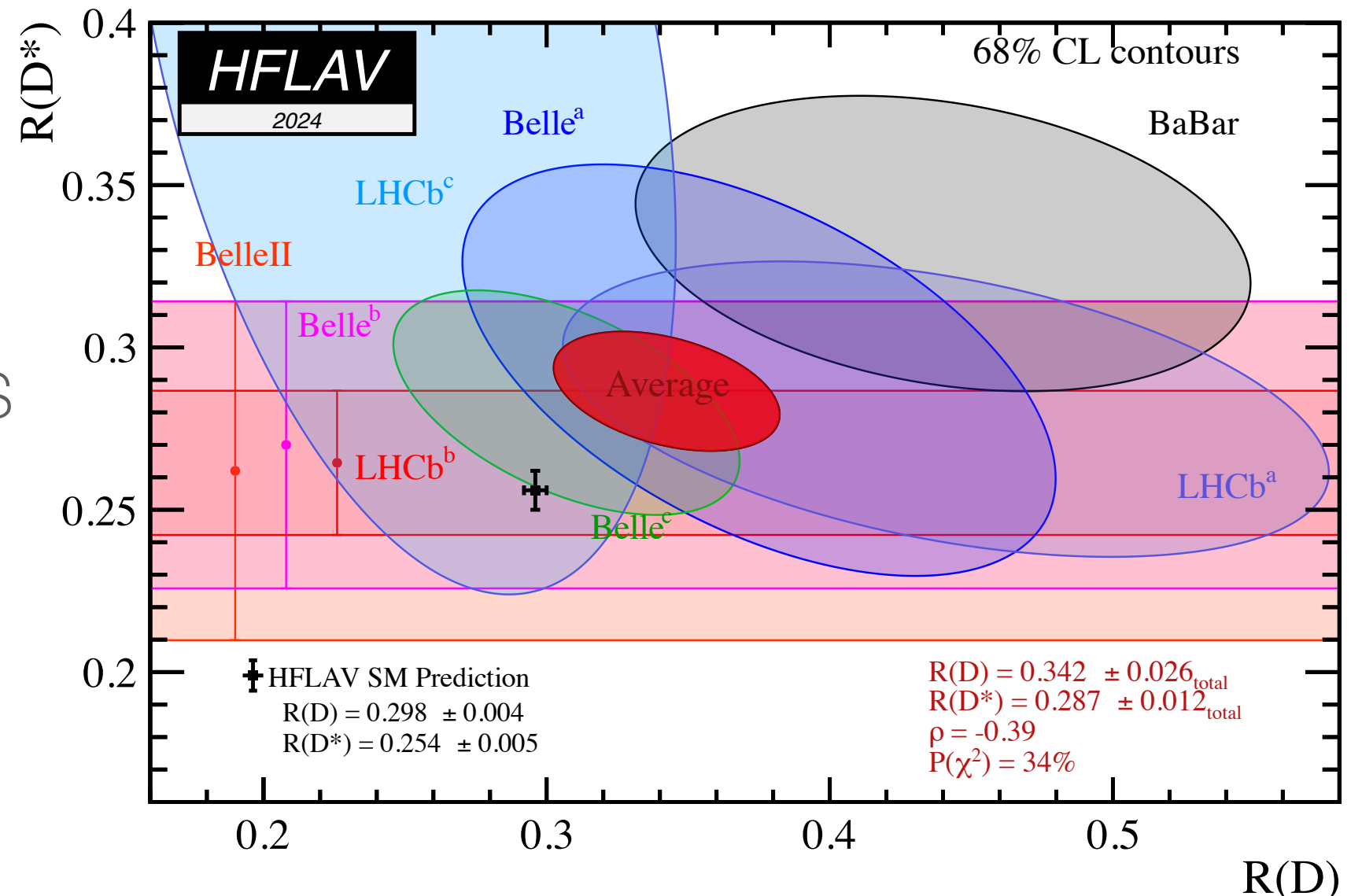
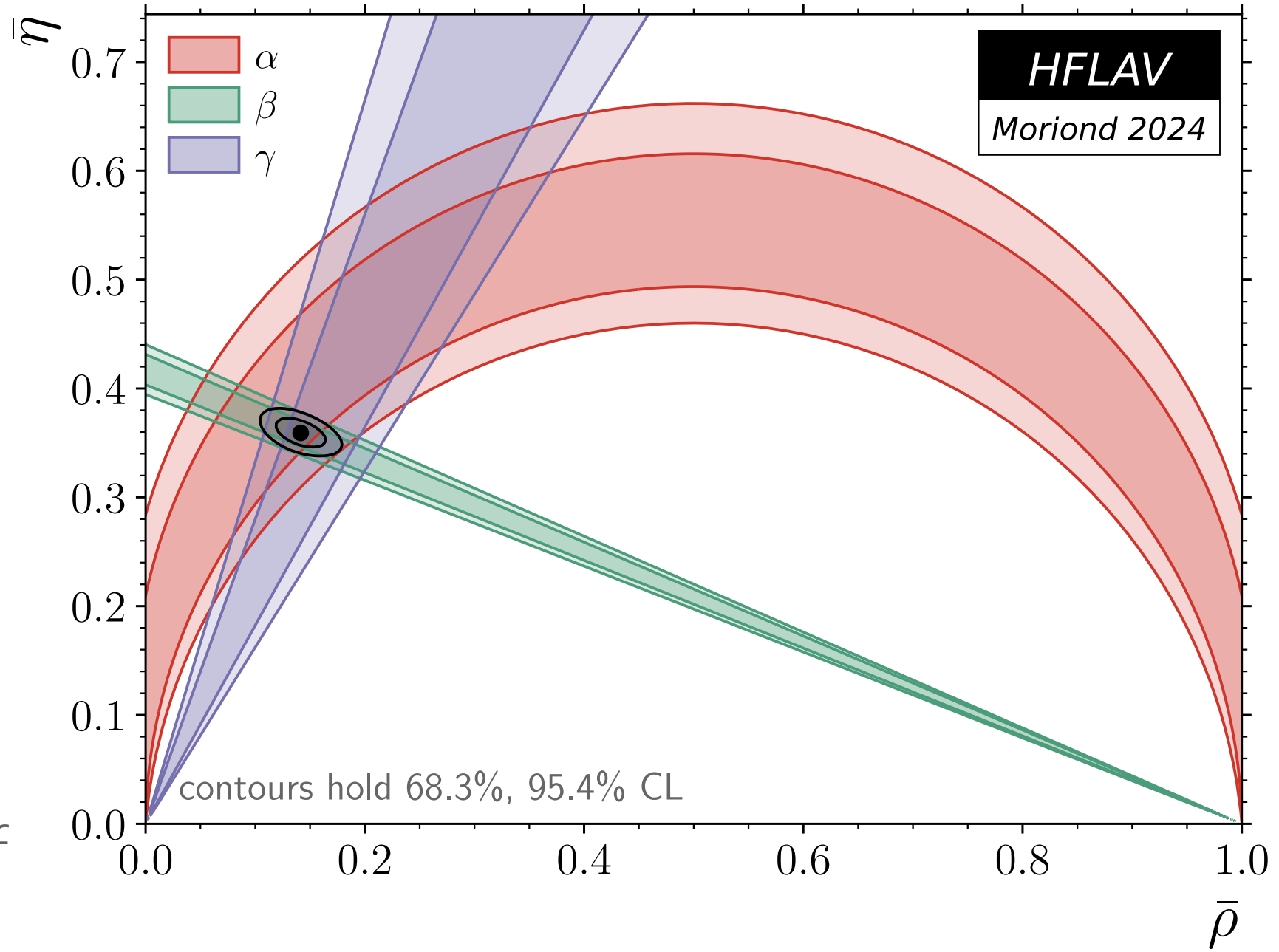
Belle (II) at (Super)KEKB

- Asymmetric e^+e^- collider, running at $Y(4s)$ resonance*
 - ▶ KEKB (1999-2012) => SuperKEKB (2019-present)
 - ▶ Achieved world's record instantaneous luminosity of $5.1 \times 10^{34} \text{cm}^{-2}\text{s}^{-1}$ (December 2024)
 - ▶ Recorded 772M (387M) $B\bar{B}$ pairs at Belle (II), Run 2 data-taking ongoing
- Beauty (and tau/charm) factory experiment
 - ▶ Improved performance (vertexing, tracking, neutral particle reconstruction, PID, flavor tagging)
 - ▶ Hermetic detector and known initial energy (ideal for decays with missing energy)



Recent results on beauty and charm*

- CPV in charm: understand nature of CPV observed in $D^0 \rightarrow \pi^+\pi^-$
 - ▶ $D^0 \rightarrow K^0_S K^0_S$ approaching precision to observe SM-induced CPV, first measurement using opposite-side charm tagging **NEW**
 - ▶ $D^0 \rightarrow \pi^0\pi^0$ important ingredient for the $D \rightarrow \pi\pi\pi$ isospin sum rule, least known experimentally **NEW**
- CPV in beauty: constrain the angles of the unitarity triangle
 - ▶ $\phi_1(\beta)$: measured in $b \rightarrow c\bar{c}s$ transitions, precision close to effect of penguin amplitudes, controlled with $B^0 \rightarrow J/\psi\pi^0$
 - ▶ $\phi_2(\alpha)$: least known experimentally, determined from isospin analysis of $B \rightarrow \pi\pi$ and $B \rightarrow \rho\rho$
- (Semi)tauonic and lepton-flavor violating B-decays: enhancements predicted by models explaining $b \rightarrow c\tau\nu$ anomalies and $B \rightarrow K\nu\nu$
 - ▶ Measurement of BF of $B^+ \rightarrow \tau\nu$ (and V_{ub}) **NEW**
 - ▶ Searches for $B^0 \rightarrow K^0_S \tau\ell$ and $B^0 \rightarrow K^{*0} \tau\tau$

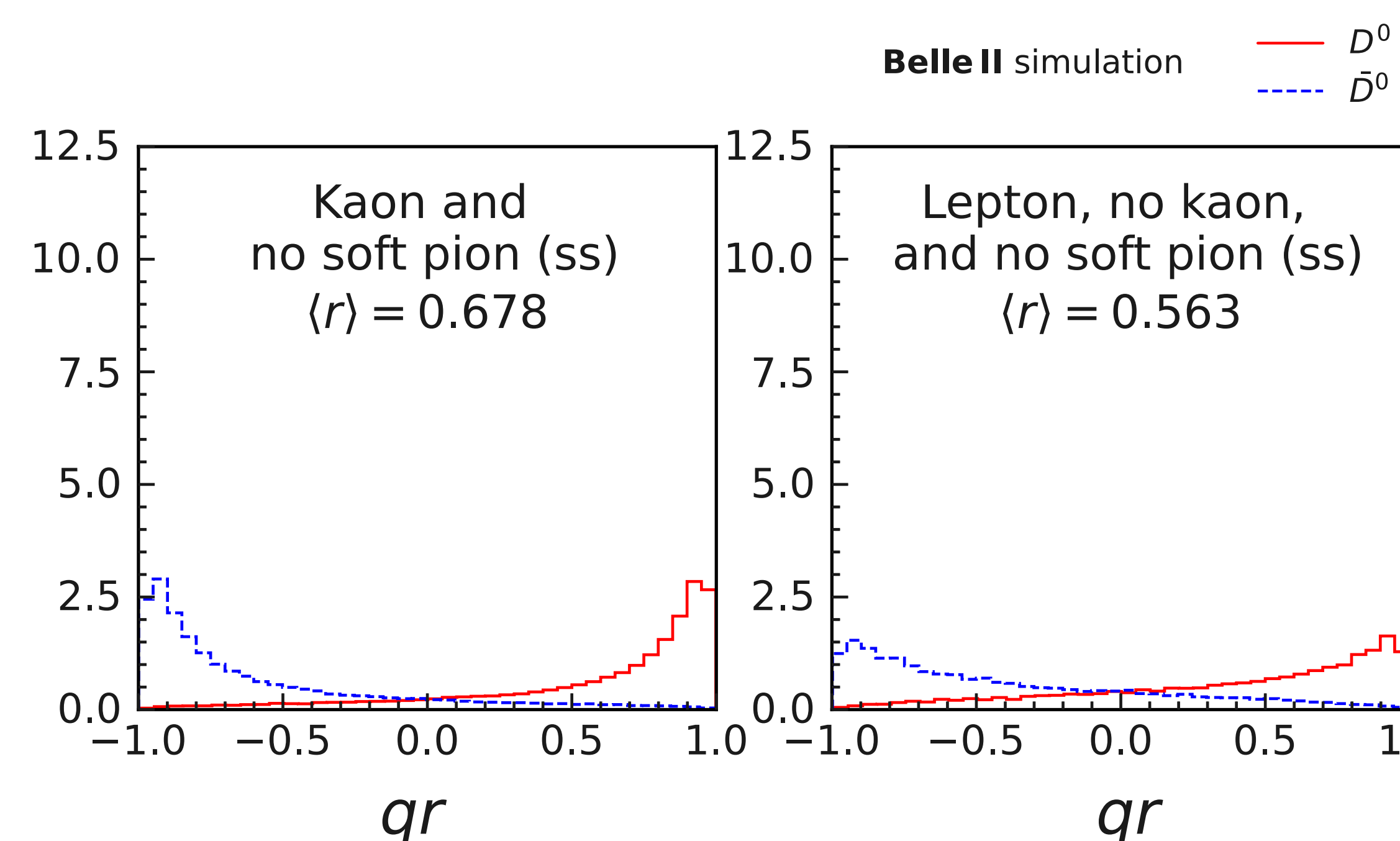
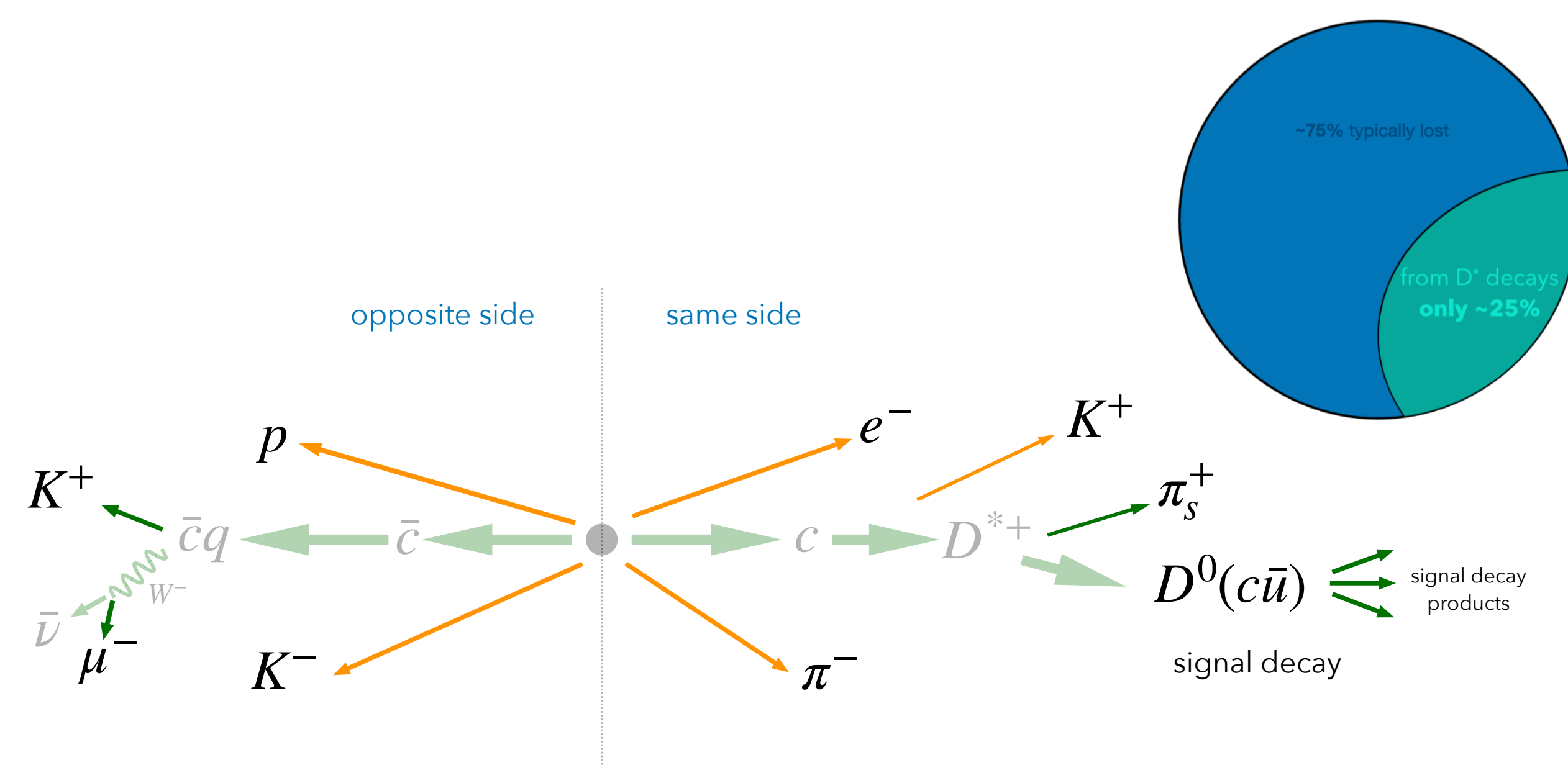


CPV in charm

Essential ingredients for charm CPV analysis:

- Knowledge of D^0 flavor, either from D^{*+} tag or charge correlation with tracks from rest of the event [[PRD 107, 112010 \(2023\)](#)]
 - ▶ Calibrated with abundant $D^0 \rightarrow K^- \pi^+$
- Knowledge of production and detection asymmetries affecting raw asymmetry
 - ▶ Subtracted using asymmetries measured in control modes

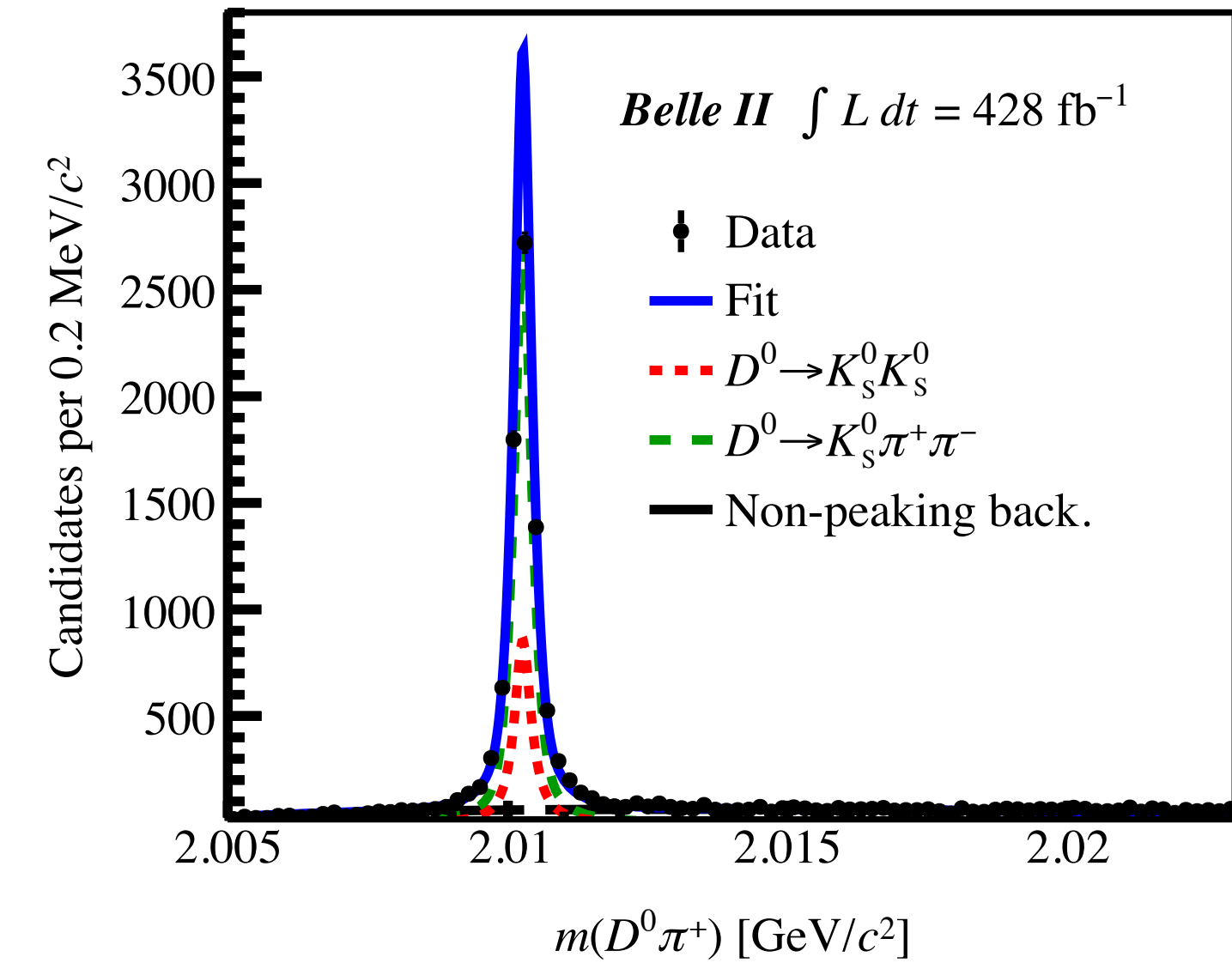
$$A_{\text{raw}}^f = A_{CP}(D^0 \rightarrow f) + A_P^{D^{*+}}(D^0 \rightarrow f) + A_\epsilon^\pi(D^0 \rightarrow f)$$



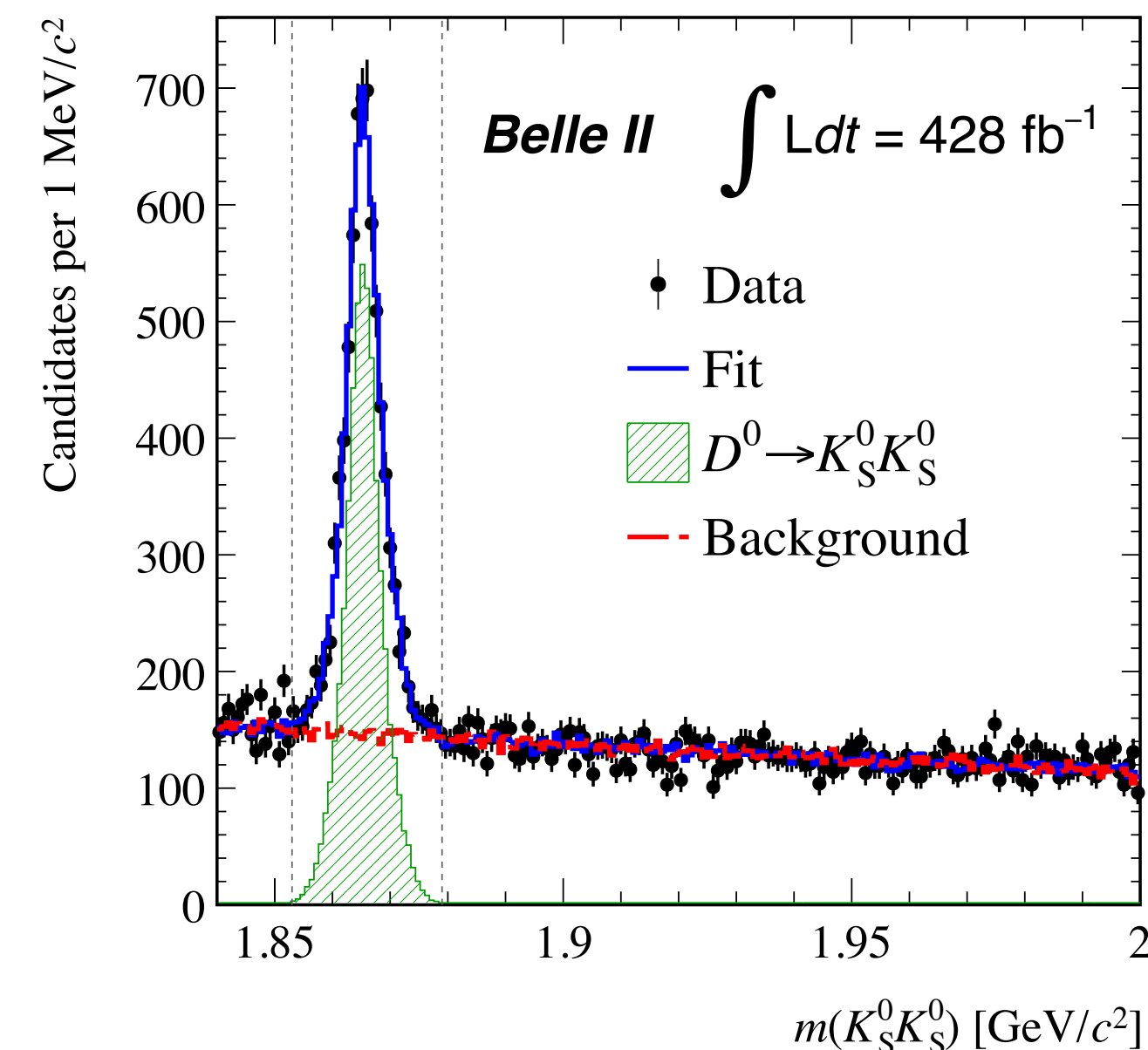
A_{CP} in $D^0 \rightarrow K_S^0 K_S^0$

- Color and CKM-suppressed transition, interference between $c \rightarrow us\bar{s}$, udd amplitudes $\sim O(1\%)$ CPV in SM
- Using Belle (980fb⁻¹) + Belle II (428fb⁻¹) datasets, combining D^{*+} tag ($\sim 7k$ signal candidates) and opposite-side tag ($\sim 20k$) samples
 - ▶ Improved calibration of nuisance asymmetries in D^{*+} tag analysis with $D^0 \rightarrow K^+ K^-$ control sample
 - ▶ Removing D^{*+} tagged events from OS-tag analysis
- Combination of two analyses gives most precise determination of the CP asymmetry in this mode

D^{*+} tag [[PRD 111, 012015 \(2025\)](#)]



Opposite-side tag [paper in preparation]



$$A_{CP}(D^0 \rightarrow K_S^0 K_S^0) = (-0.6 \pm 1.1 \pm 0.1)\% \quad \text{NEW}$$

A_{CP} in $D^0 \rightarrow \pi^0 \pi^0$

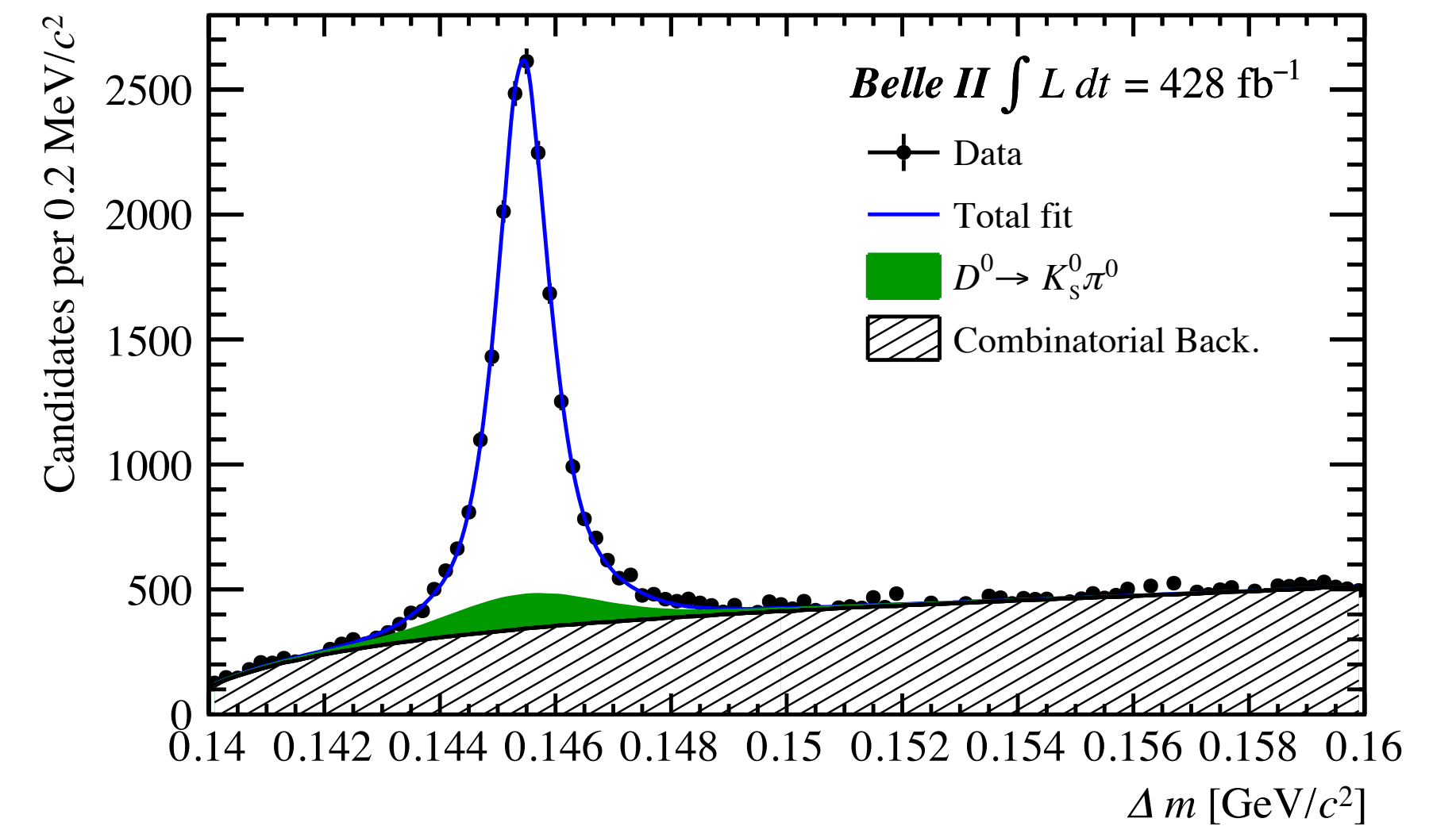
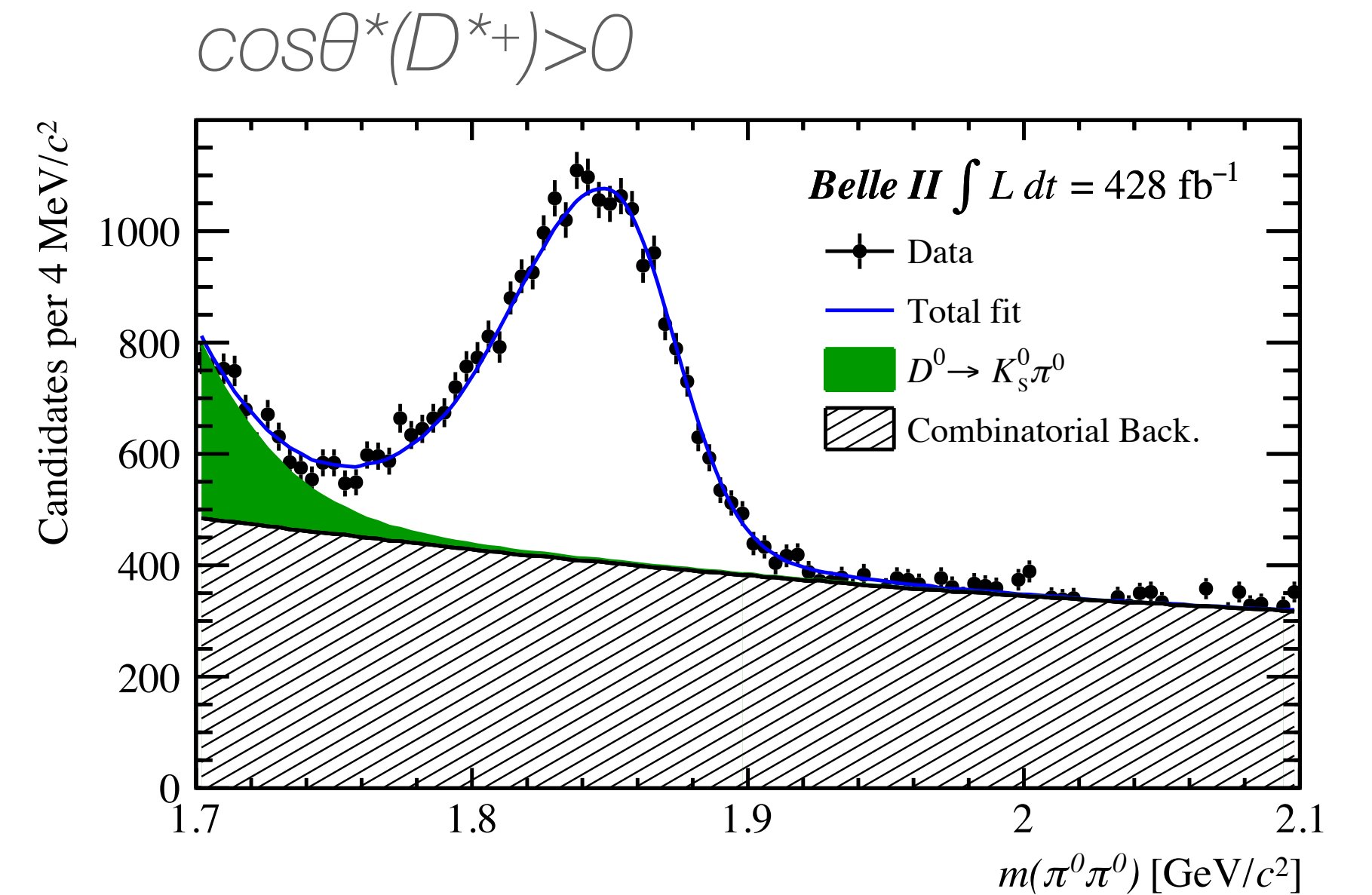
[paper in preparation]

- Non-zero CP asymmetries arise from interference of CKM-suppressed and QCD-penguin amplitudes
 - ▶ Current data suggest $\sim O(1\%)$ CPV in $D^0 \rightarrow \pi^0 \pi^0$ in SM
 - ▶ Isospin sum rule of $D \rightarrow \pi\pi$ to identify source of charm CPV
- Using D^{*+} tagged Belle II sample ($\sim 16k$ signal candidates)
 - ▶ Detection asymmetries cancelled with (un)tagged $D^0 \rightarrow K^+ \pi^-$
 - ▶ Production asymmetry cancelled by averaging over $\cos\theta^*$
- Precision comparable to Belle result and 18% improvement on the isospin sum rule

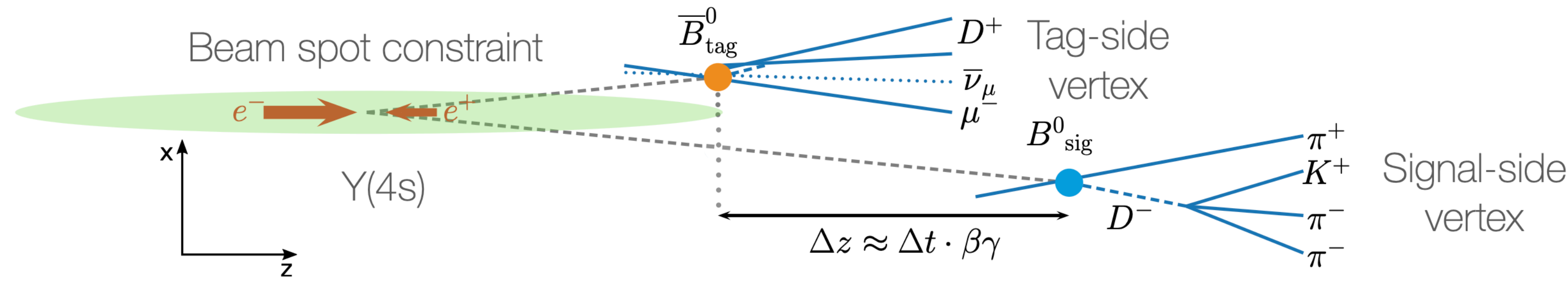
$$A_{CP}(D^0 \rightarrow \pi^0 \pi^0) = (0.30 \pm 0.72(\text{stat}) \pm 0.20(\text{syst}))\%$$

$$R = (1.5 \pm 2.5) \times 10^{-3}$$

NEW



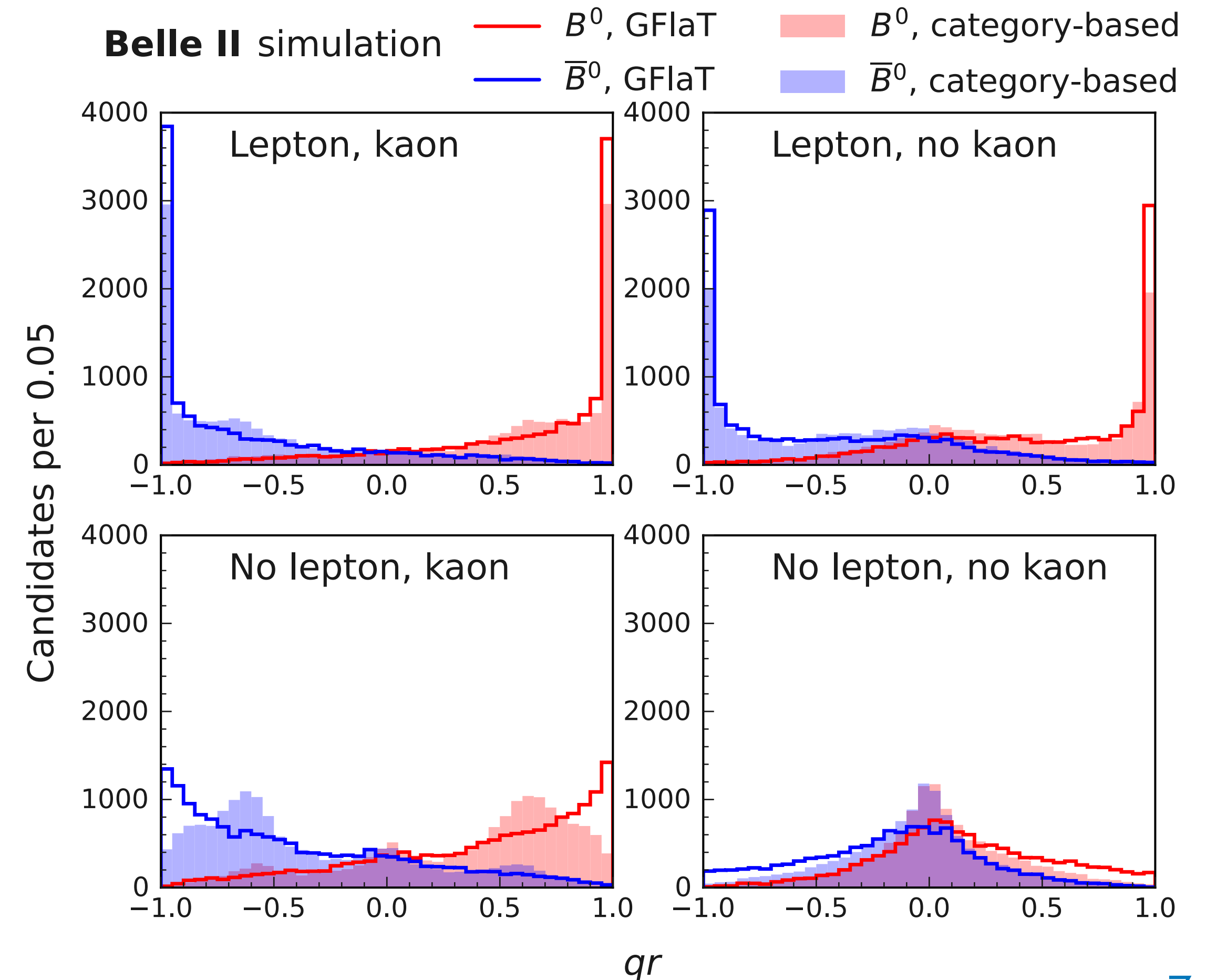
CPV in beauty



Essential ingredients for B^0 CPV analysis:

- Tag initial flavor from partially reconstructed tag-side B^0 [[PRD 110, 012001 \(2024\)](#)]
 - ▶ Improved efficiency with Graph-NN (~37%)
- Exploit correlation of $B^0\bar{B}^0$ pairs to measure Δt asymmetries
 - ▶ Improved Δt resolution from pixel detector and constraints from nano-beams

$$\mathcal{P}(\Delta t, q) = \frac{e^{-|\Delta t|/\tau_{B^0}}}{4\tau_{B^0}} \{1 + q[S_{CP} \sin(\Delta m_d \Delta t) - C_{CP} \cos(\Delta m_d \Delta t)]\}$$

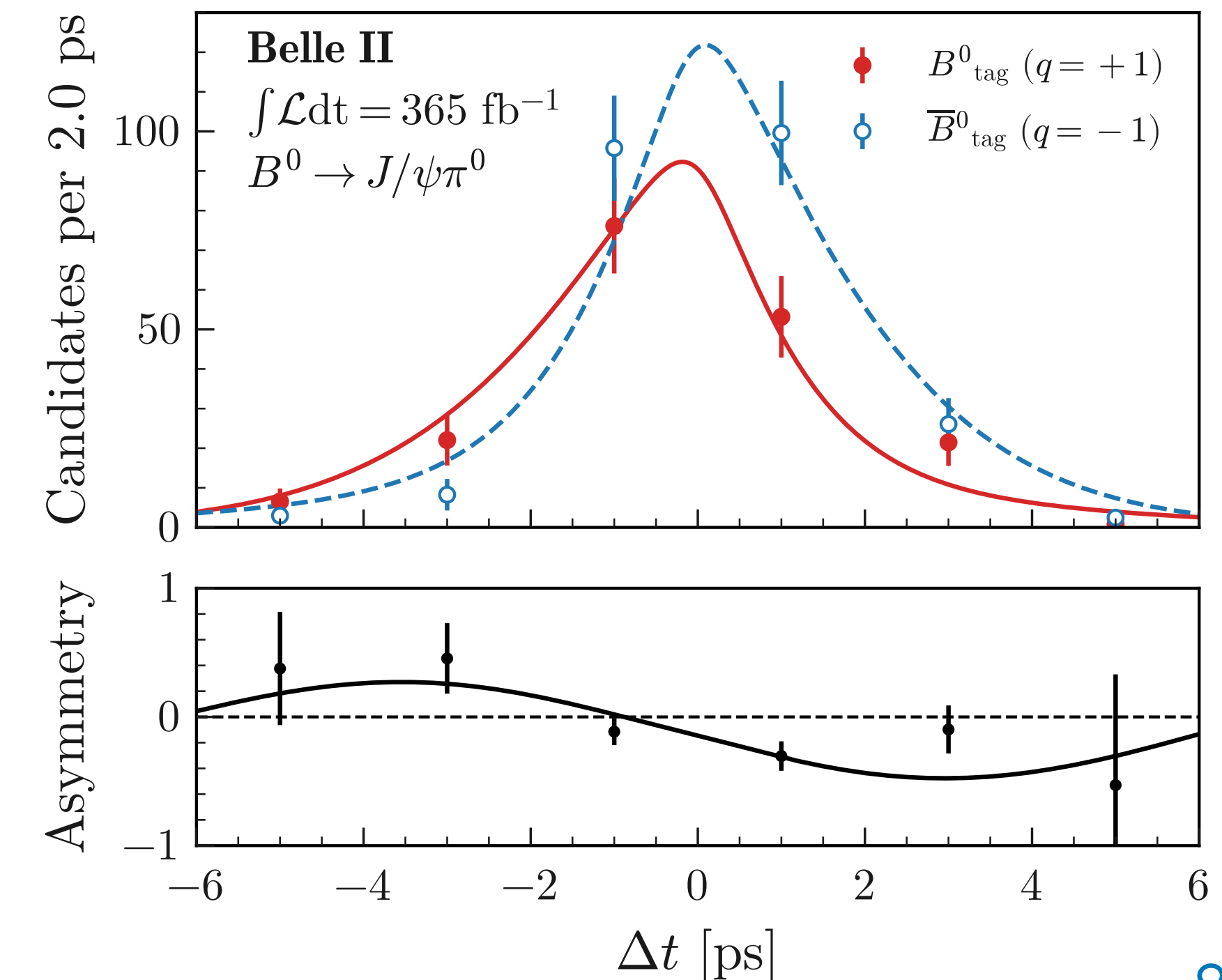
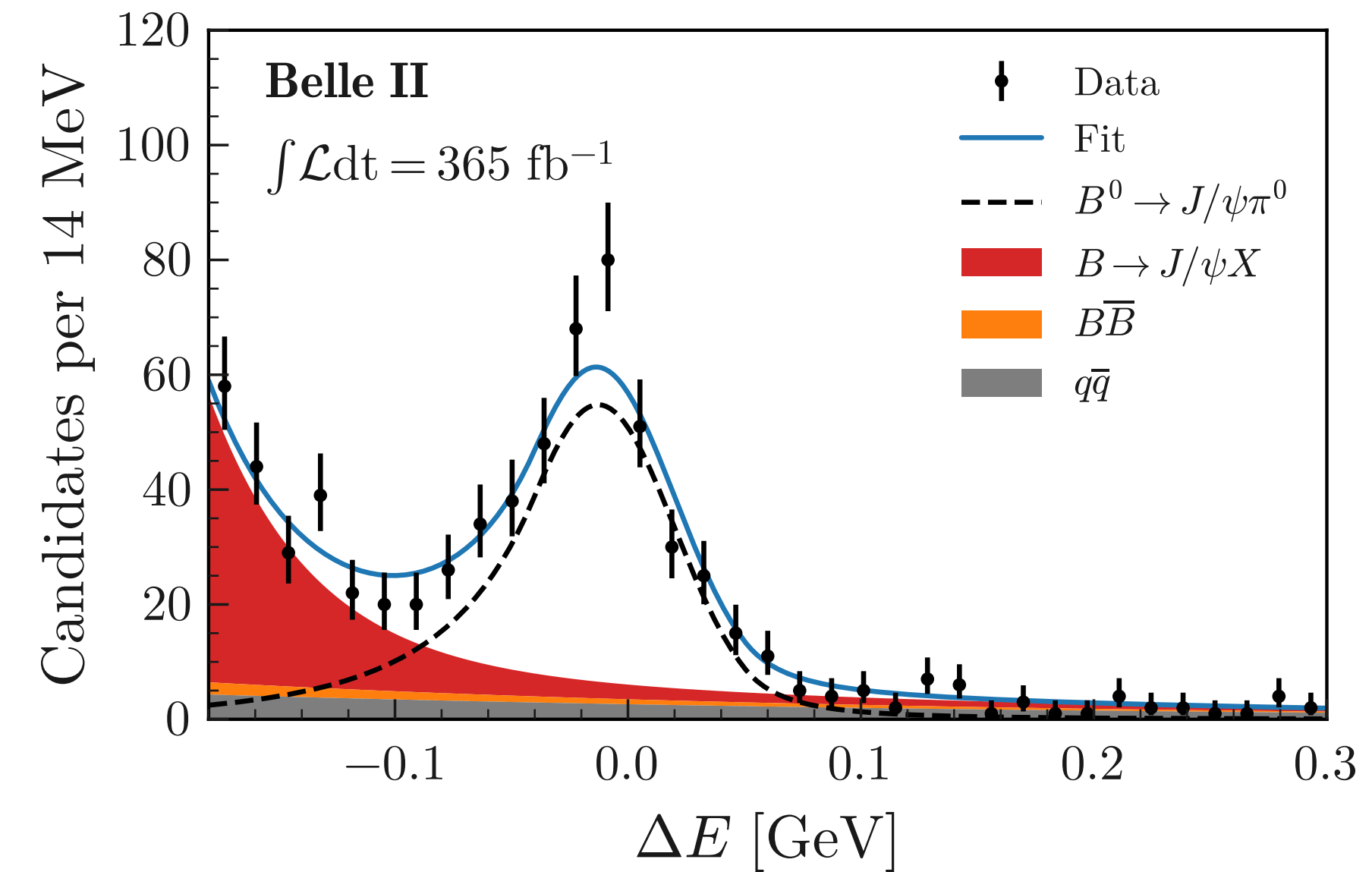


$(\Delta)\phi_1$ in $B^0 \rightarrow J/\psi\pi^0$

- Doubly-CKM suppressed (“penguin”) amplitudes can shift the value of $\phi_d=2\phi_1$ measured in $B^0 \rightarrow J/\psi K^0$ by $\sim O(0.5^\circ)$
 - ▶ Current experimental knowledge $\phi_d^{eff} = [45.12 \pm 0.94]^\circ$
 - ▶ BF and CP asymmetries in $B^0 \rightarrow J/\psi\pi^0$ constrain $\Delta\phi_d$
- First observation of indirect CPV and competitive BF with 392 ± 24 signal candidates
 - ▶ Experimental error on $\phi_d = [45.6^{+1.1}_{-1.0}(\text{exp}) \pm 0.3(\text{SU}(3))]^\circ$ reduced by $\sim 10\%$ with this result [[arxiv:2501.09414](https://arxiv.org/abs/2501.09414)]

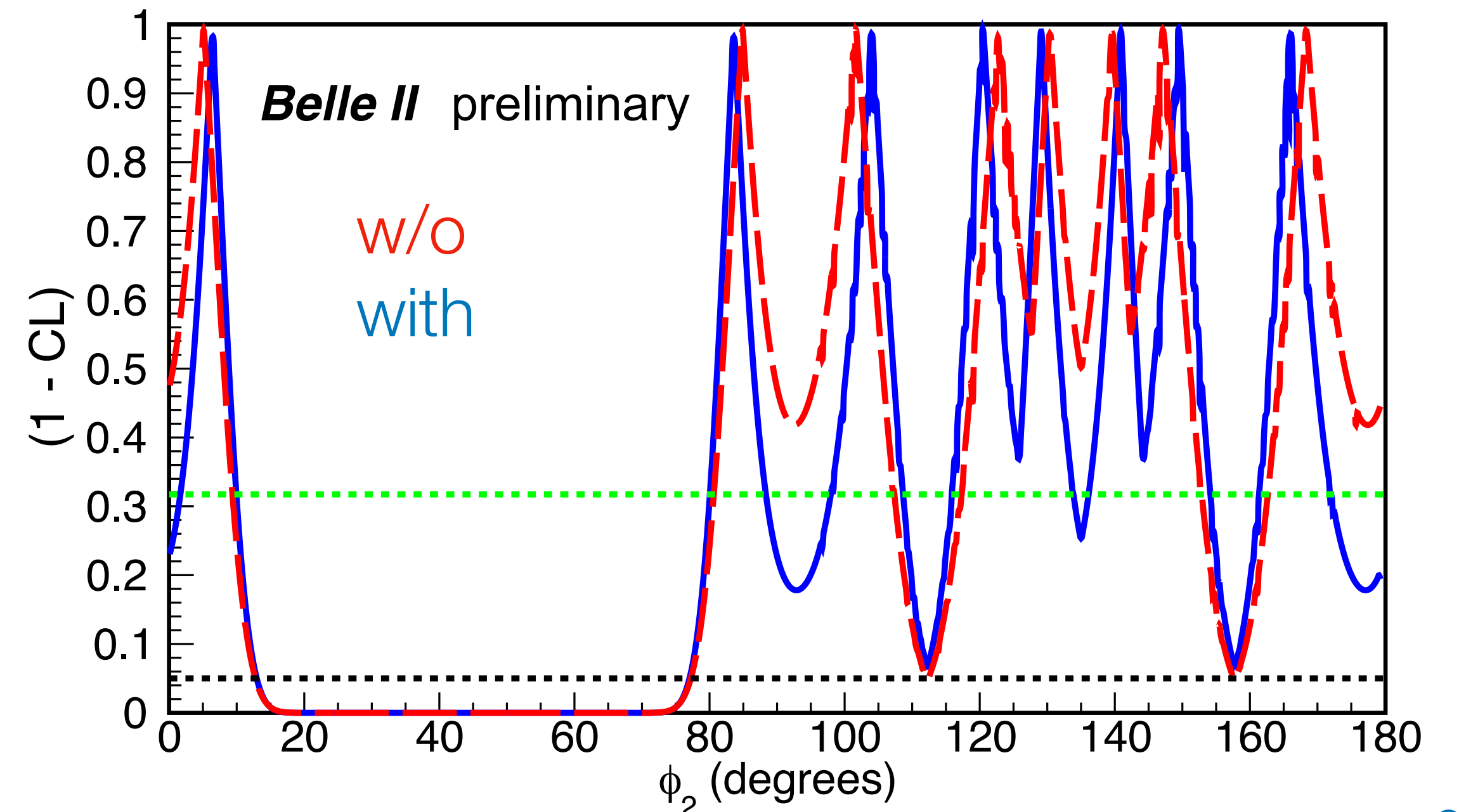
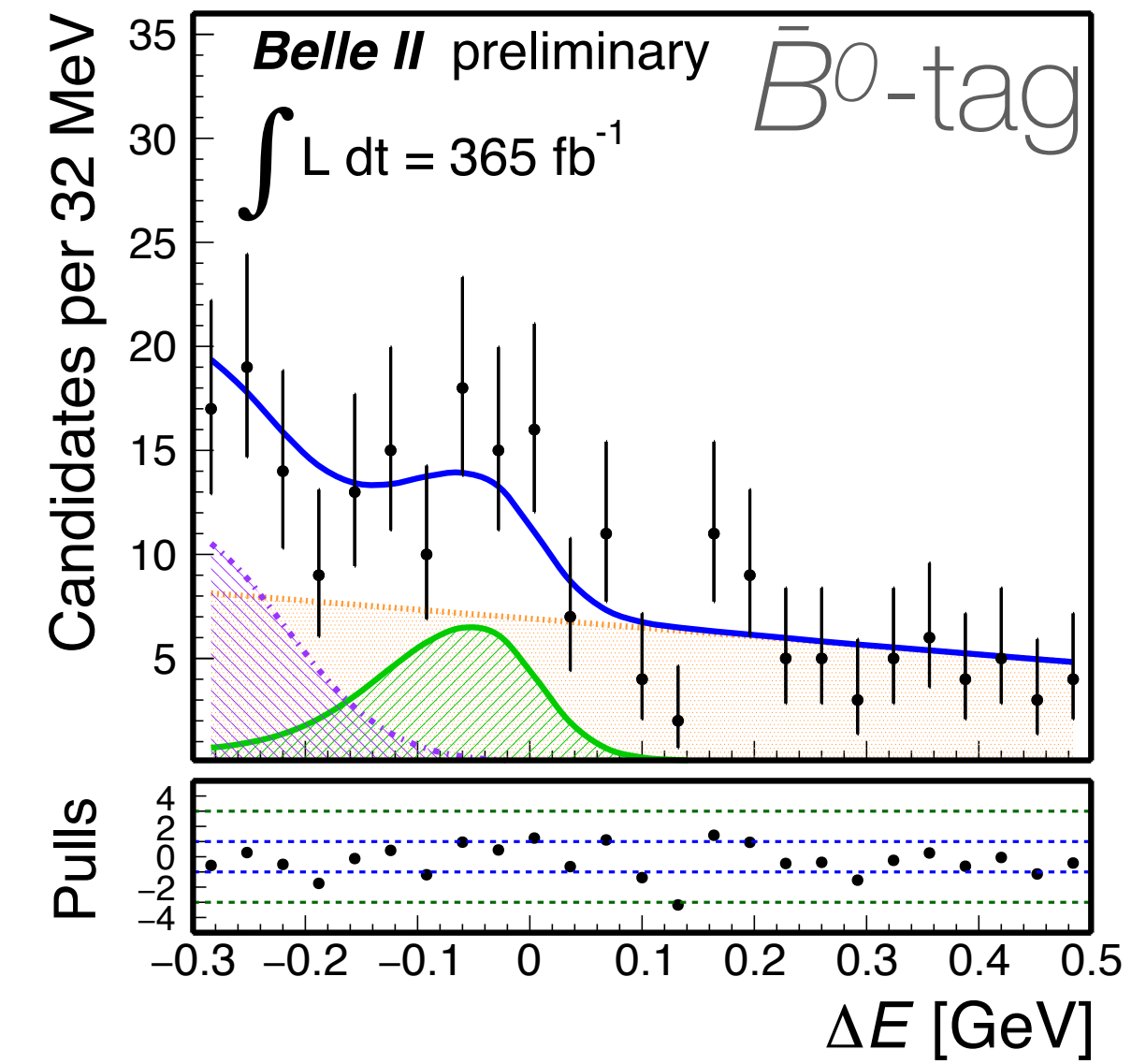
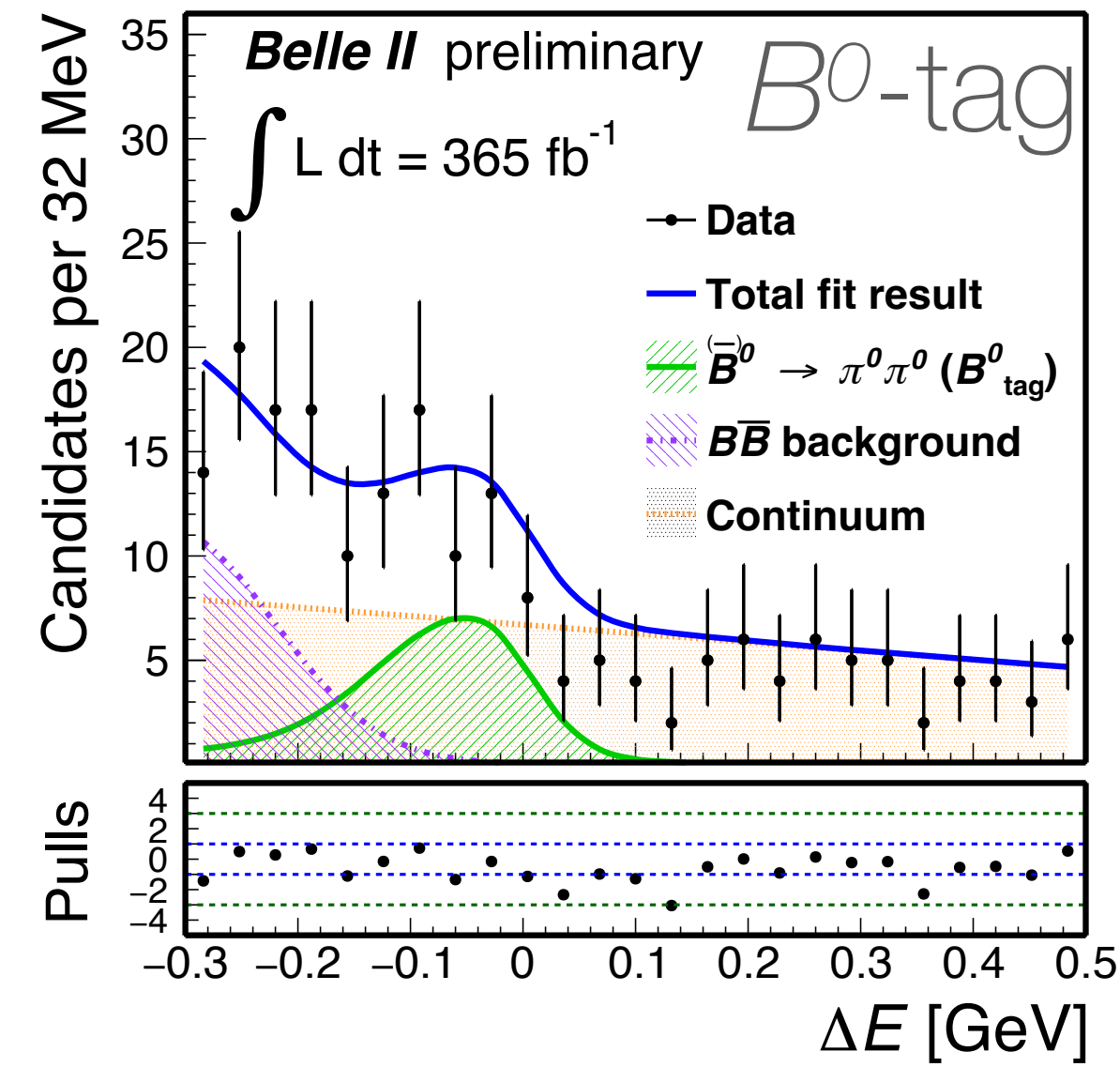
$$\mathcal{B}(B^0 \rightarrow J/\psi\pi^0) = (2.00 \pm 0.12 \pm 0.09) \times 10^{-5},$$

$$C_{CP} = 0.13 \pm 0.12 \pm 0.03, \quad S_{CP} = -0.88 \pm 0.17 \pm 0.03$$



ϕ_2 in $B^0 \rightarrow \pi^0 \pi^0$

- Knowledge of BF and CP asymmetries in $B^0 \rightarrow \pi^0 \pi^0$ limits the precision on ϕ_2 extracted from the $B \rightarrow \pi\pi$ system
- Experimentally reconstruct $2\pi^0$'s (i.e. 4 photons and no vertex) among large continuum background
- Found 126 ± 20 signal candidates, achieving competitive precision on BF and A_{CP}
 - ▶ ~30% fractional increase in ϕ_2 precision from $B \rightarrow \pi\pi$ system including this result



$$\mathcal{B}(B^0 \rightarrow \pi^0 \pi^0) = (1.25 \pm 0.20 \pm 0.11) \times 10^{-6}$$

$$\mathcal{A}_{CP}(B^0 \rightarrow \pi^0 \pi^0) = 0.03 \pm 0.30 \pm 0.04$$

ϕ_2 in $B^0 \rightarrow \rho^+ \rho^-$

- $B^0 \rightarrow \rho^+ \rho^-$ dominates precision on ϕ_2 due to small loop contribution
- Experimentally reconstruct $2\pi^0$'s in the final state and angular analysis to separate longitudinal/transverse polarization in $P \rightarrow VV$ decay
- Found 436 ± 35 longitudinally polarized signal candidates, from which competitive precision on Δt -dependent CP-asymmetries is achieved
 - ▶ ~8% relative improvement on the precision of ϕ_2 from $B \rightarrow \rho\rho$ isospin analysis

$$\mathcal{B}(B^0 \rightarrow \rho^+ \rho^-) = (2.88^{+0.23+0.29}_{-0.22-0.27}) \times 10^{-5},$$

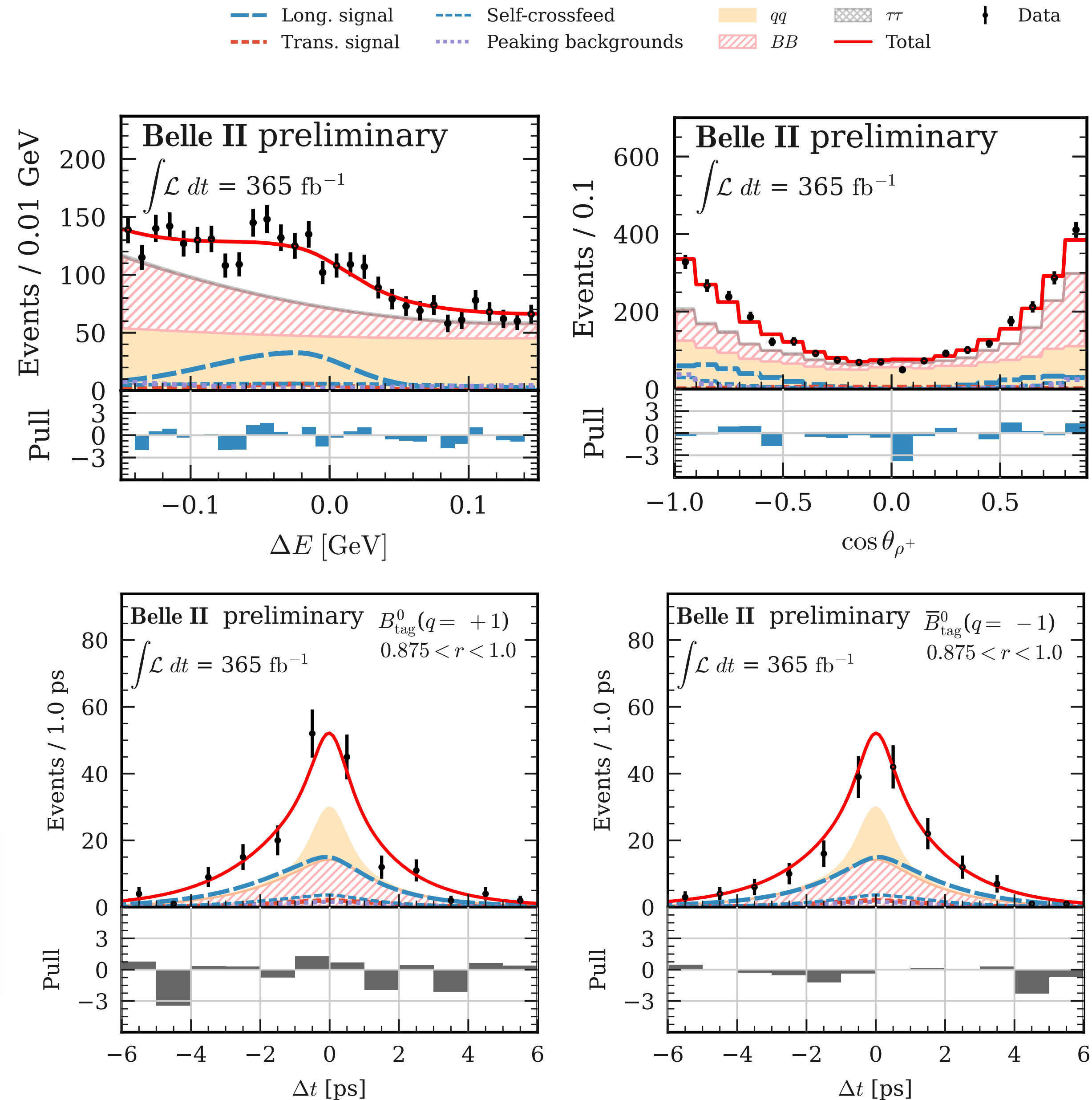
$$f_L = 0.921^{+0.024+0.017}_{-0.025-0.015},$$

$$S = -0.26 \pm 0.19 \pm 0.08,$$

$$C = -0.02 \pm 0.12^{+0.06}_{-0.05},$$

$$\phi_2 = (92.6^{+4.5}_{-4.7})^\circ$$

$$\Delta\phi_2 = (2.4^{+3.8}_{-3.7})^\circ$$



B-tagging

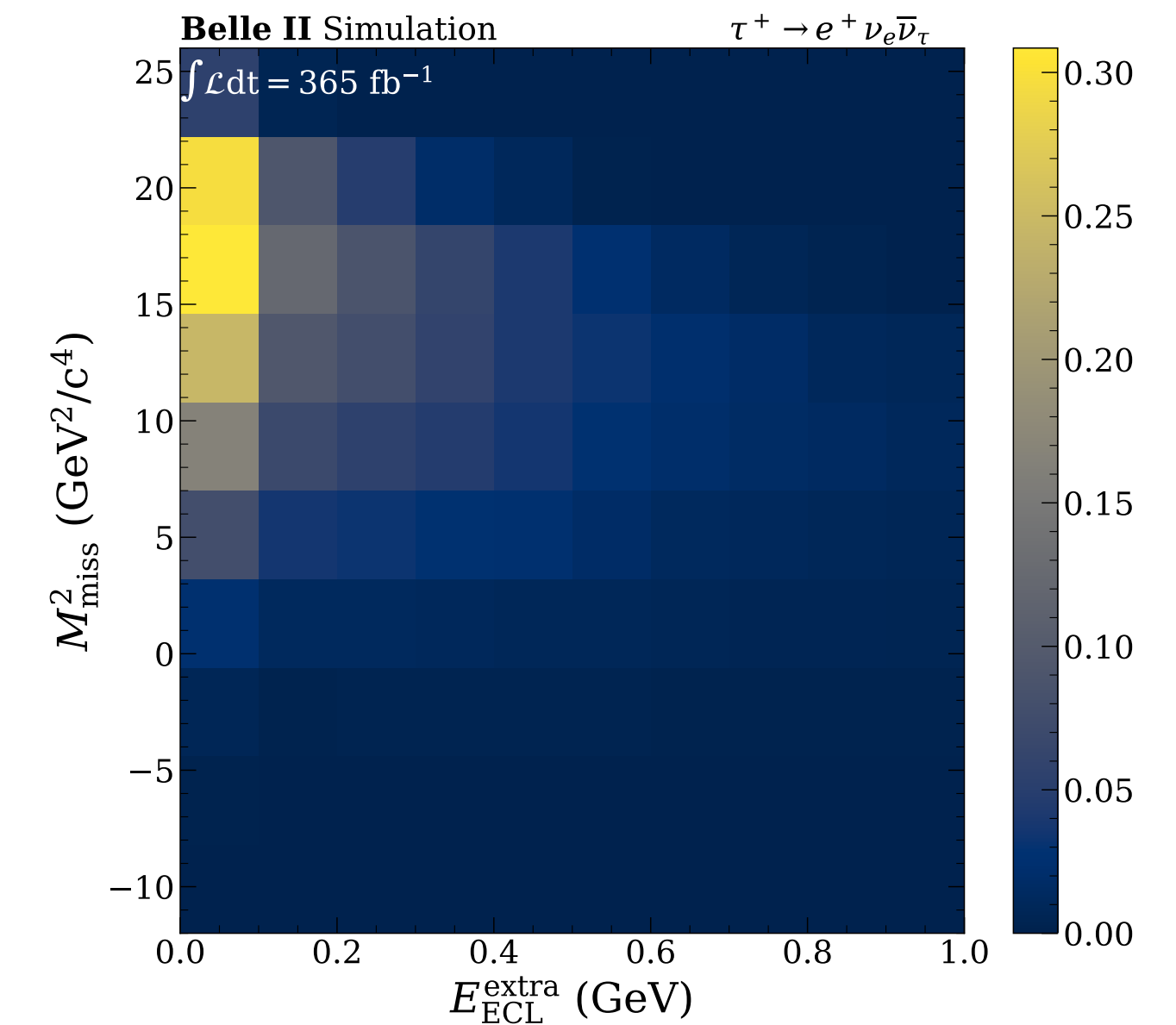
Essential ingredient for analyses with $>1\nu$ in the final state

- Fully reconstruct tag-side B-meson with hadronic decays (e.g. $B \rightarrow D^{(*)}n\pi$)
- Calibrate tagging efficiency ($<1\%$) in data using $B \rightarrow Xl\nu$ and partially reconstructed $B \rightarrow D^{(*)}\pi$ decays

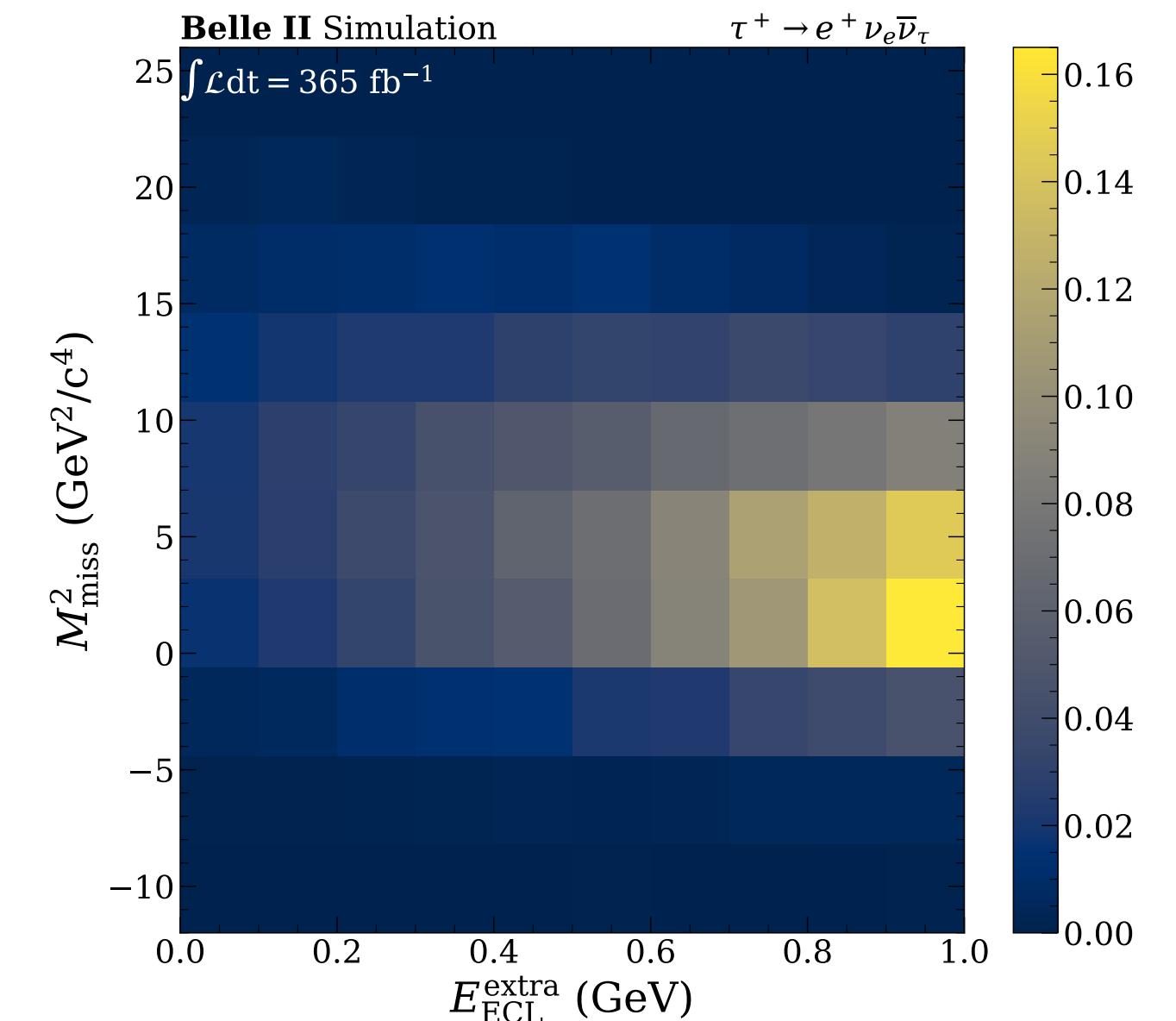
Separate signal and background distributions in

- ▶ Sum of the energy deposits in the calorimeter not associated with B_{tag} and B_{sig} (E_{ECL})
- ▶ Missing mass squared of the event from the known beam energies (M_{miss}^2)

$B^+ \rightarrow \tau\nu$ signal



$B^+ \rightarrow \tau\nu$ background



BF of $B^+ \rightarrow \tau \nu$

- Leptonic B decay with largest BF, sensitive to BSM (charged Higgs, 2HDM) and theoretically clean probe for V_{ub}

$$\mathcal{B}(B^+ \rightarrow \tau^+ \nu_\tau) = \frac{G_F^2 m_B m_\tau^2}{8\pi} \left[1 - \frac{m_\tau^2}{m_B^2} \right]^2 f_B^2 |V_{ub}|^2 \tau_B$$

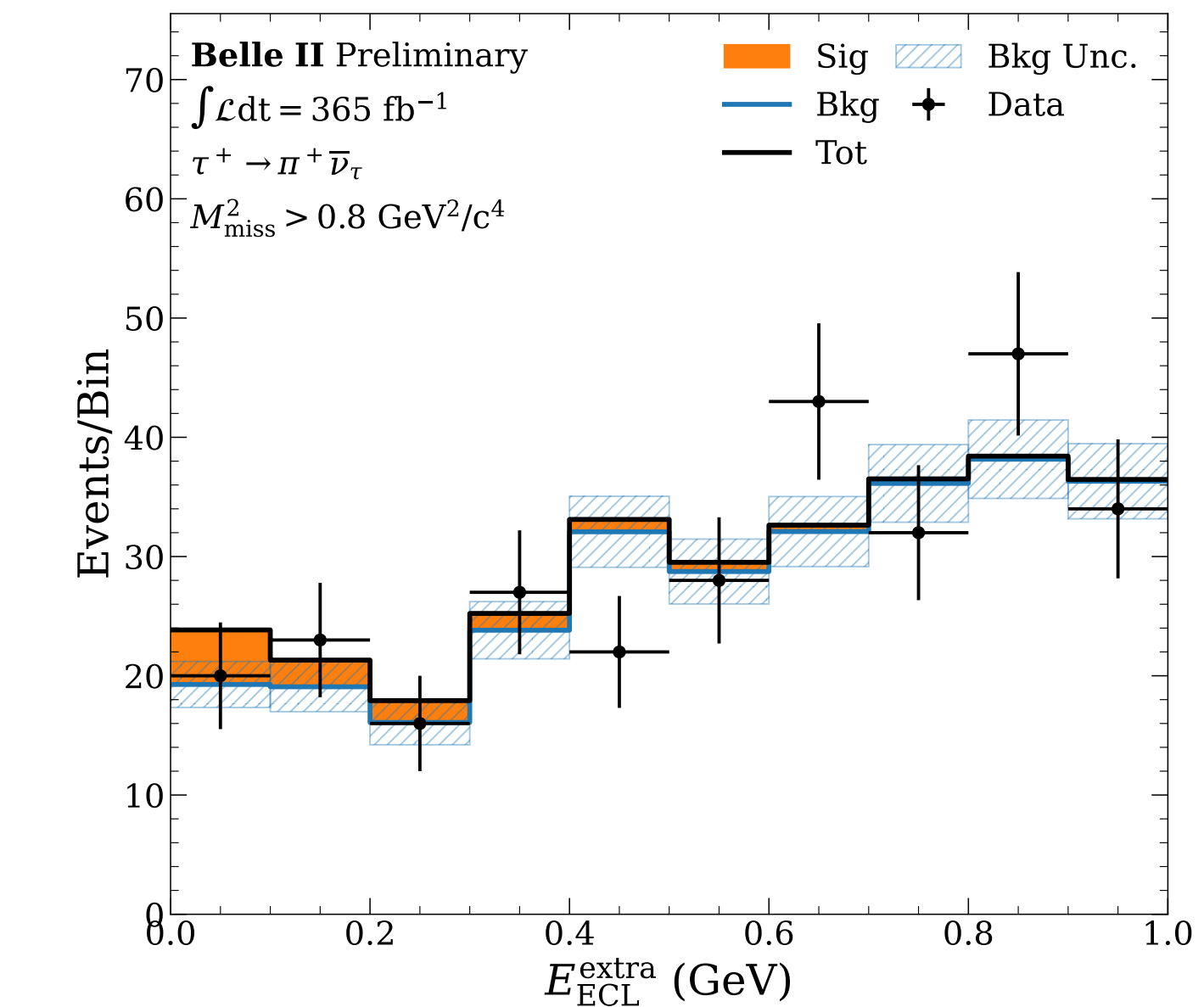
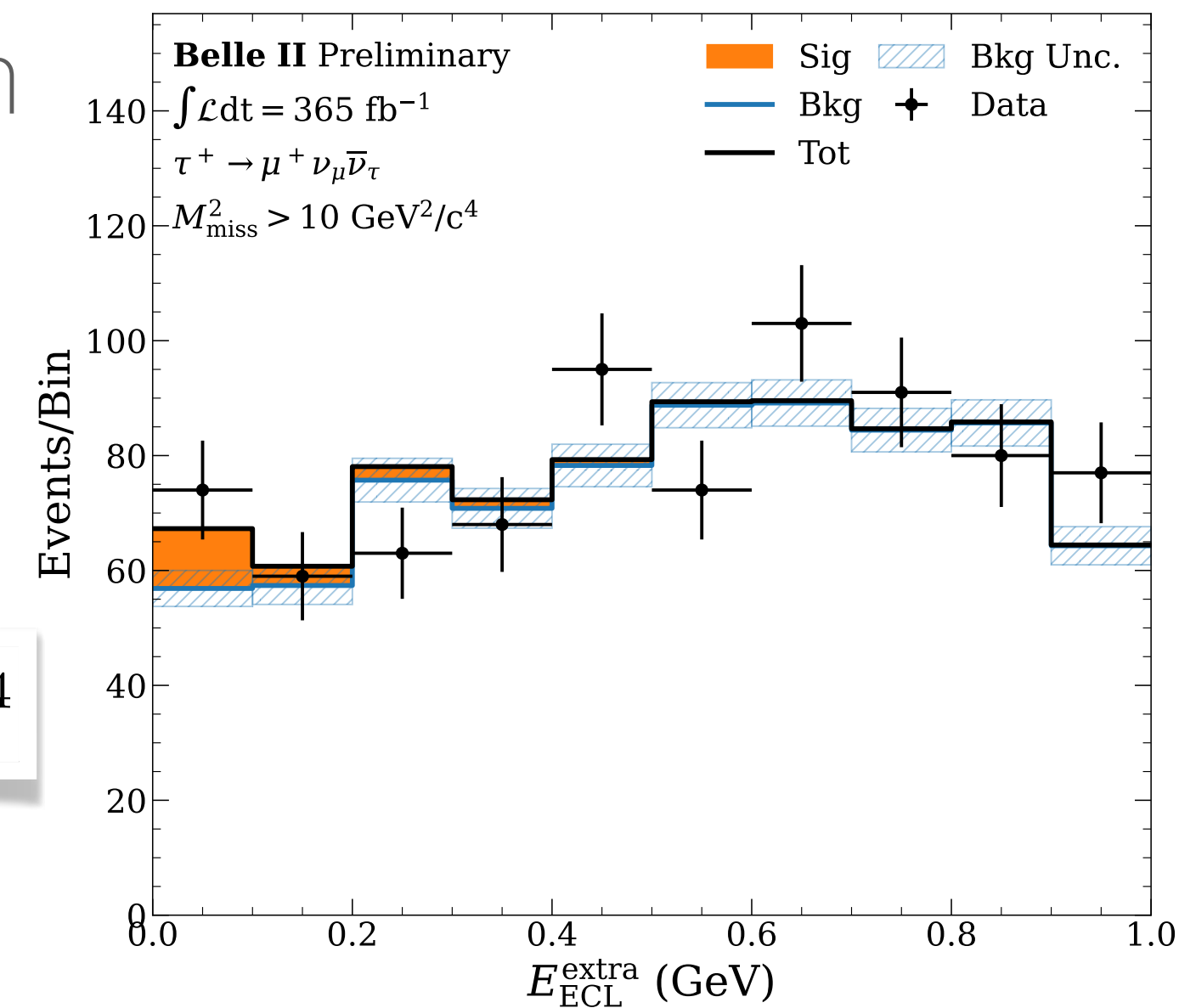
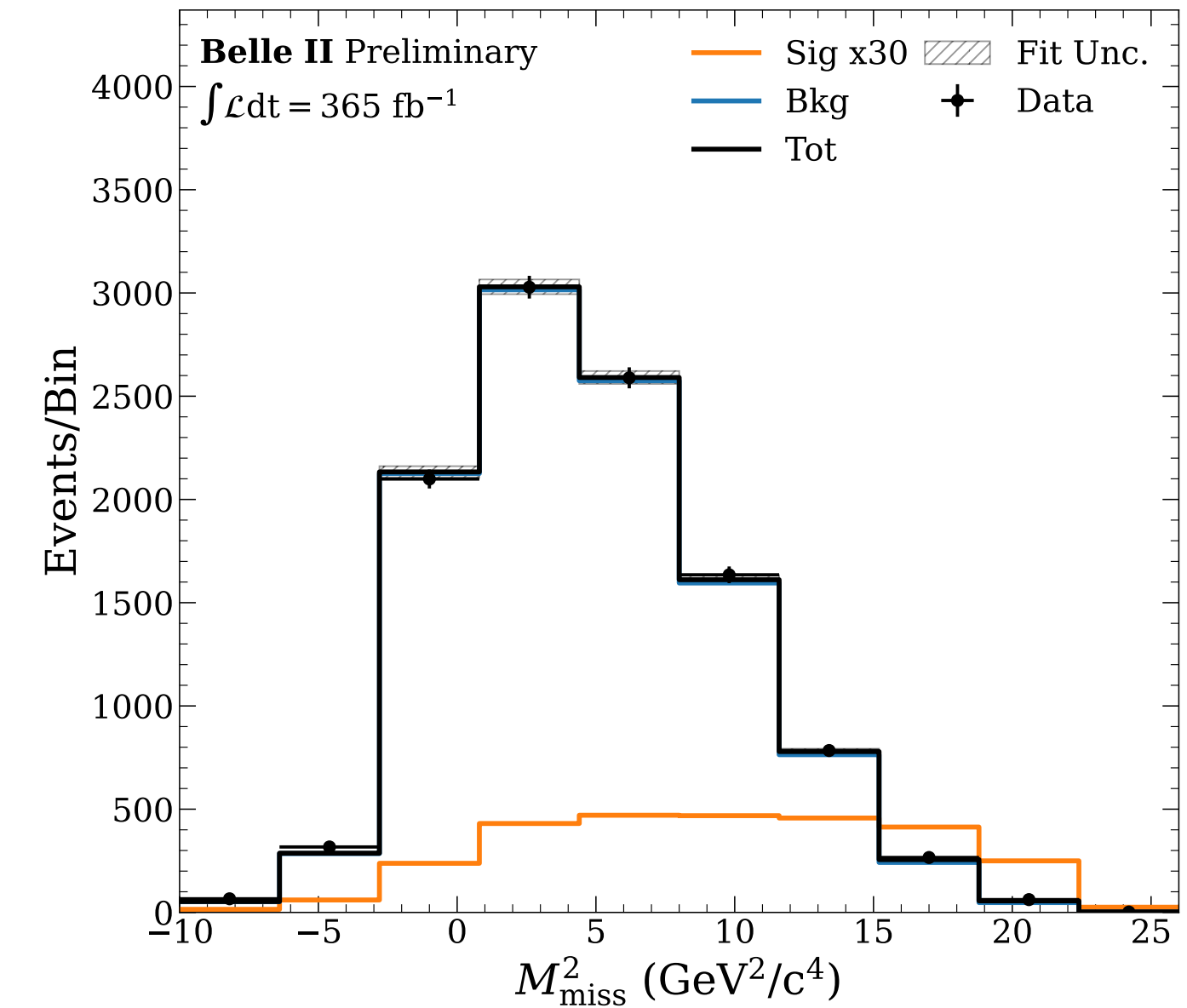
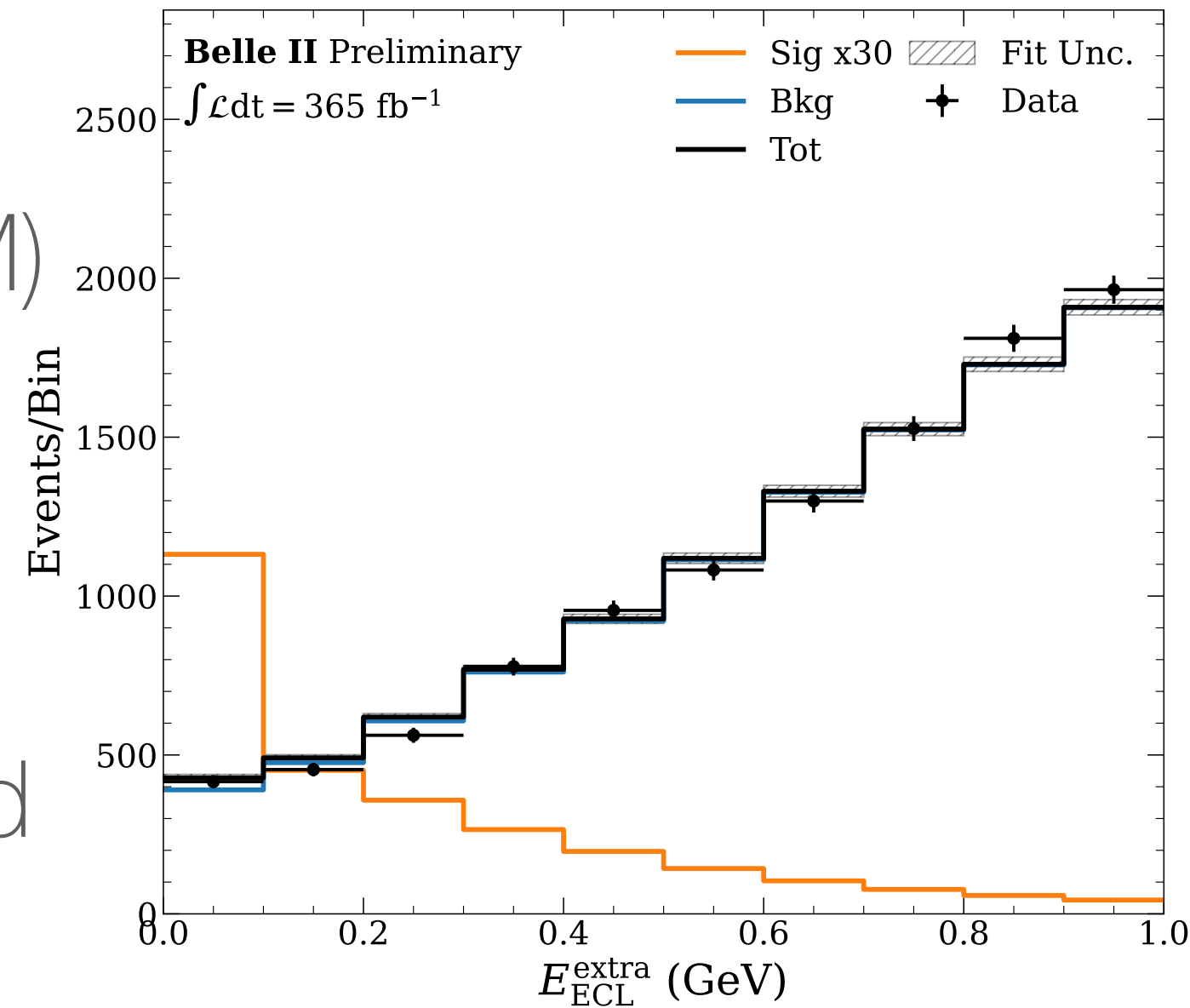
- Using hadronic B -tag and $\tau \rightarrow (e, \mu) \nu \nu$ and $\tau \rightarrow (\pi, \rho) \nu$ modes ($\sim 72\%$ of τ decays)

- Observed 94 ± 31 signal candidates from fit to E_{ECL} and M_{miss}^2 (3σ evidence)

- Sensitivity comparable to previous hadronic-tagged analyses

NEW

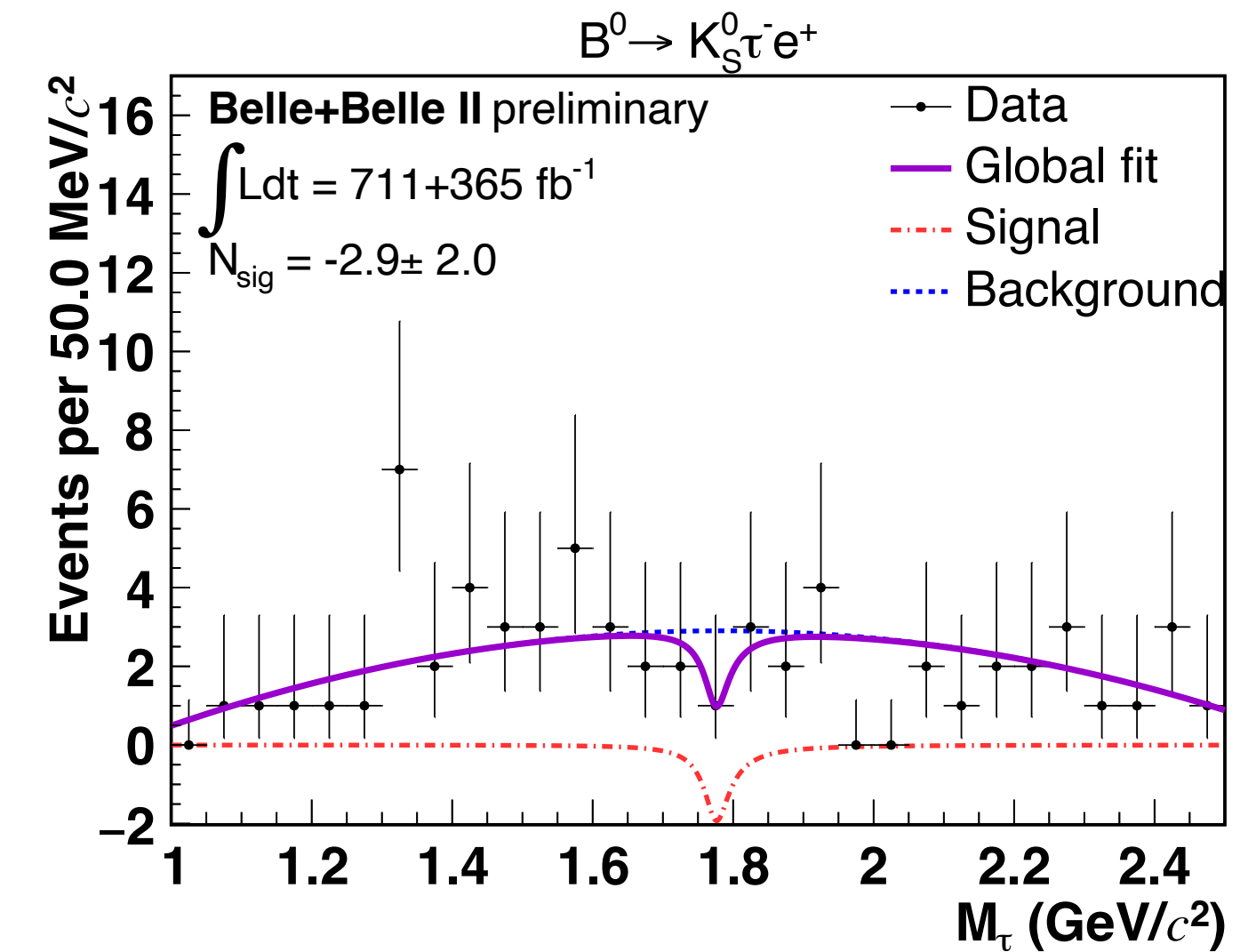
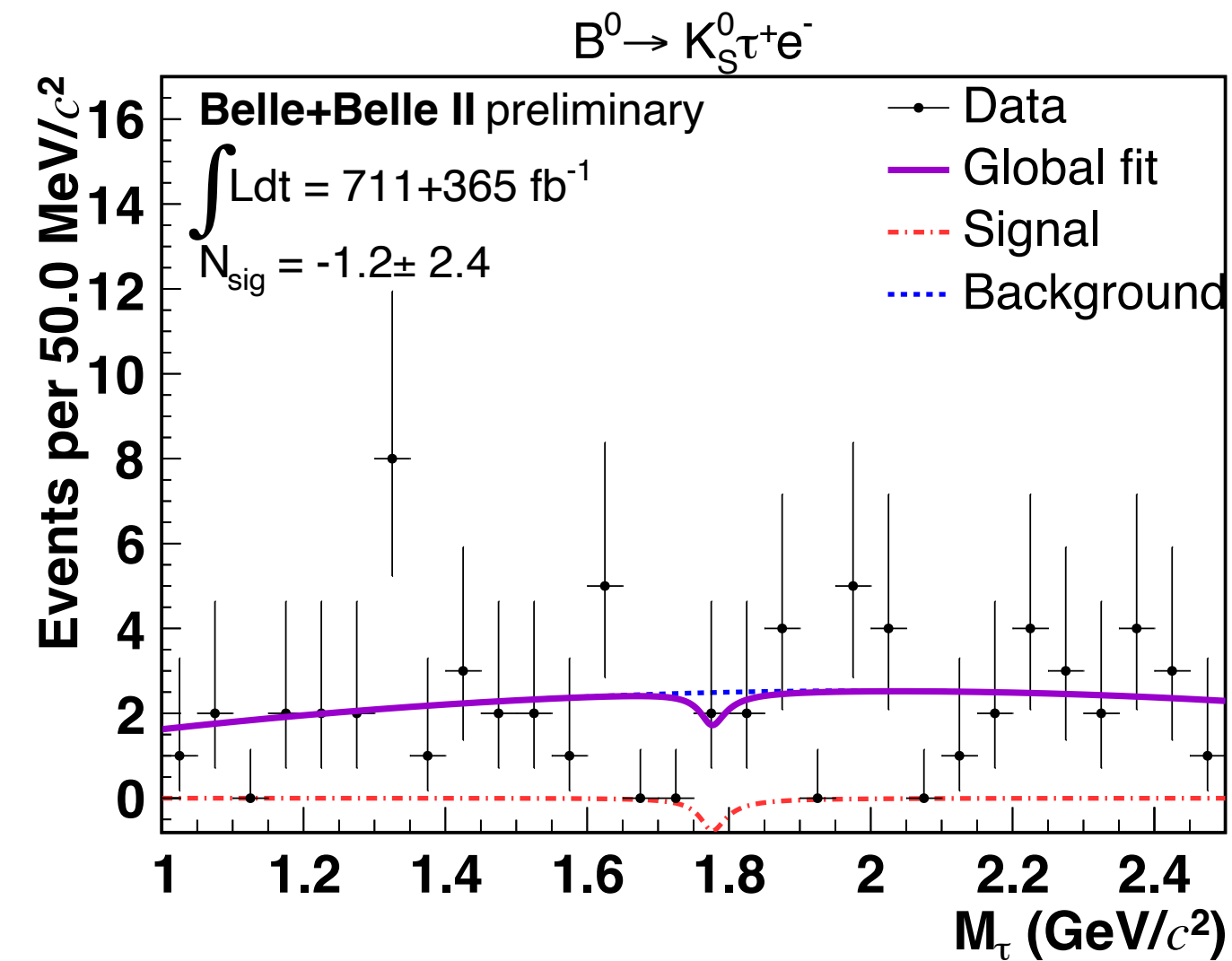
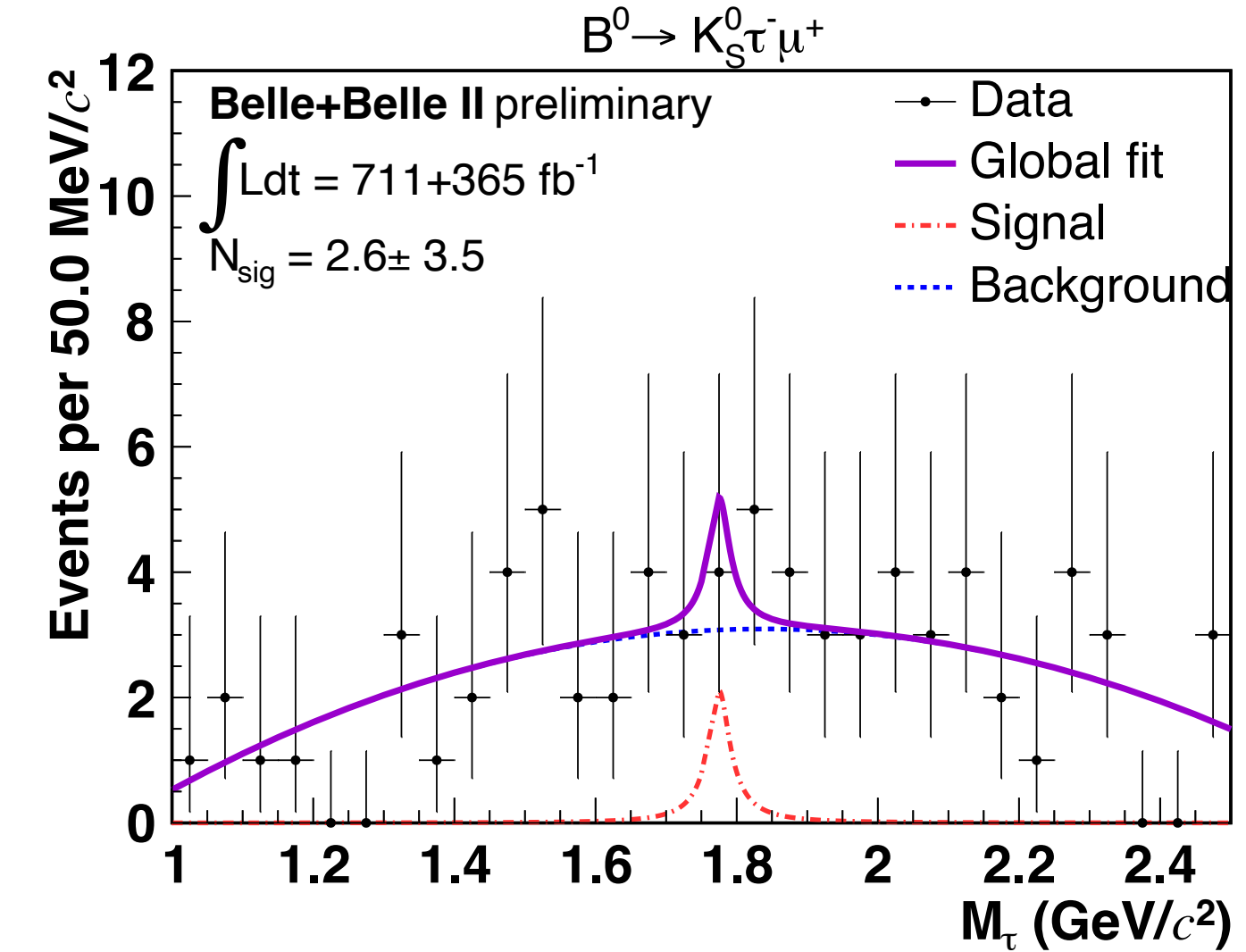
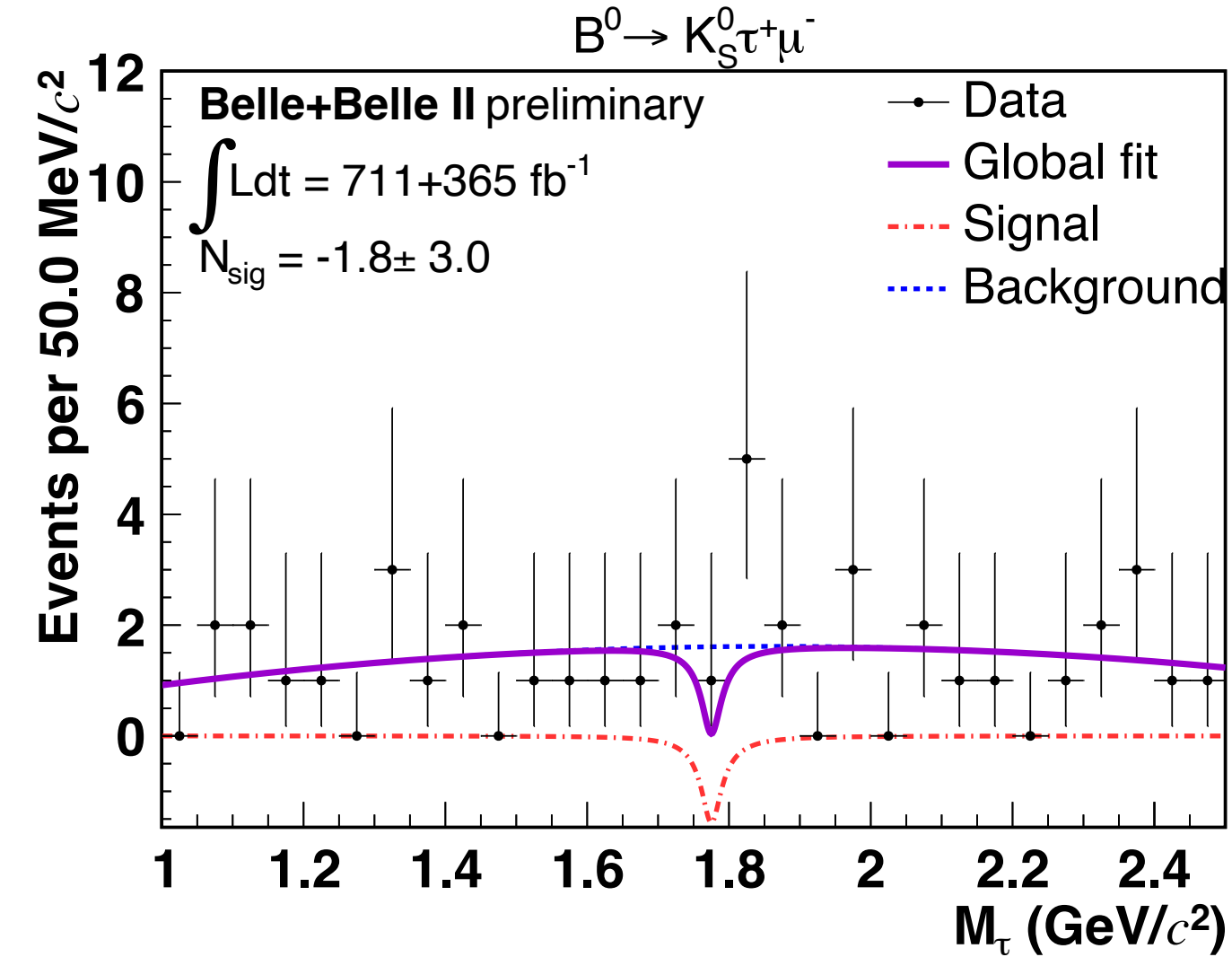
$$\mathcal{B}(B^+ \rightarrow \tau^+ \nu_\tau) = [1.24 \pm 0.41(\text{stat.}) \pm 0.19(\text{syst.})] \times 10^{-4}$$



Search for $B^0 \rightarrow K_S^0 \tau \ell$

- LFV $b \rightarrow s \tau \ell$ transitions arise in models explaining $b \rightarrow c \tau \nu$ anomalies with $\text{BF} \sim \mathcal{O}(10^{-6})$, close to experimental sensitivity
- First search for $B^0 \rightarrow K_S^0 \tau \ell$ using hadronic B-tagging and recoil mass to reconstruct M_τ
 - Clean $K_S^0 \rightarrow \pi^+ \pi^-$ signature, first $B \rightarrow K \tau \ell$ analysis including $\tau \rightarrow \rho \nu$ channel
 - Most stringent ULs on $b \rightarrow s \tau e$ transitions

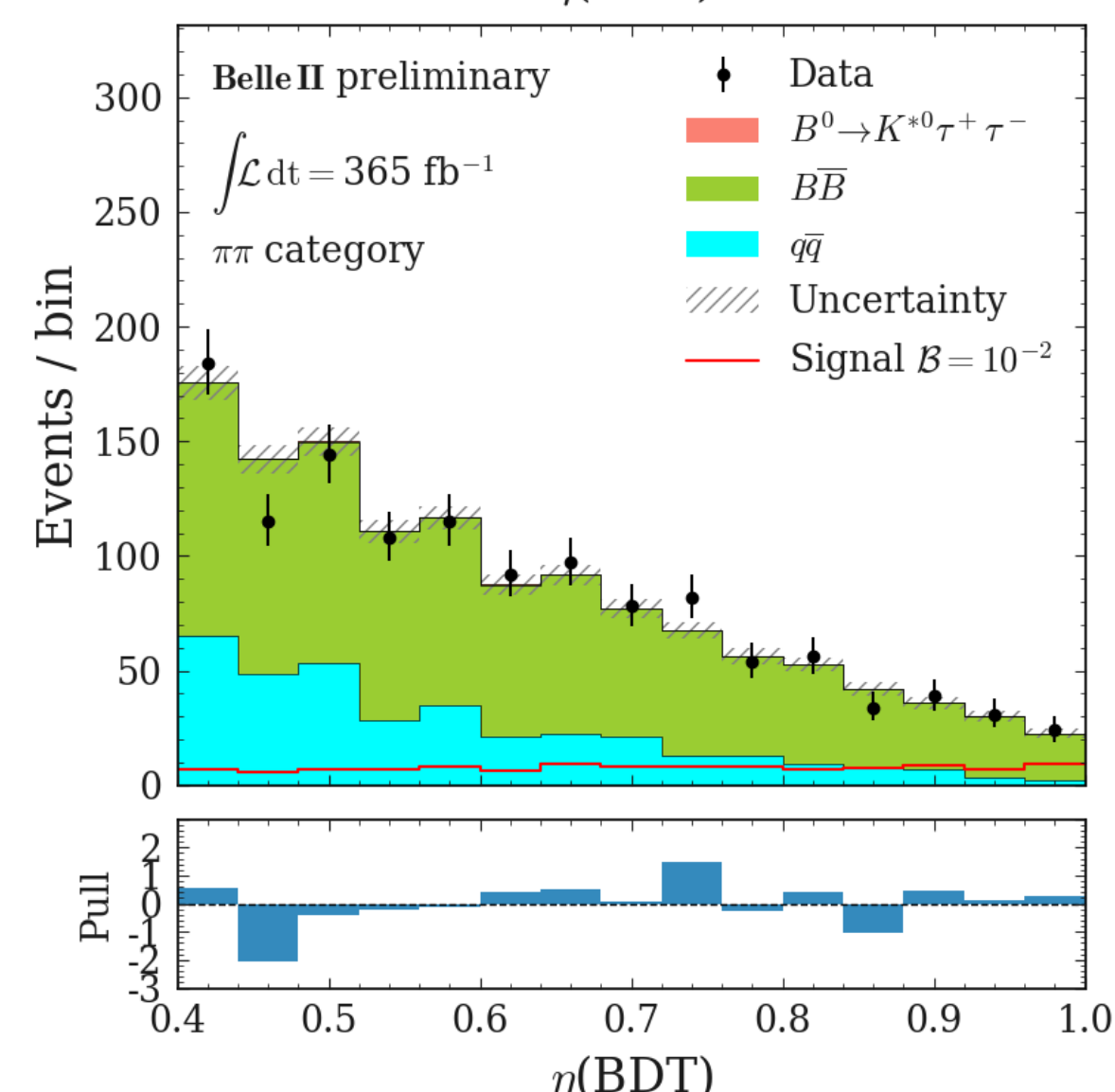
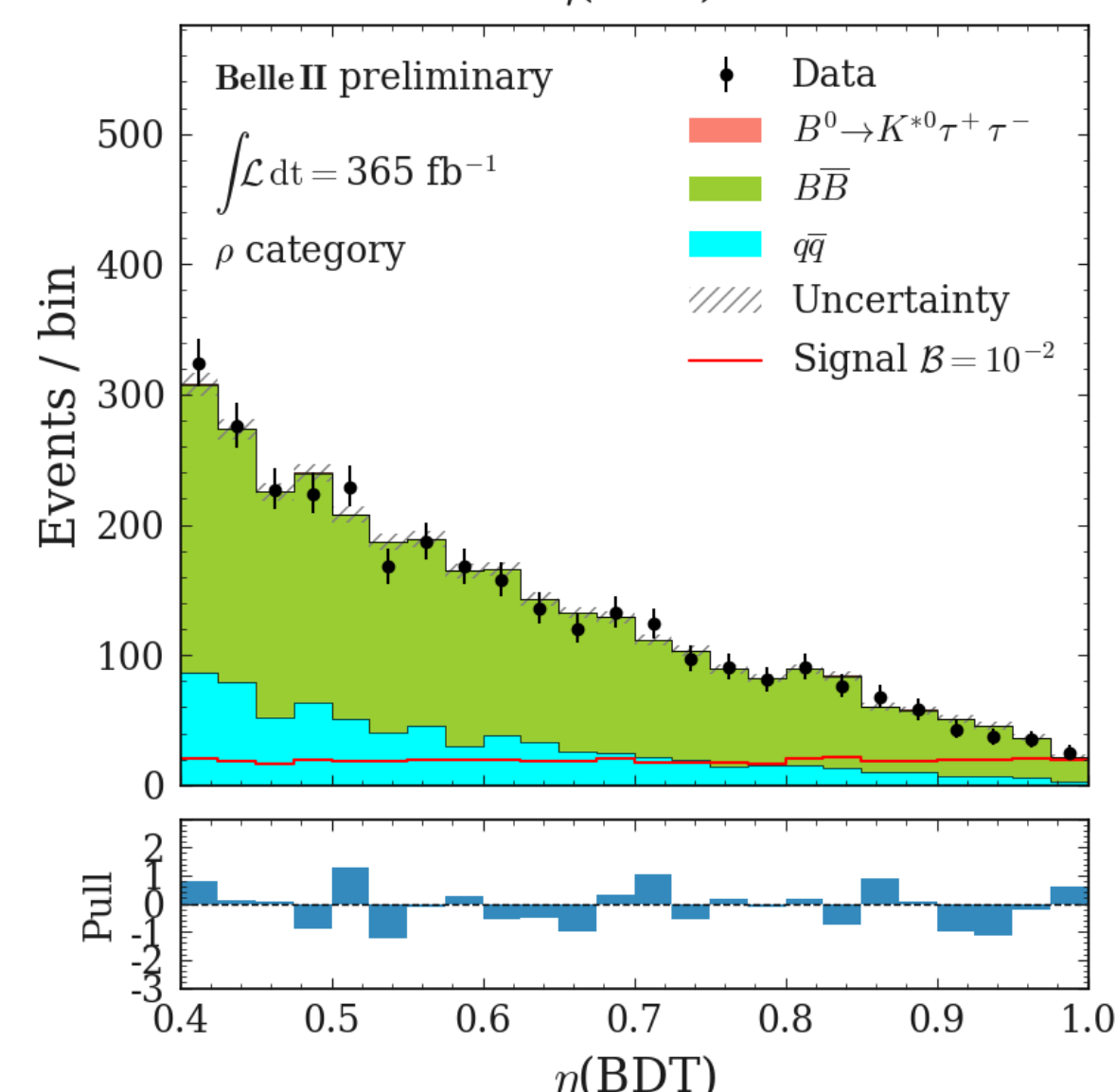
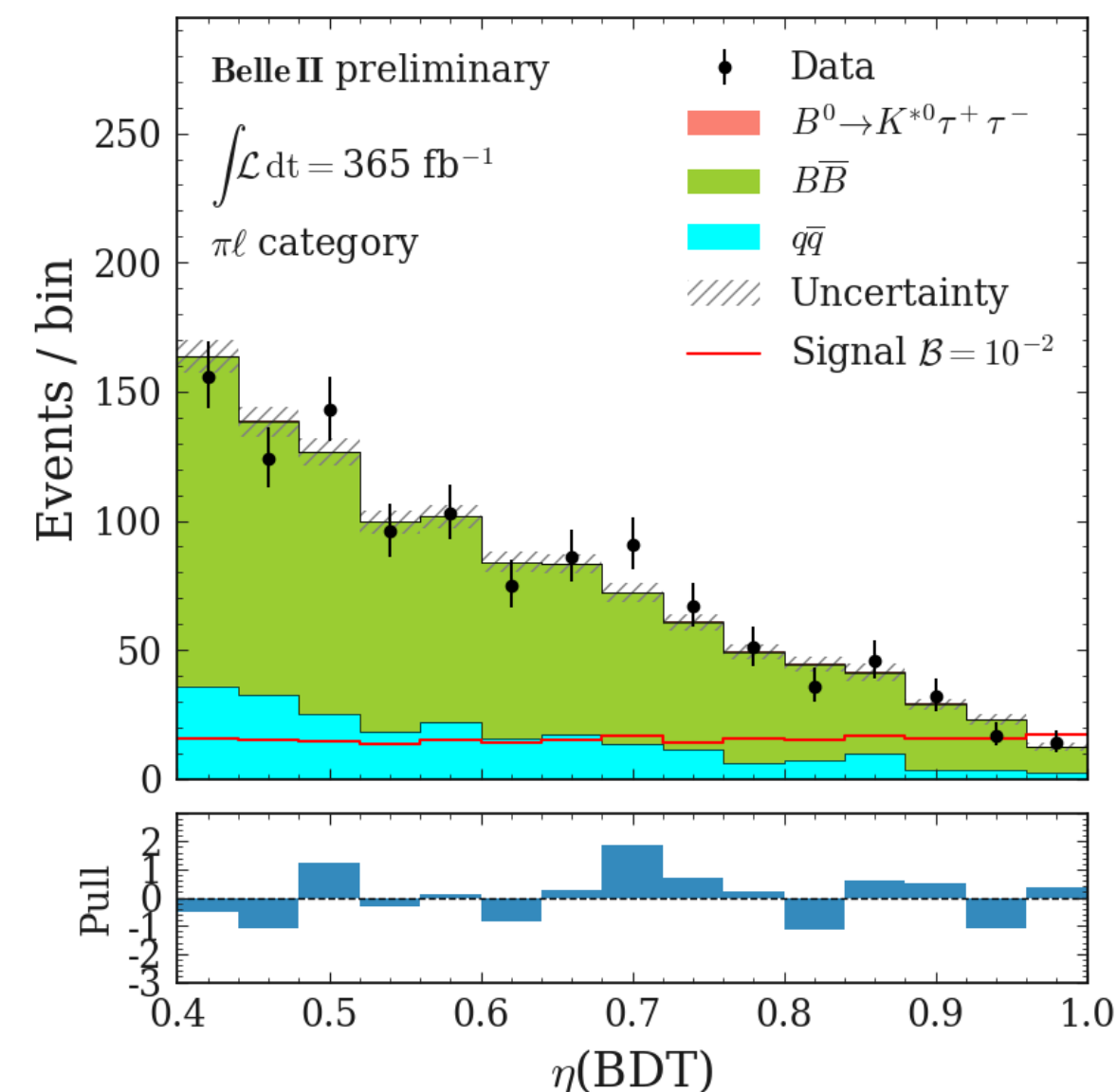
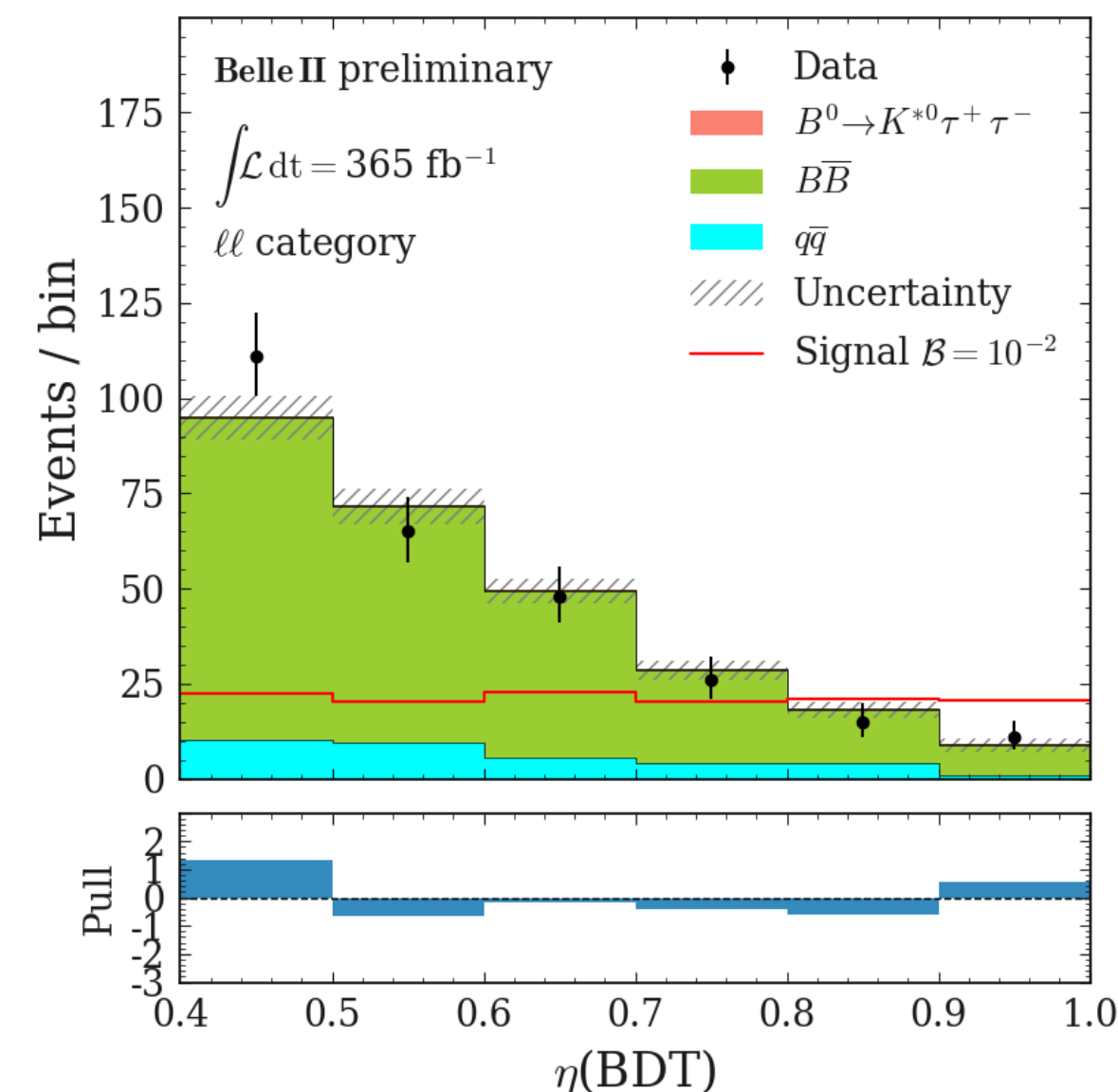
$$\begin{aligned} \mathcal{B}(B^0 \rightarrow K_S^0 \tau^+ \mu^-) &< 1.1 \times 10^{-5} \\ \mathcal{B}(B^0 \rightarrow K_S^0 \tau^- \mu^+) &< 3.6 \times 10^{-5} \\ \mathcal{B}(B^0 \rightarrow K_S^0 \tau^+ e^-) &< 1.5 \times 10^{-5} \\ \mathcal{B}(B^0 \rightarrow K_S^0 \tau^- e^+) &< 0.8 \times 10^{-5} \end{aligned}$$



Search for $B^0 \rightarrow K^{*0} \tau \tau$

[paper in preparation]

- $BF \sim O(10^{-7})$ in SM, enhanced up to $\sim O(10^{-4})$ in models explaining $b \rightarrow c \tau \nu$ anomalies and $B \rightarrow K \nu \bar{\nu}$ excess, close to experimental sensitivities
- Reconstructing tag-side with hadronic decays and signal side from combinations of $\tau \rightarrow (e, \mu) \nu \bar{\nu}$ and $\tau \rightarrow (\pi, \rho) \nu$ (up to 4ν in the final state)
- Signal extracted from fit to BDT classifier combining event shape variables, kinematic of K^* and τ , missing four-momentum and E_{ECL}
 - ▶ Limit twice improved over previous Belle search (higher B -tagging efficiency and inclusion of $\tau \rightarrow \rho \nu$ channel)
 - ▶ Most stringent limit on $b \rightarrow s \tau \tau$ transitions to date

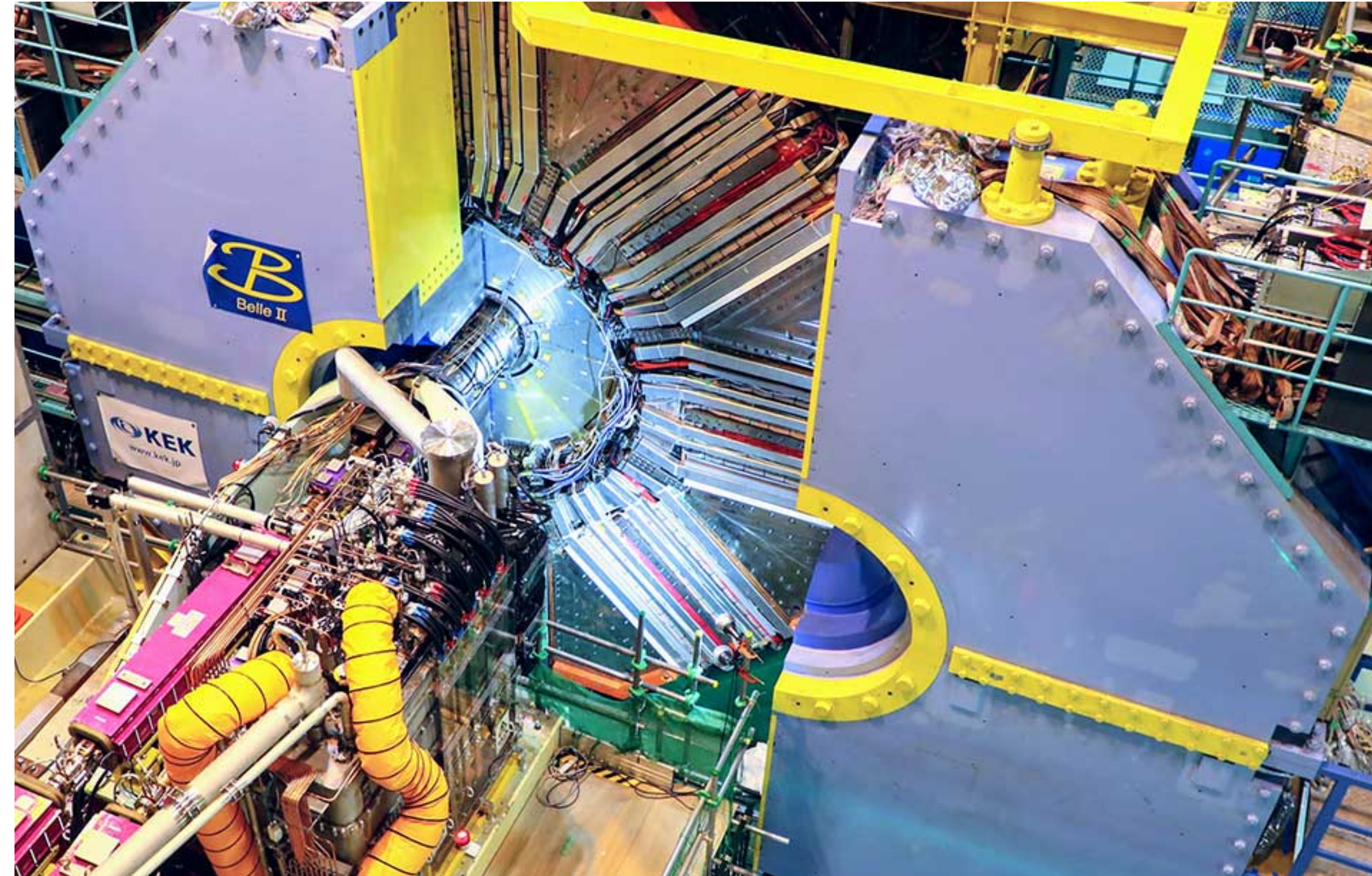


$$BF(B^0 \rightarrow K^{*0} \tau \tau) < 1.8 \times 10^{-3} \text{ @90\% C.L.}$$

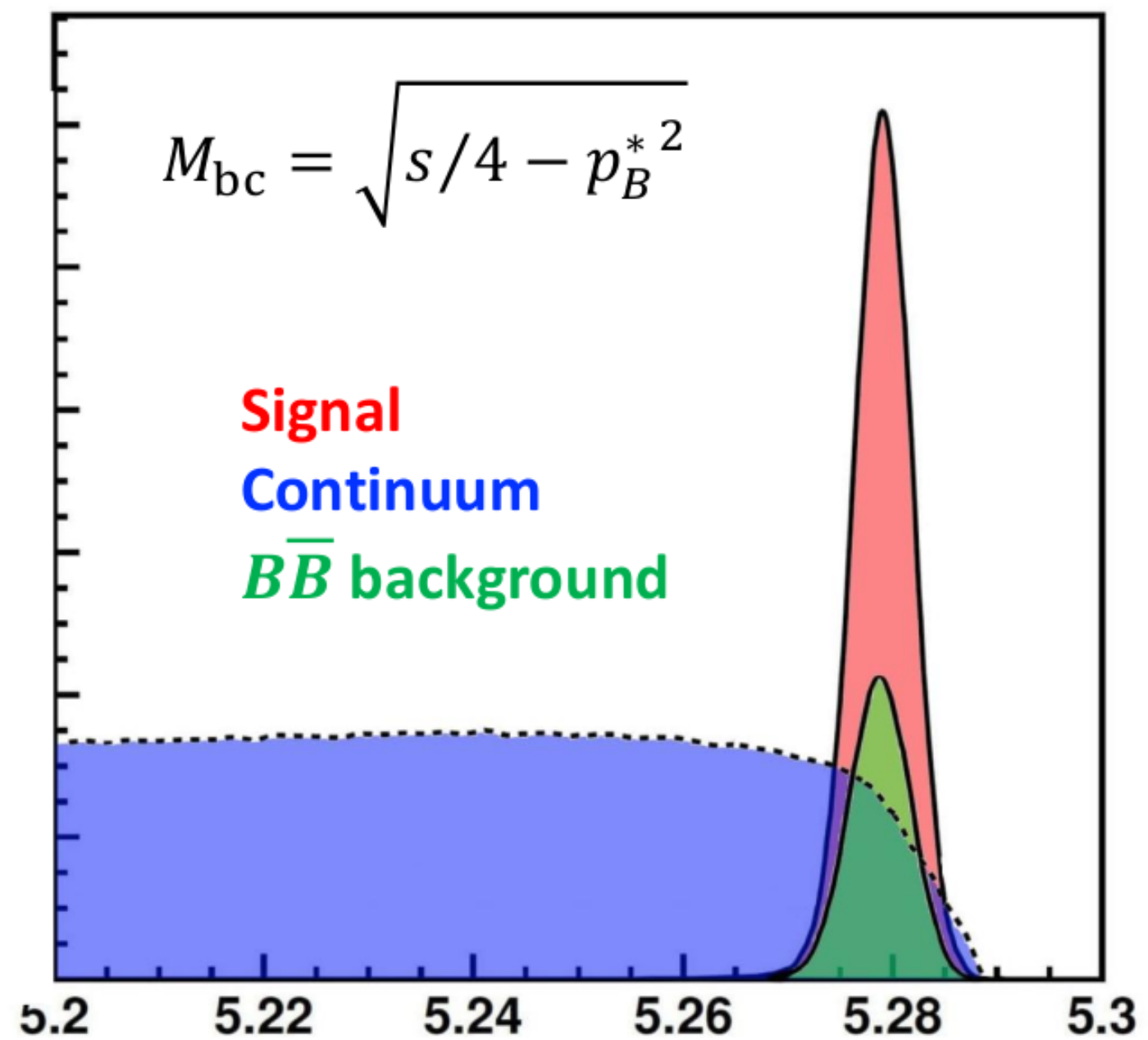
Summary and outlook

Belle II continues to provide essential inputs to test the CKM structure of the SM

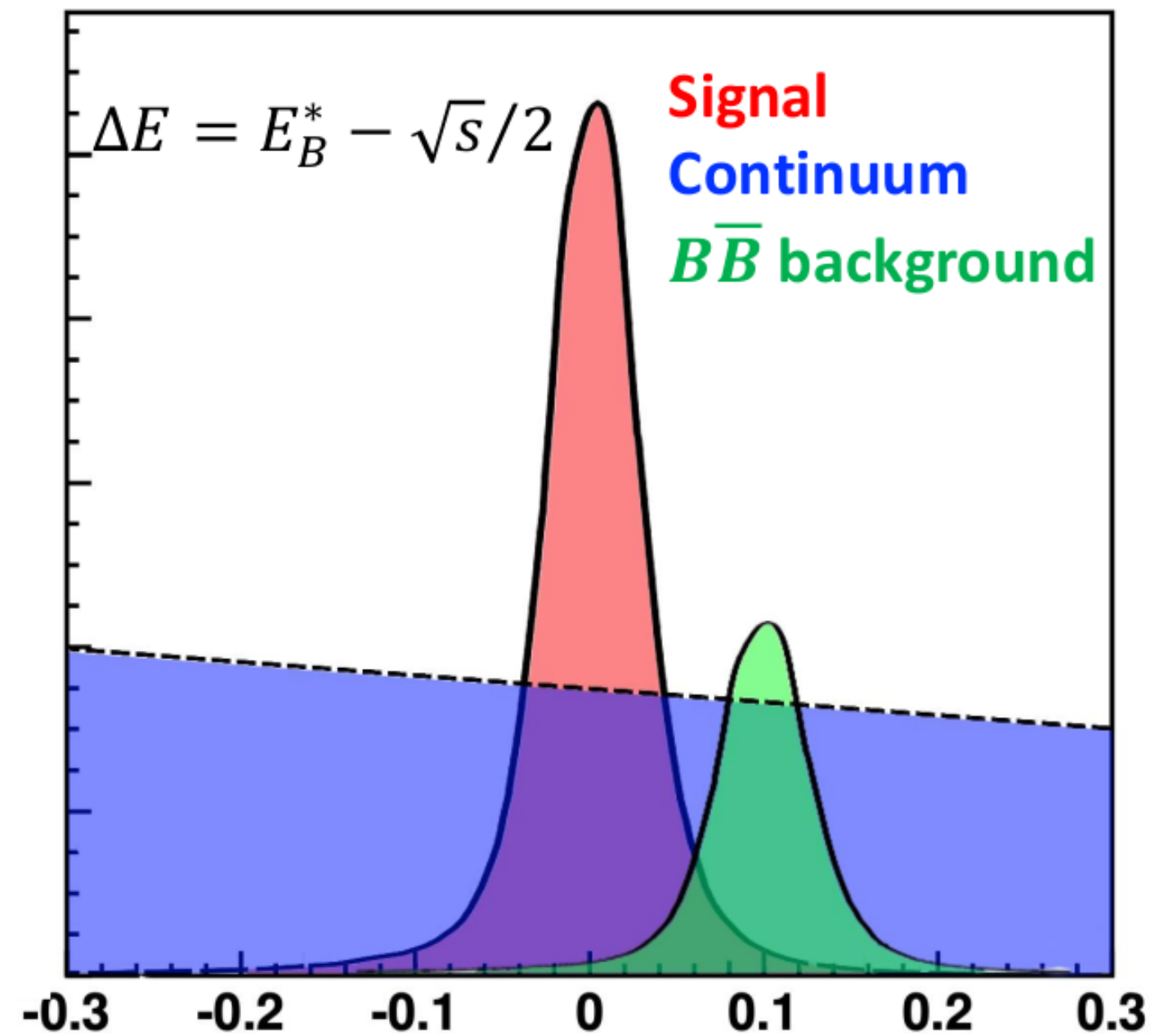
- ▶ Several world leading results and mostly unique measurements with neutrals and missing energy
- ▶ Improved detector performance and analysis techniques
- ▶ Expecting significant increase in sample size with ongoing run



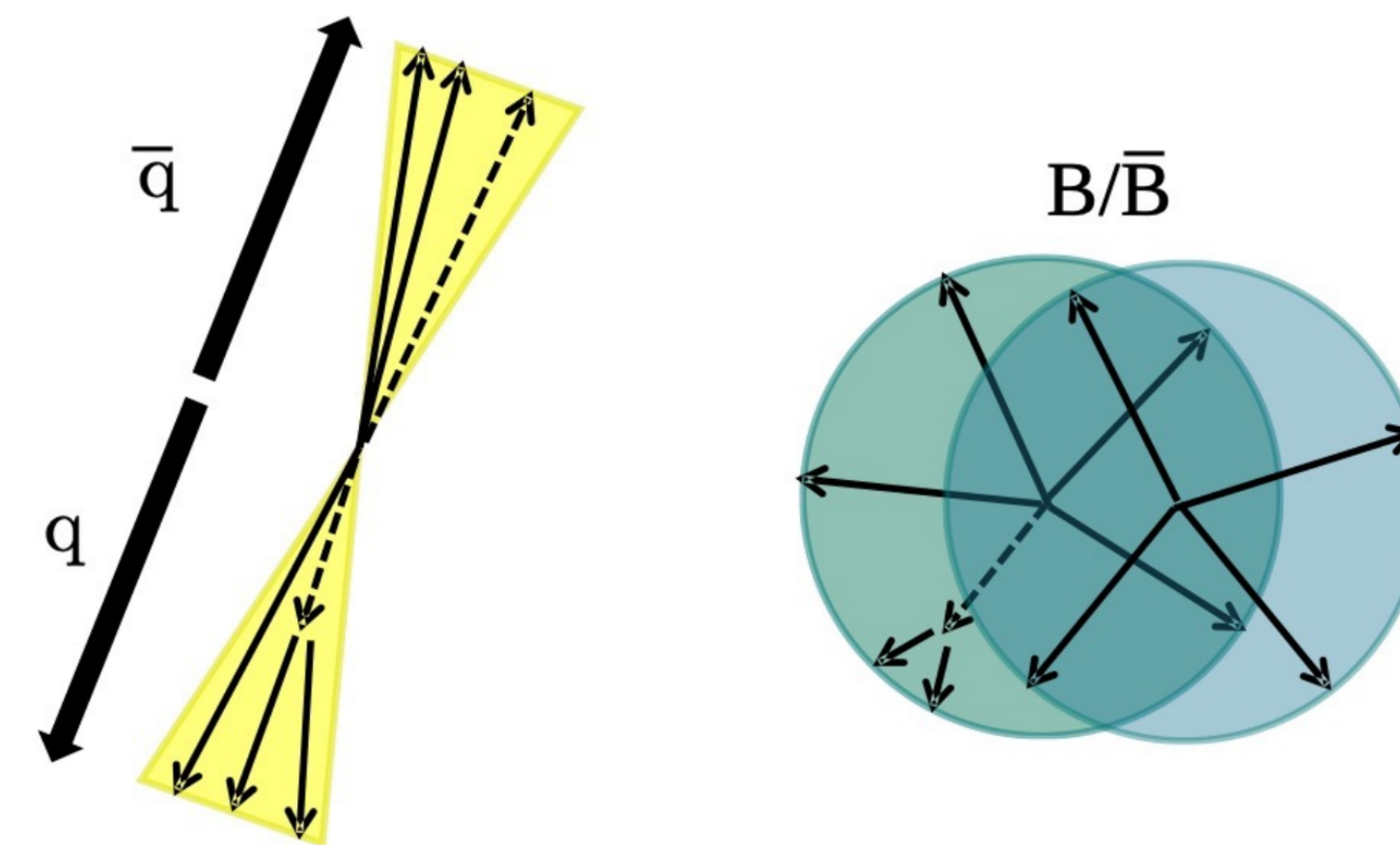
Backup



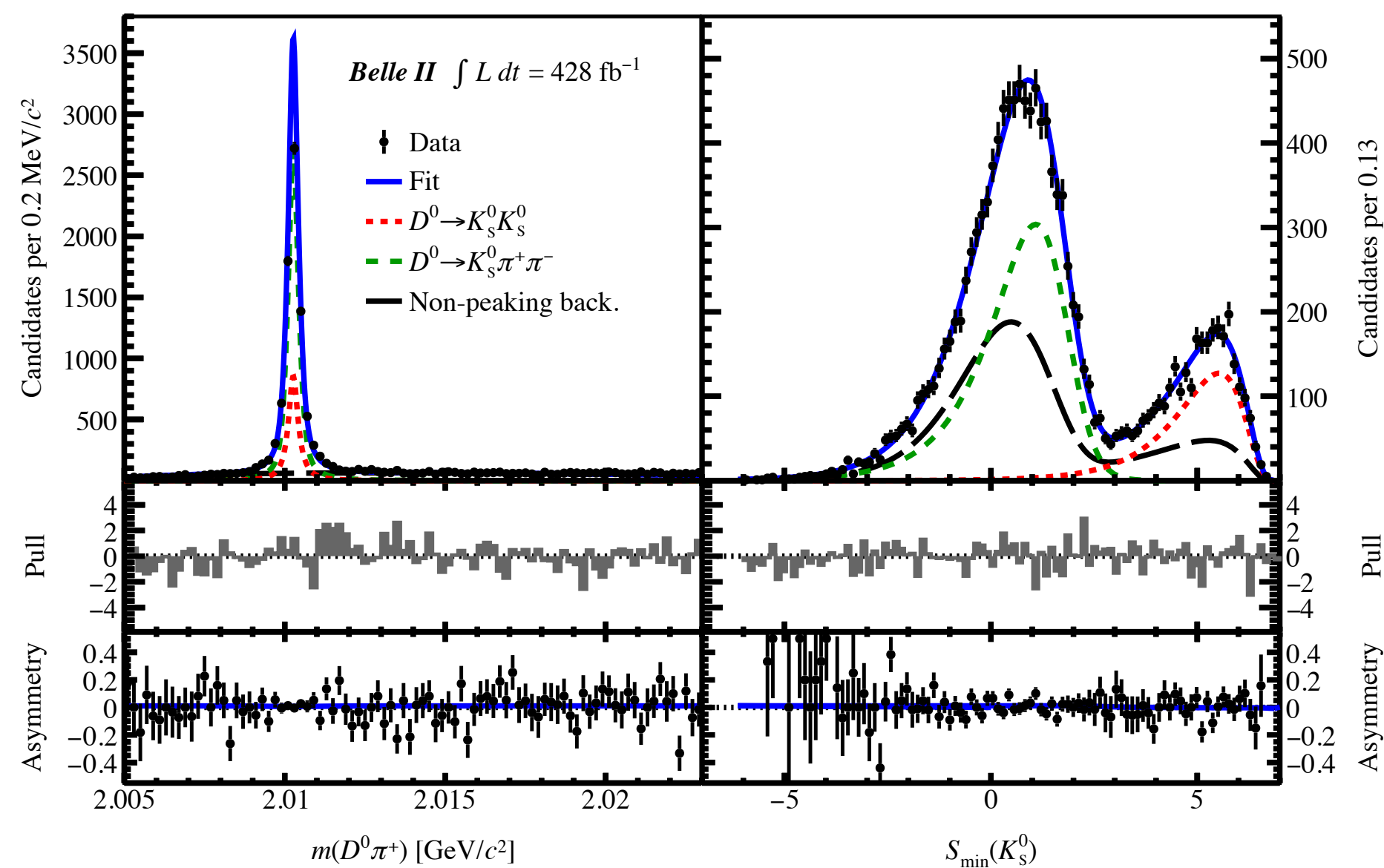
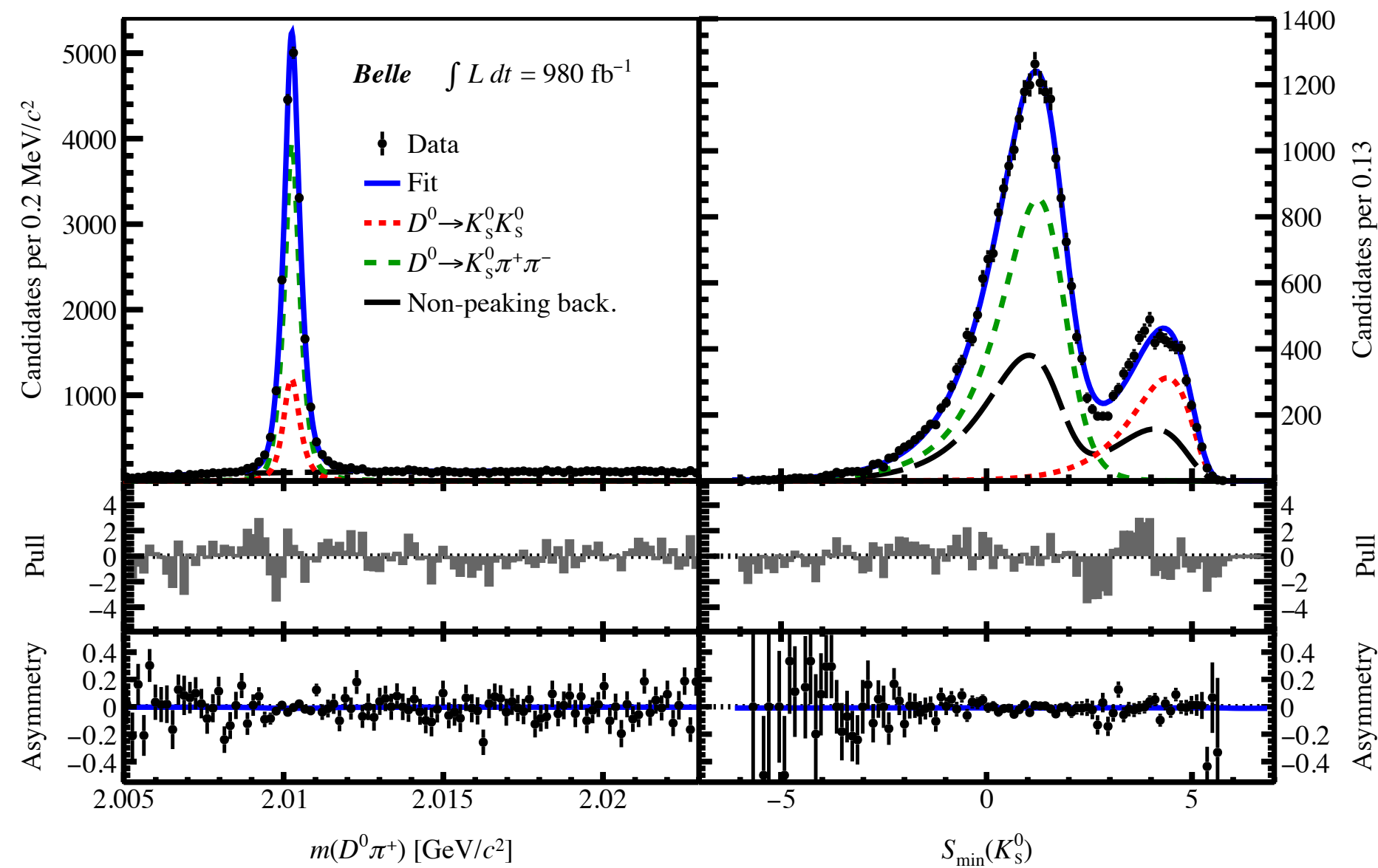
Beam-constrained mass [GeV/c²]



Energy difference [GeV]



Event shape



Systematic uncertainties

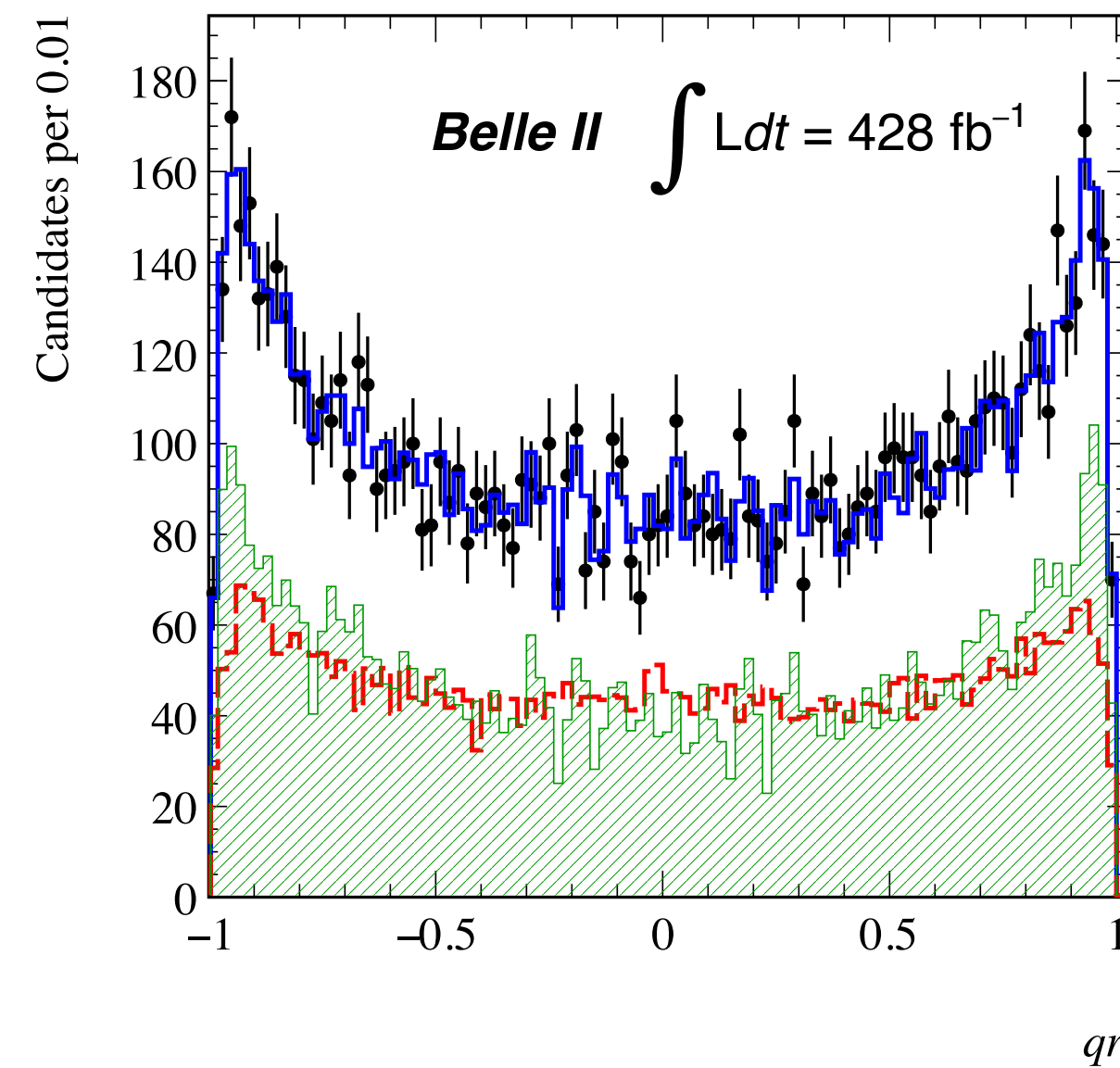
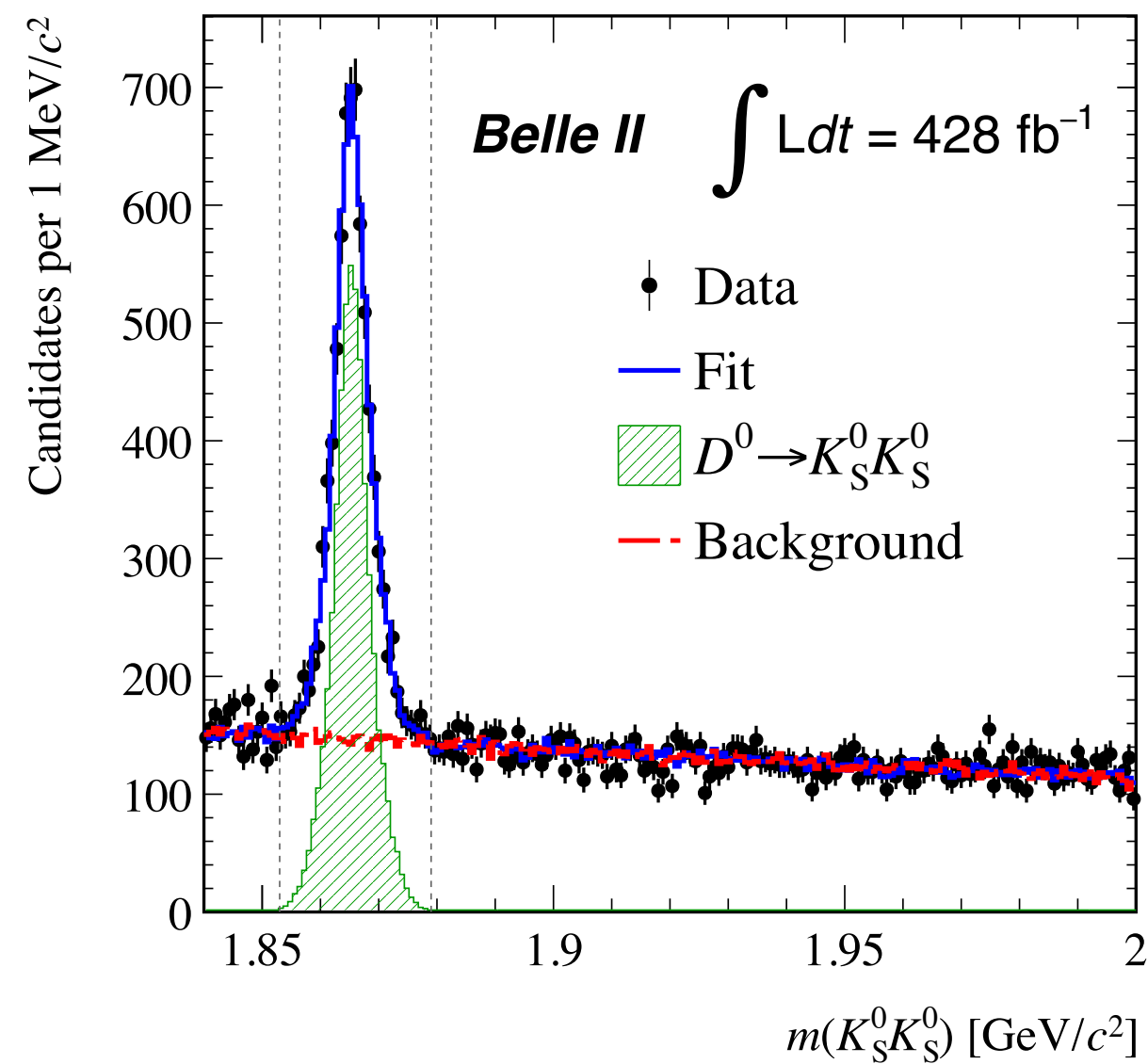
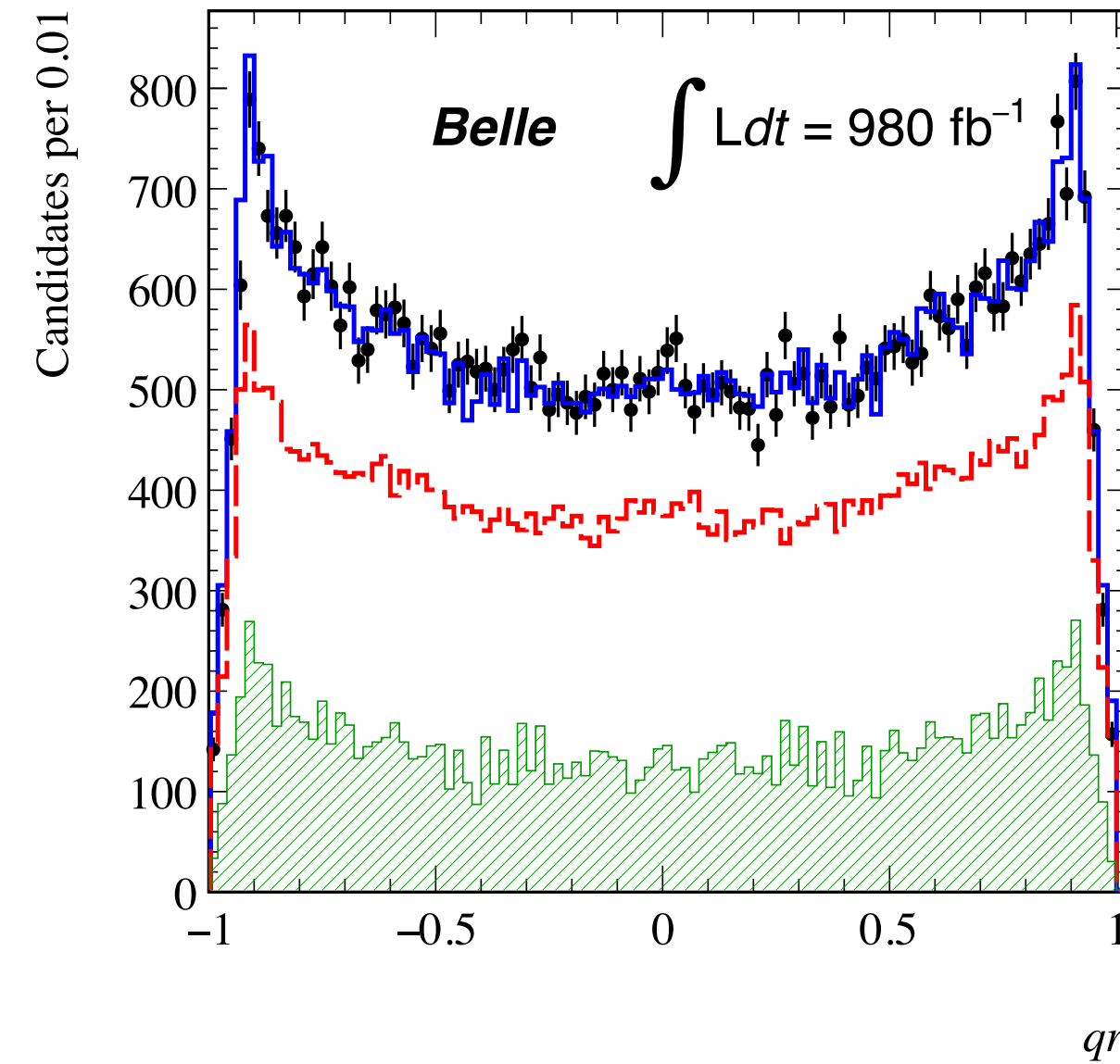
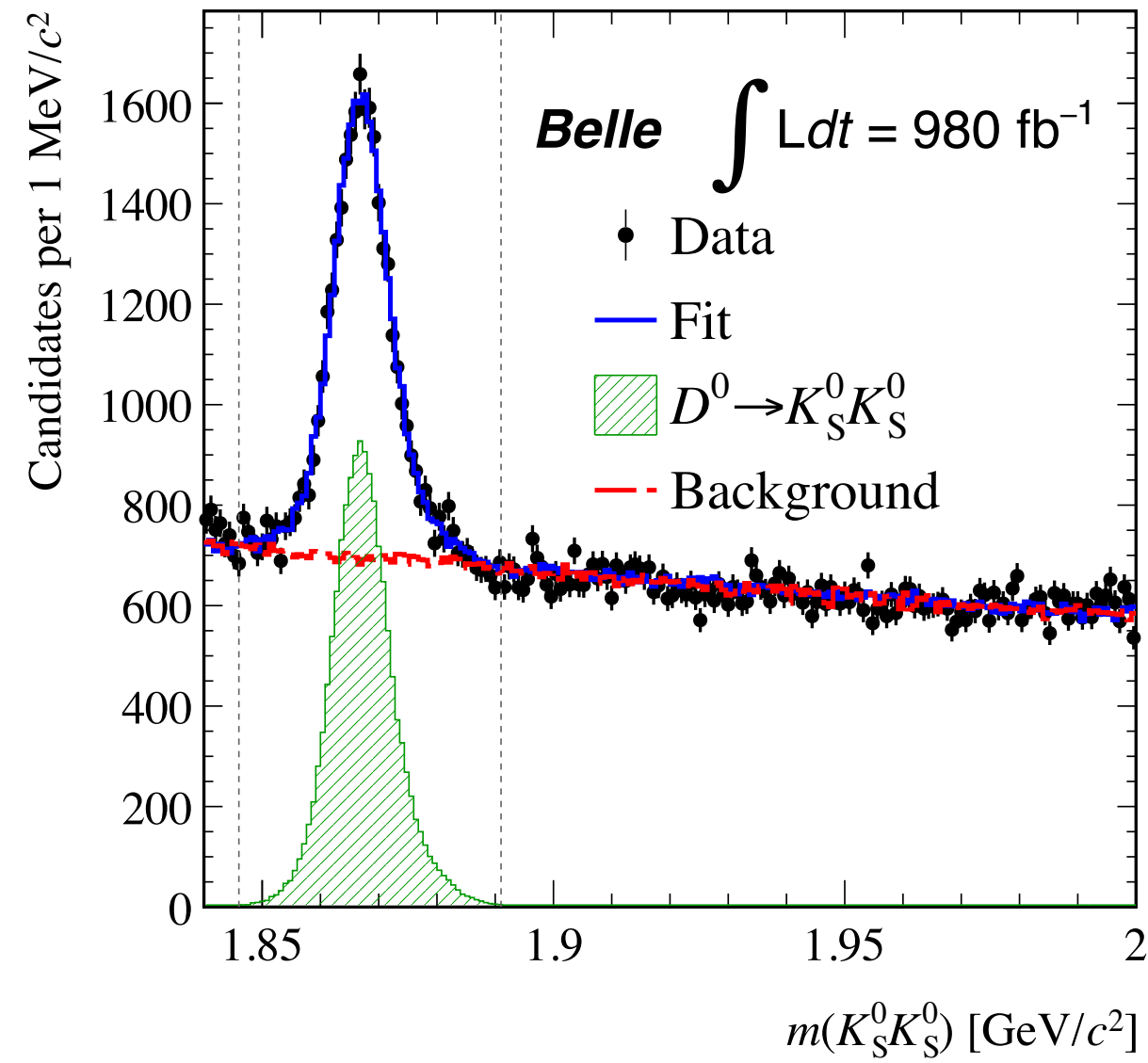
Source	Uncertainty (%)	
	Belle	Belle II
Modeling in the $D^0 \rightarrow K_S^0 K_S^0$ fit	0.04	0.05
Modeling in the $D^0 \rightarrow K^+ K^-$ fit	0.02	<0.01
Kinematic weighting	0.06	0.07
Input $A_{CP}(D^0 \rightarrow K^+ K^-)$	0.05	0.05
Total systematic	0.09	0.10
Statistical	1.60	2.30

Belle

$$A_{CP}(D^0 \rightarrow K_S^0 K_S^0) = (-1.1 \pm 1.6(\text{stat}) \pm 0.1(\text{syst}))\%$$

Belle II

$$A_{CP}(D^0 \rightarrow K_S^0 K_S^0) = (-2.2 \pm 2.3(\text{stat}) \pm 0.1(\text{syst}))\%$$



Systematic uncertainties

Source	Uncertainty [%]	
	Belle	Belle II
Fit modeling	0.35	0.10
$K_S^0\pi\pi$ contamination	0.25	0.23
Total systematics	0.43	0.25
Statistical	2.7	3.0

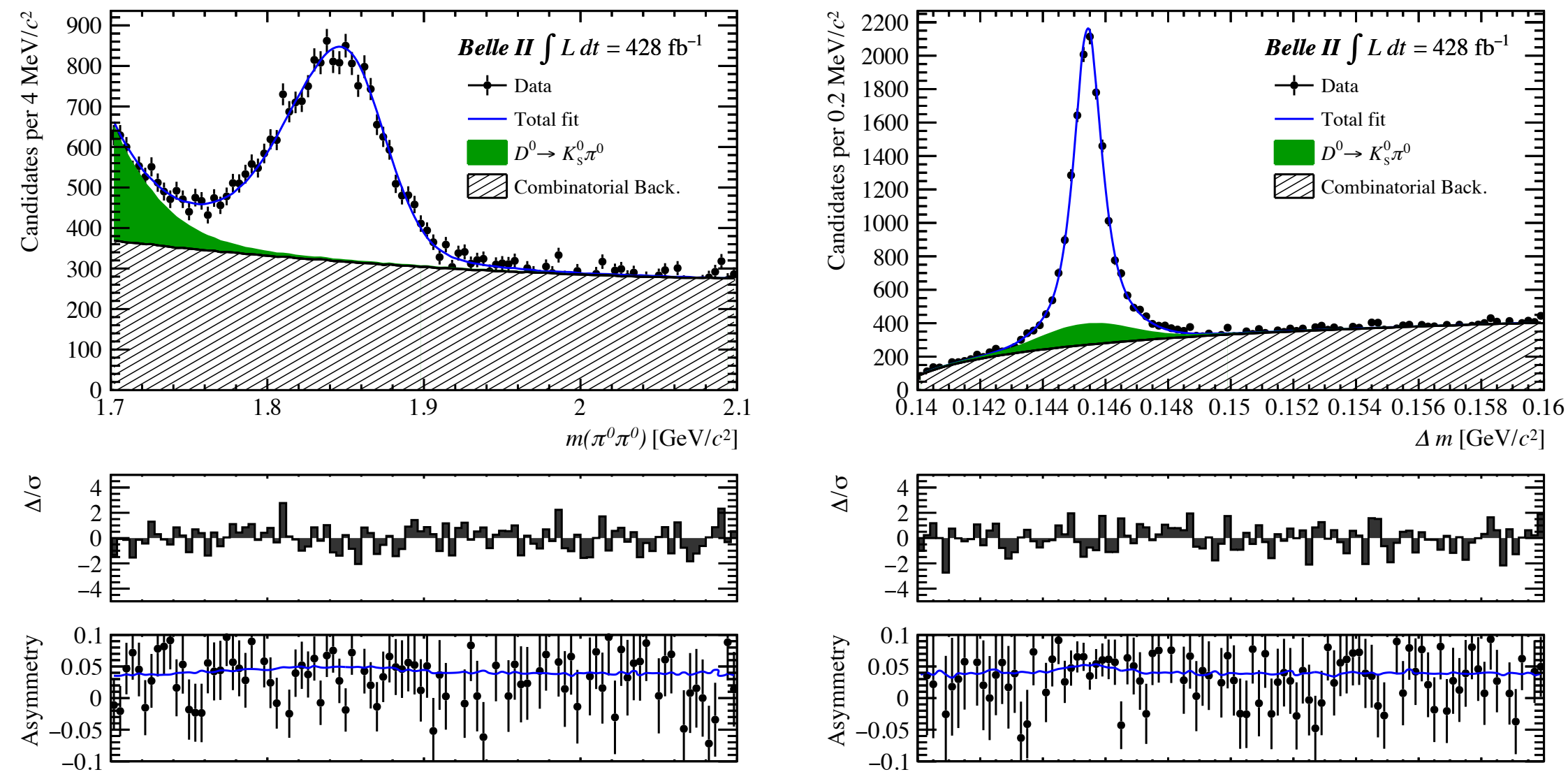
Belle

$$A_{CP}(D^0 \rightarrow K_S^0 K_S^0) = (2.5 \pm 2.7 \pm 0.4)\%$$

Belle II

$$A_{CP}(D^0 \rightarrow K_S^0 K_S^0) = (-0.1 \pm 3.0 \pm 0.3)\%$$

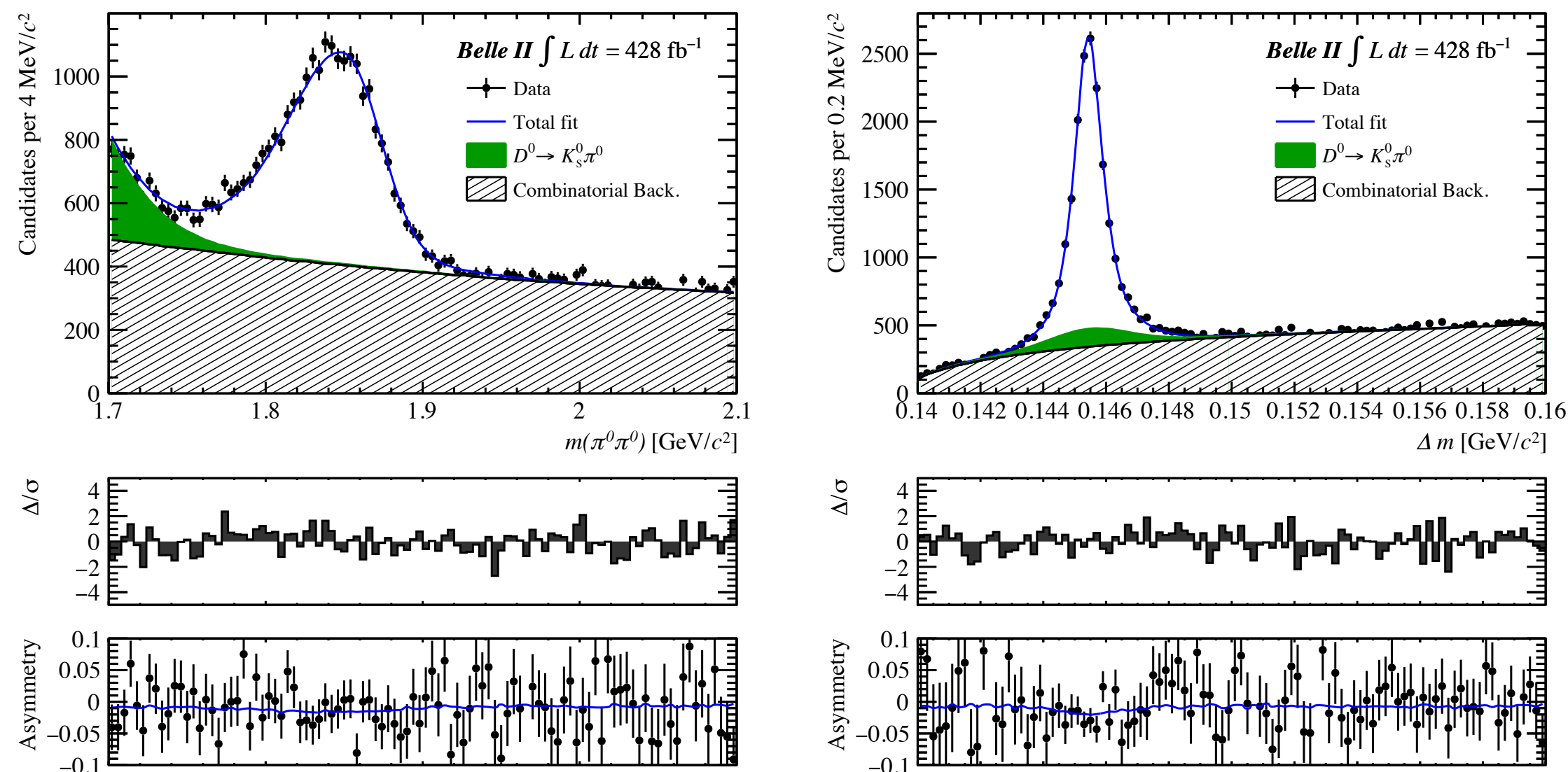
$$\cos\theta^*(D^{*+}) < 0$$



Systematic uncertainties

Source	Uncertainty (%)
Modeling of the $D^0 \rightarrow \pi^0\pi^0$ fit	0.15
Modeling of the tagged $D^0 \rightarrow K^-\pi^+$ fit	0.05
Modeling of the untagged $D^0 \rightarrow K^-\pi^+$ fit	0.09
Kinematic weighting	0.09
Total systematic	0.20
Statistical	0.72

$$\cos\theta^*(D^{*+}) > 0$$



Isospin sum rule

$$R = \frac{A_{CP}^{\text{dir}}(D^0 \rightarrow \pi^+\pi^-)}{1 + \frac{\tau_{D^0}}{\mathcal{B}_{+-}} \left(\frac{\mathcal{B}_{00}}{\tau_{D^0}} - \frac{2}{3} \frac{\mathcal{B}_{+0}}{\tau_{D^+}} \right)} + \frac{A_{CP}^{\text{dir}}(D^0 \rightarrow \pi^0\pi^0)}{1 + \frac{\tau_{D^0}}{\mathcal{B}_{00}} \left(\frac{\mathcal{B}_{+-}}{\tau_{D^0}} - \frac{2}{3} \frac{\mathcal{B}_{+0}}{\tau_{D^+}} \right)} + \frac{A_{CP}^{\text{dir}}(D^+ \rightarrow \pi^+\pi^0)}{1 - \frac{3}{2} \frac{\tau_{D^+}}{\mathcal{B}_{+0}} \left(\frac{\mathcal{B}_{00}}{\tau_{D^0}} + \frac{\mathcal{B}_{+-}}{\tau_{D^0}} \right)}$$

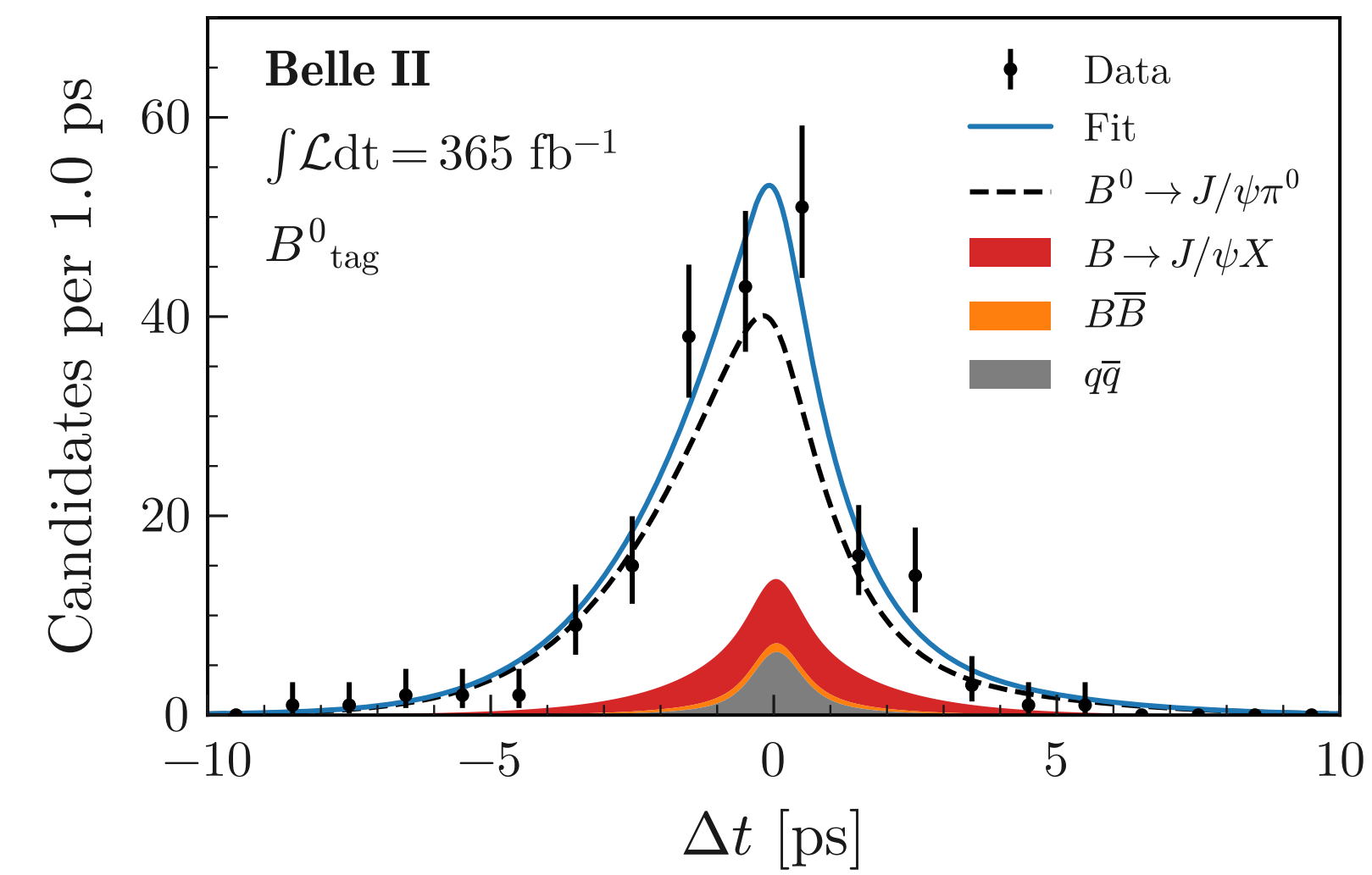
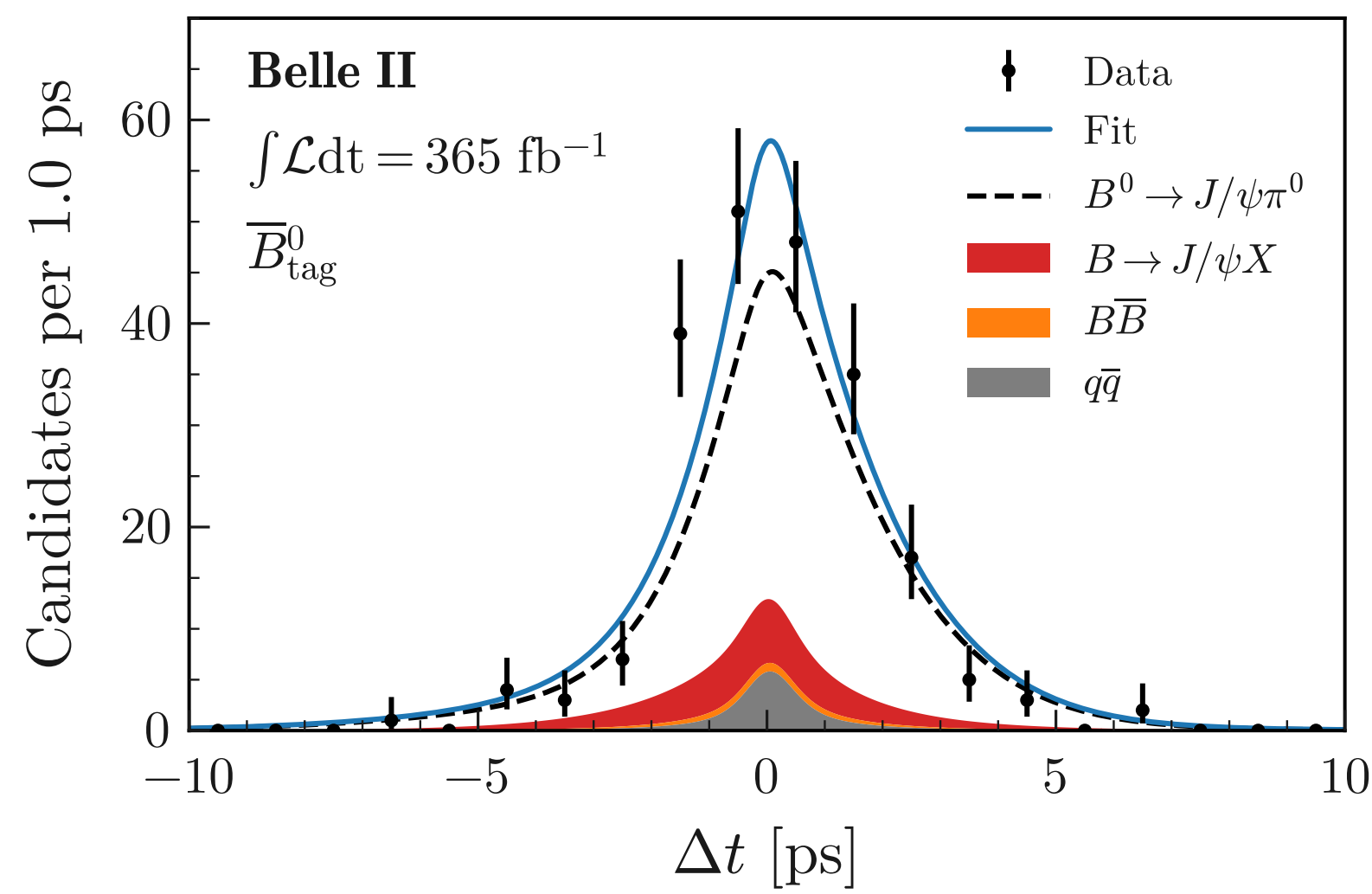
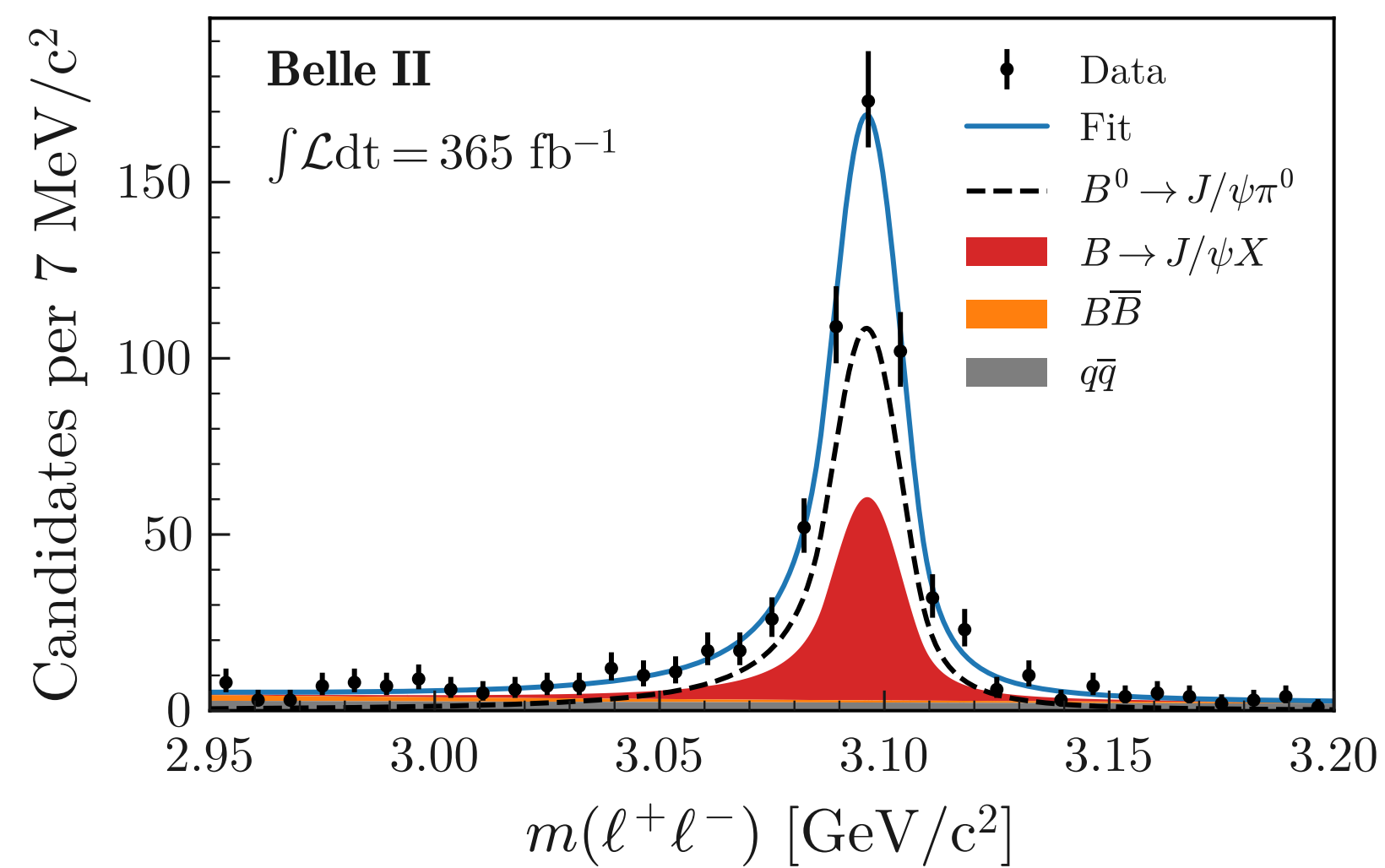
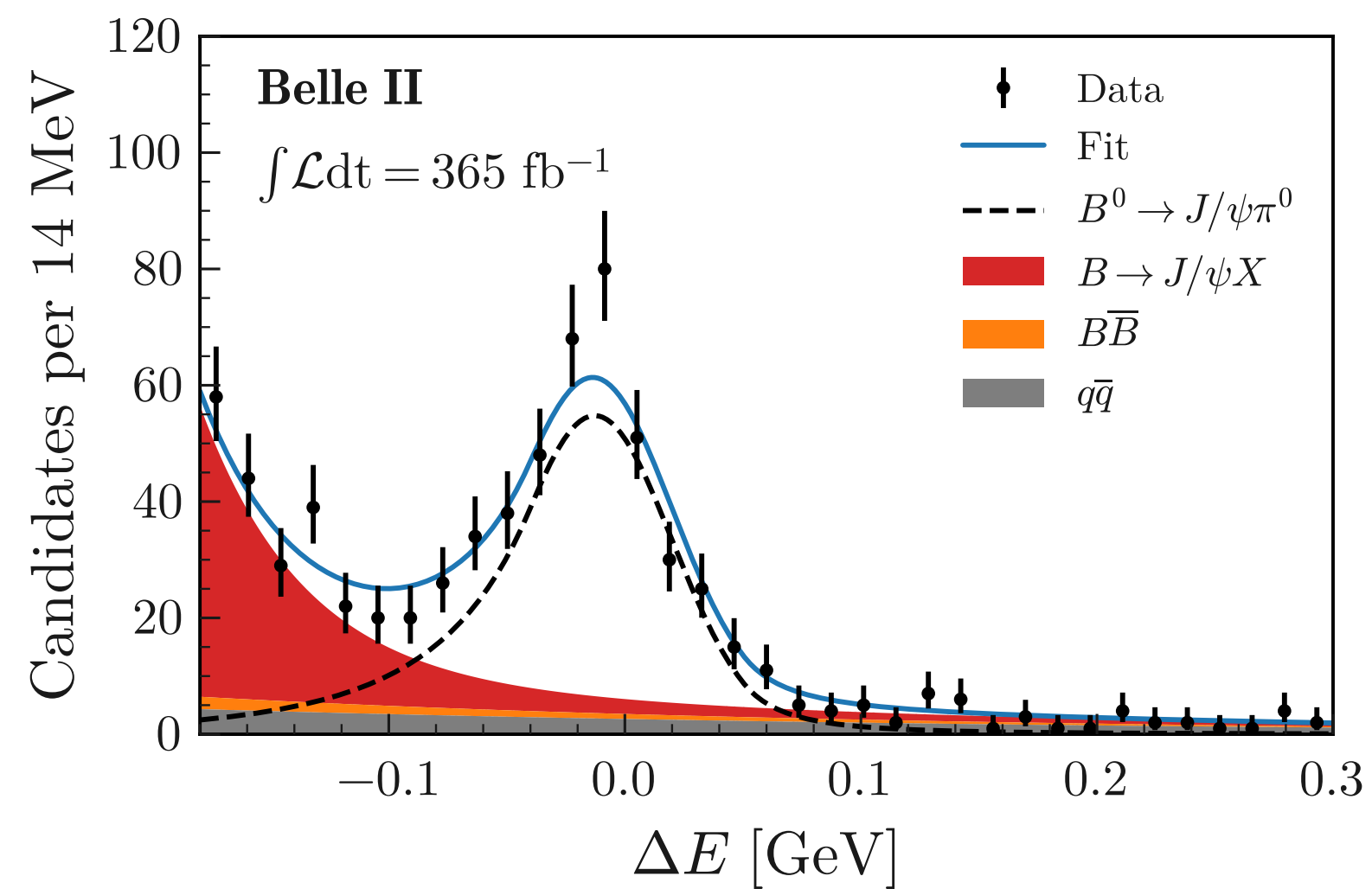


TABLE II. Relative systematic uncertainties on the branching fraction compared with the statistical uncertainties.

Source	Relative uncertainty on BF [%]
π^0 efficiency	3.7
Lepton ID	0.4
BDT	0.3
Tracking efficiencies	0.5
External inputs	0.4
$N(B\bar{B})$	1.4
f^{+-}/f^{00}	1.5
Fixed parameters	0.9
Backgrounds composition	0.4
Multiple candidates	0.5
Total systematic uncertainty	4.5
Statistical uncertainty	6.0

 TABLE III. Systematic uncertainties on the CP asymmetries compared with the statistical uncertainties.

Source	C_{CP}	$-\eta_f S_{CP}$
Calibration with $B^0 \rightarrow D^{*-}\pi^+$	0.017	0.023
Signal extraction fit	0.003	0.017
Backgrounds composition	0.005	0.009
Backgrounds Δt shapes	<0.001	0.001
Fit bias	0.010	0.010
Multiple candidates	<0.001	0.002
Tracking detector misalignment	0.002	0.002
Tag-side interference	0.027	0.001
τ_{B^0} and Δm_d	<0.001	<0.001
Total systematic uncertainty	0.034	0.032
Statistical uncertainty	0.123	0.171

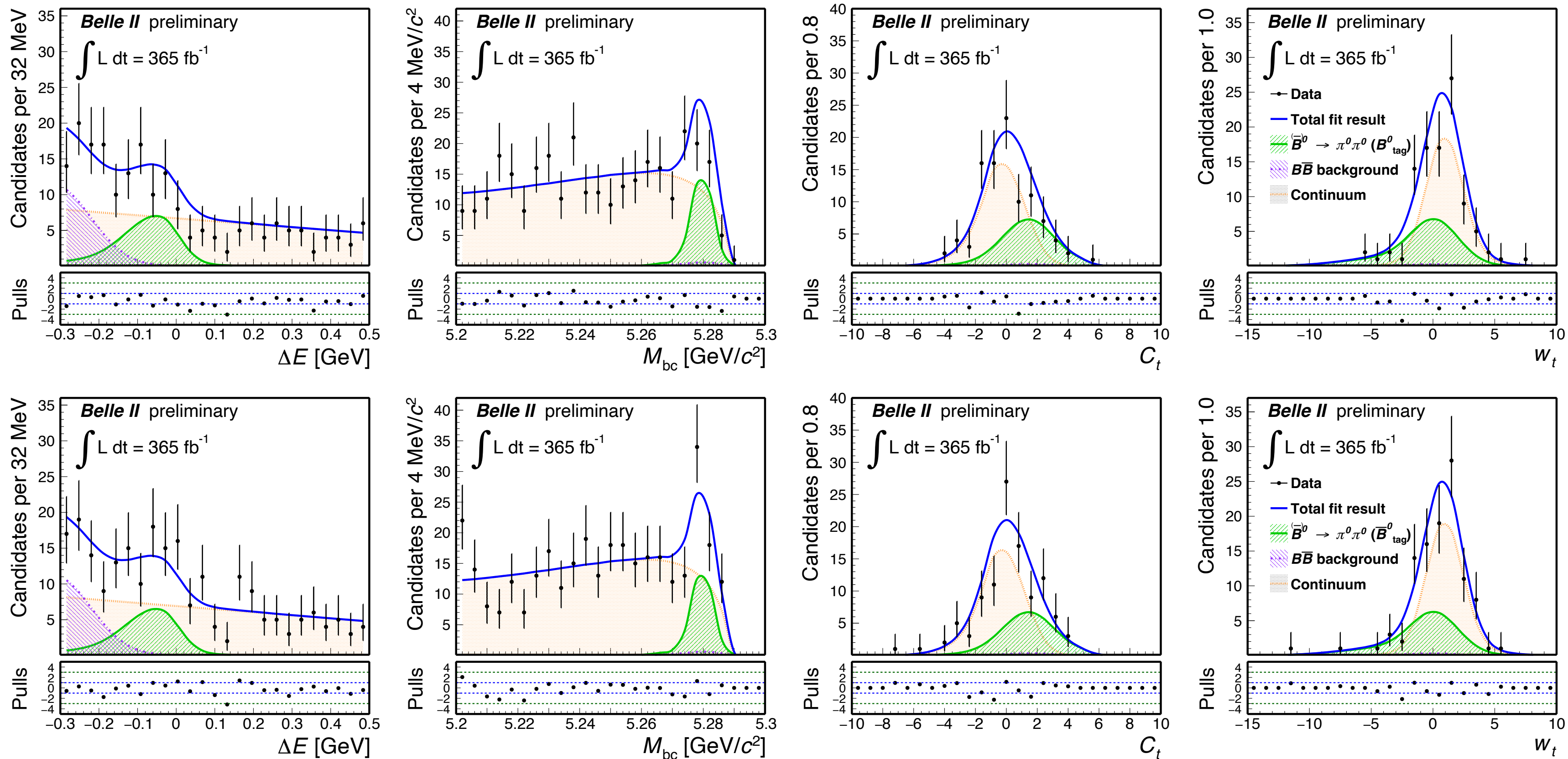
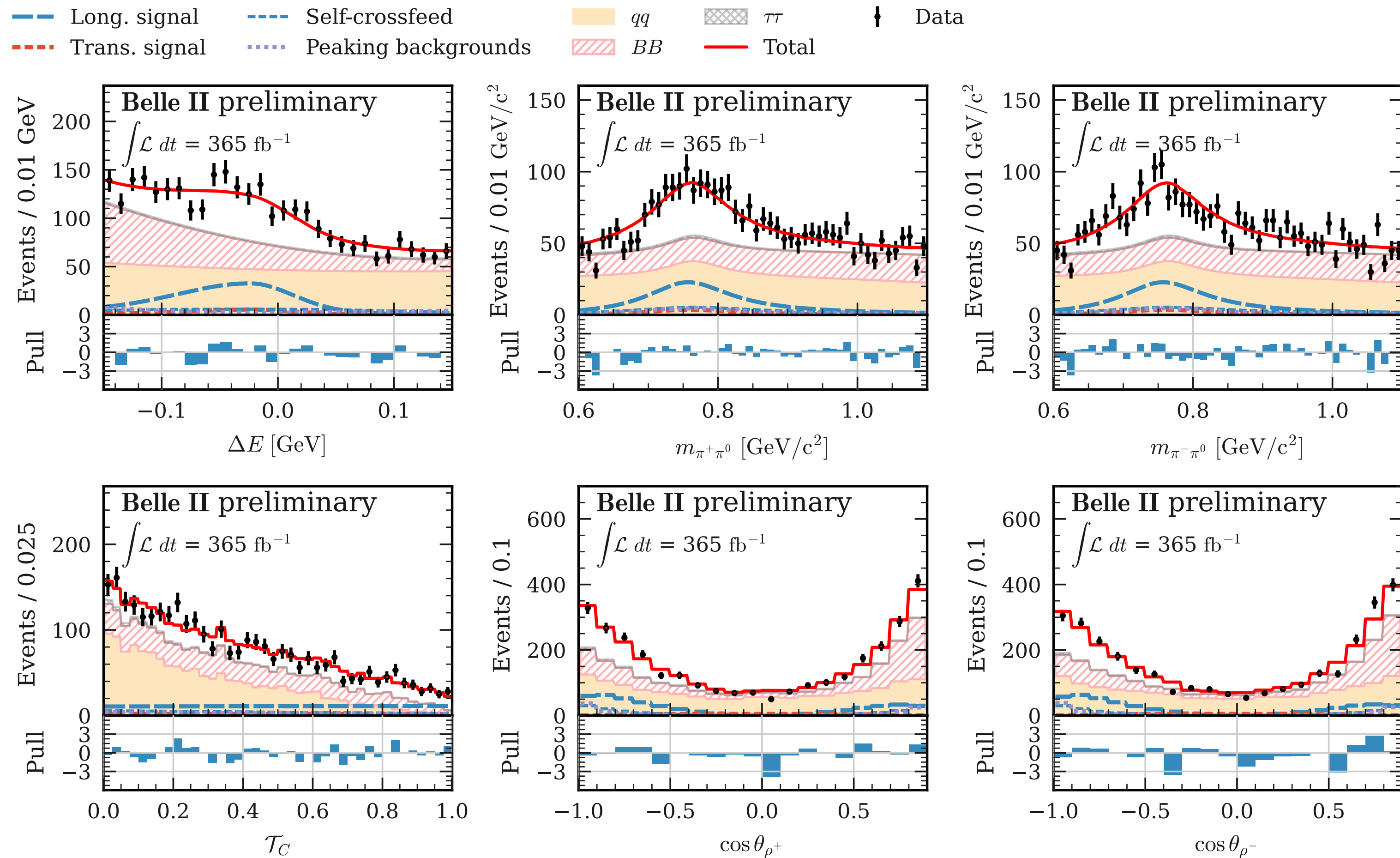
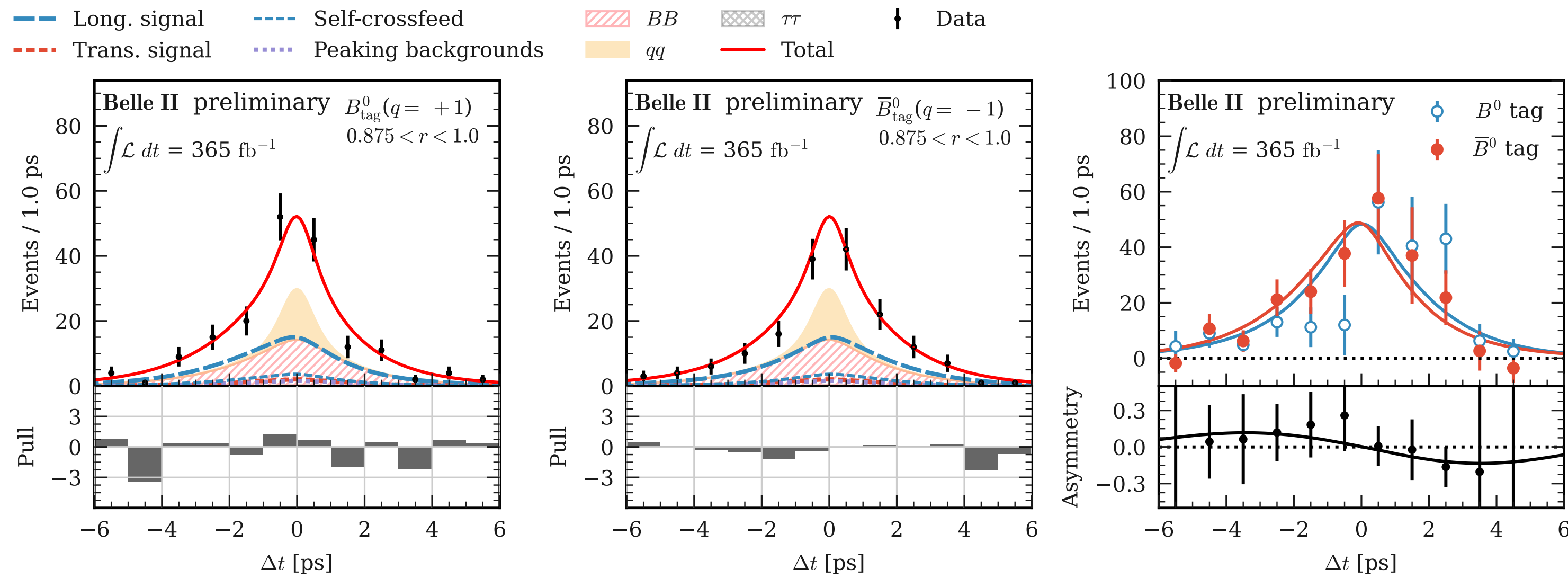


TABLE I. Fractional systematic uncertainties on the branching fraction and absolute systematic uncertainties on the CP asymmetry. Total systematic uncertainties, resulting from their sums in quadrature, are also given and compared with statistical uncertainties.

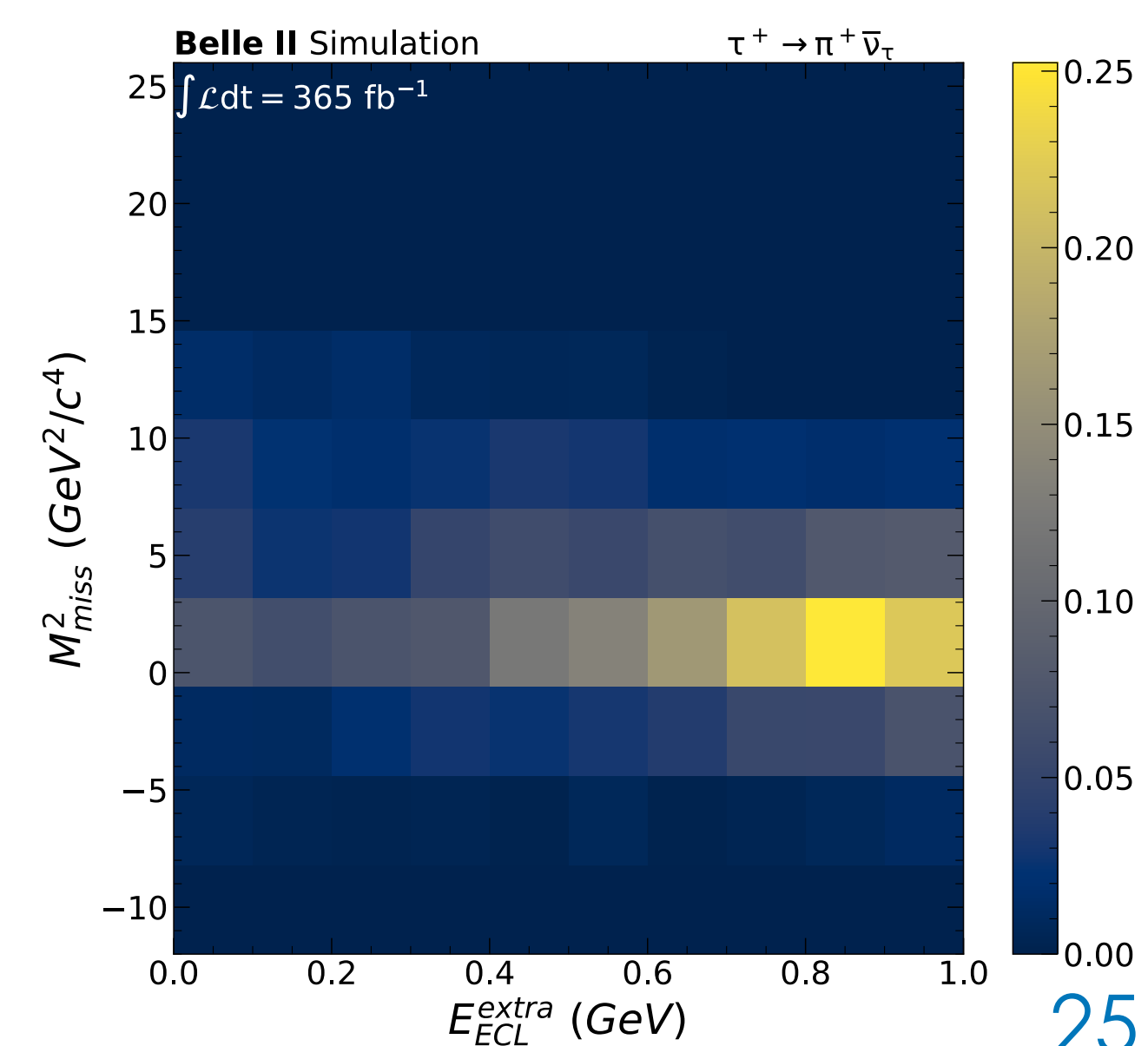
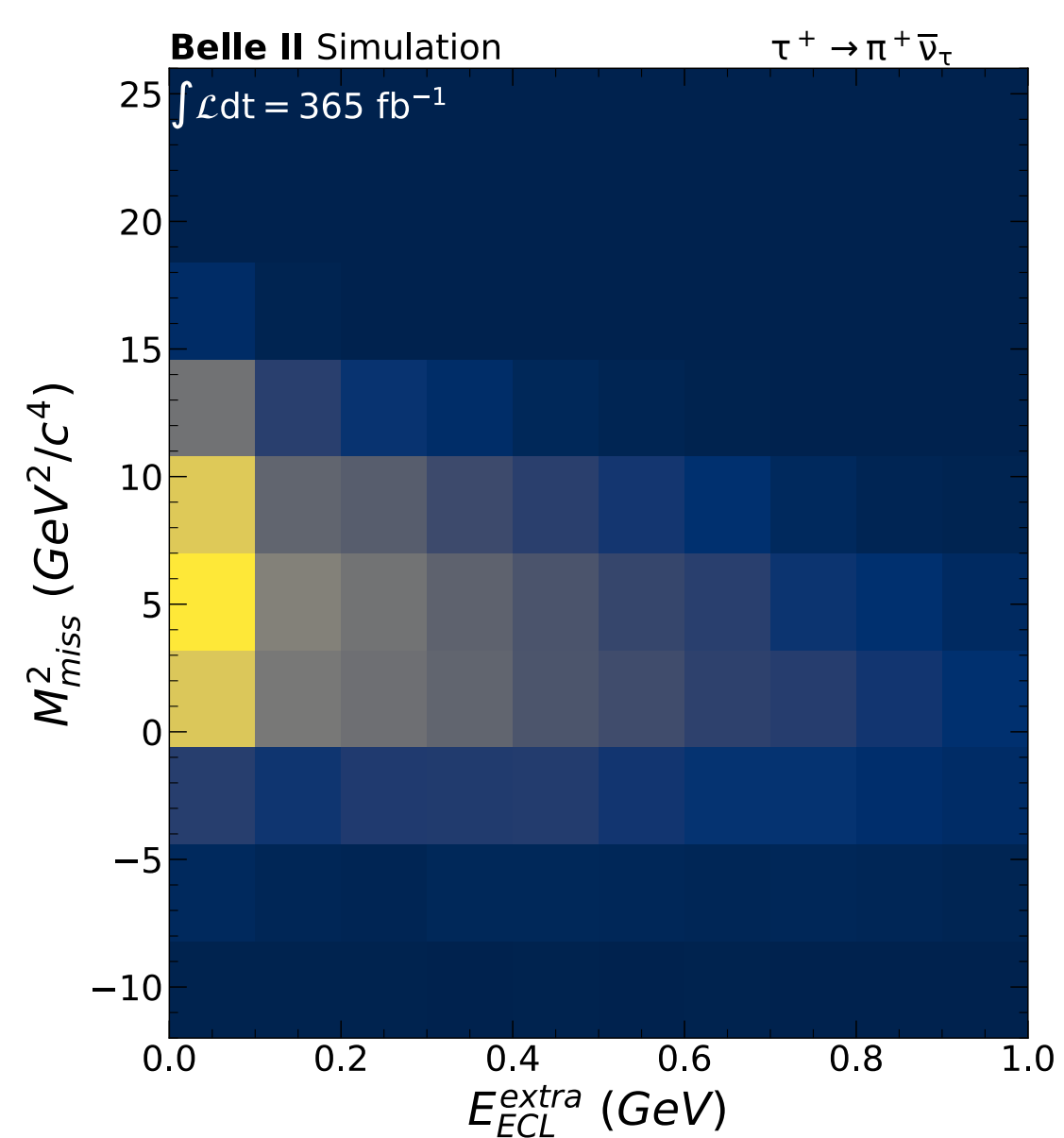
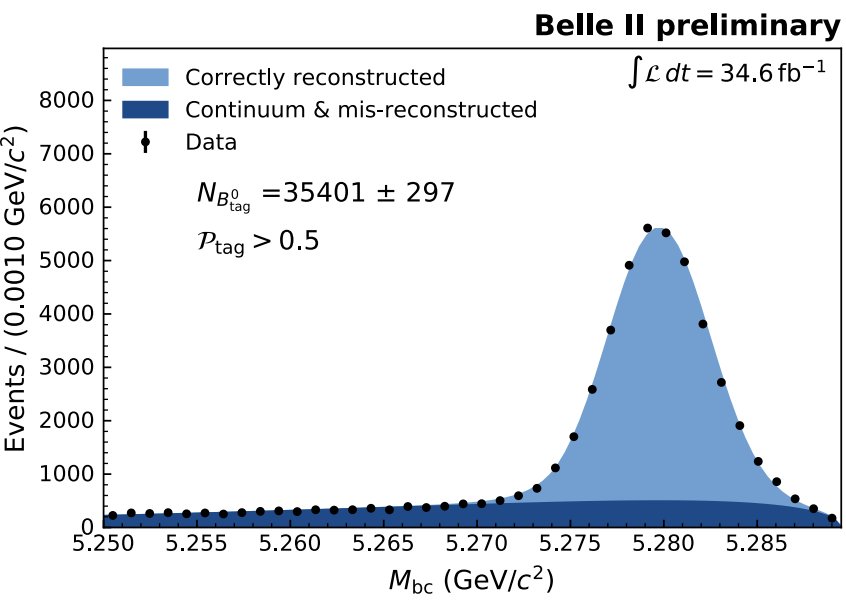
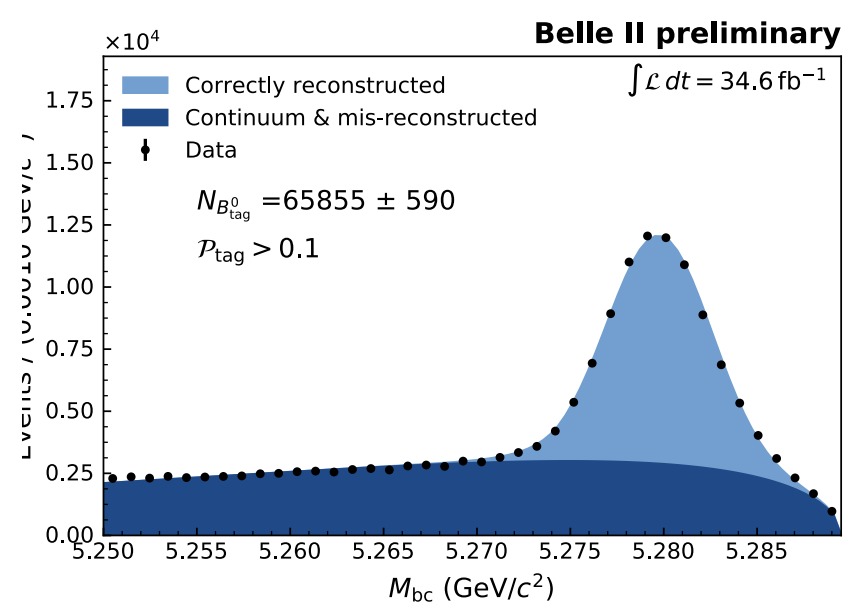
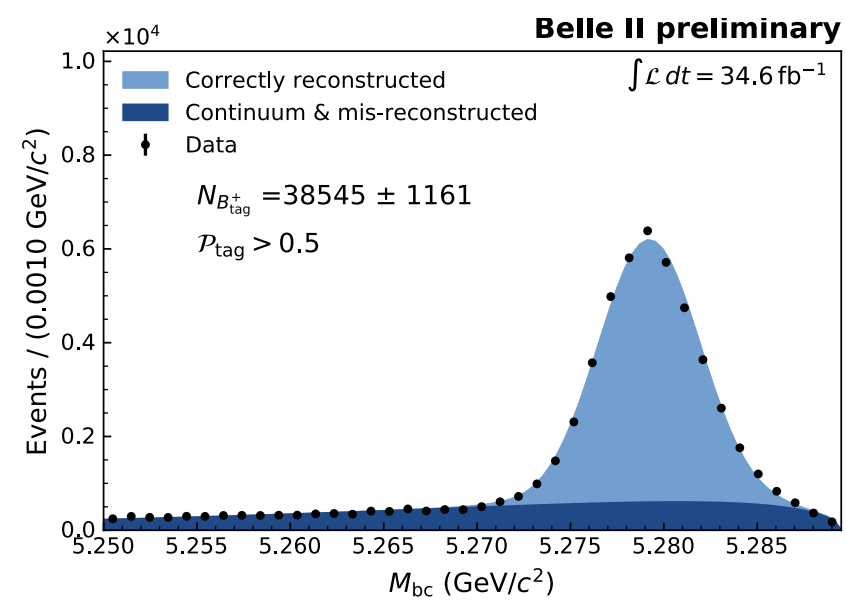
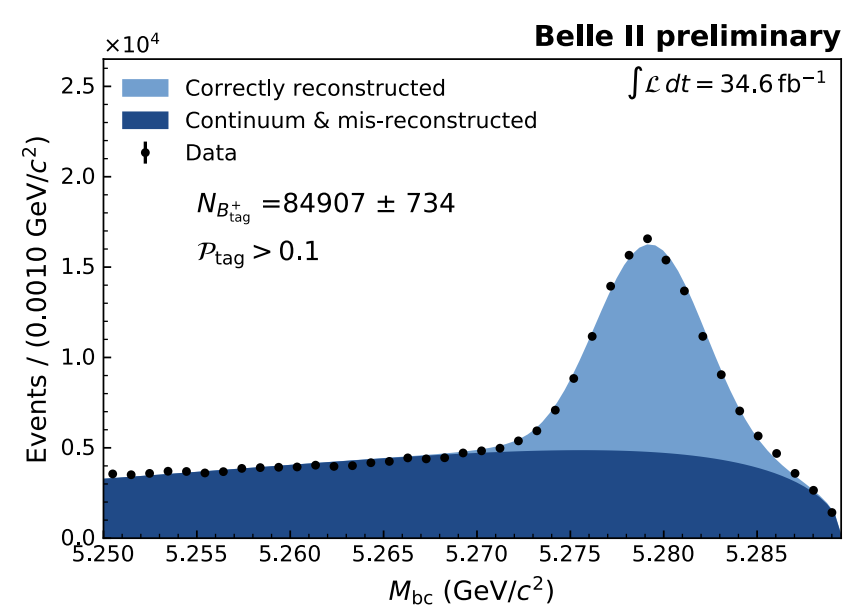
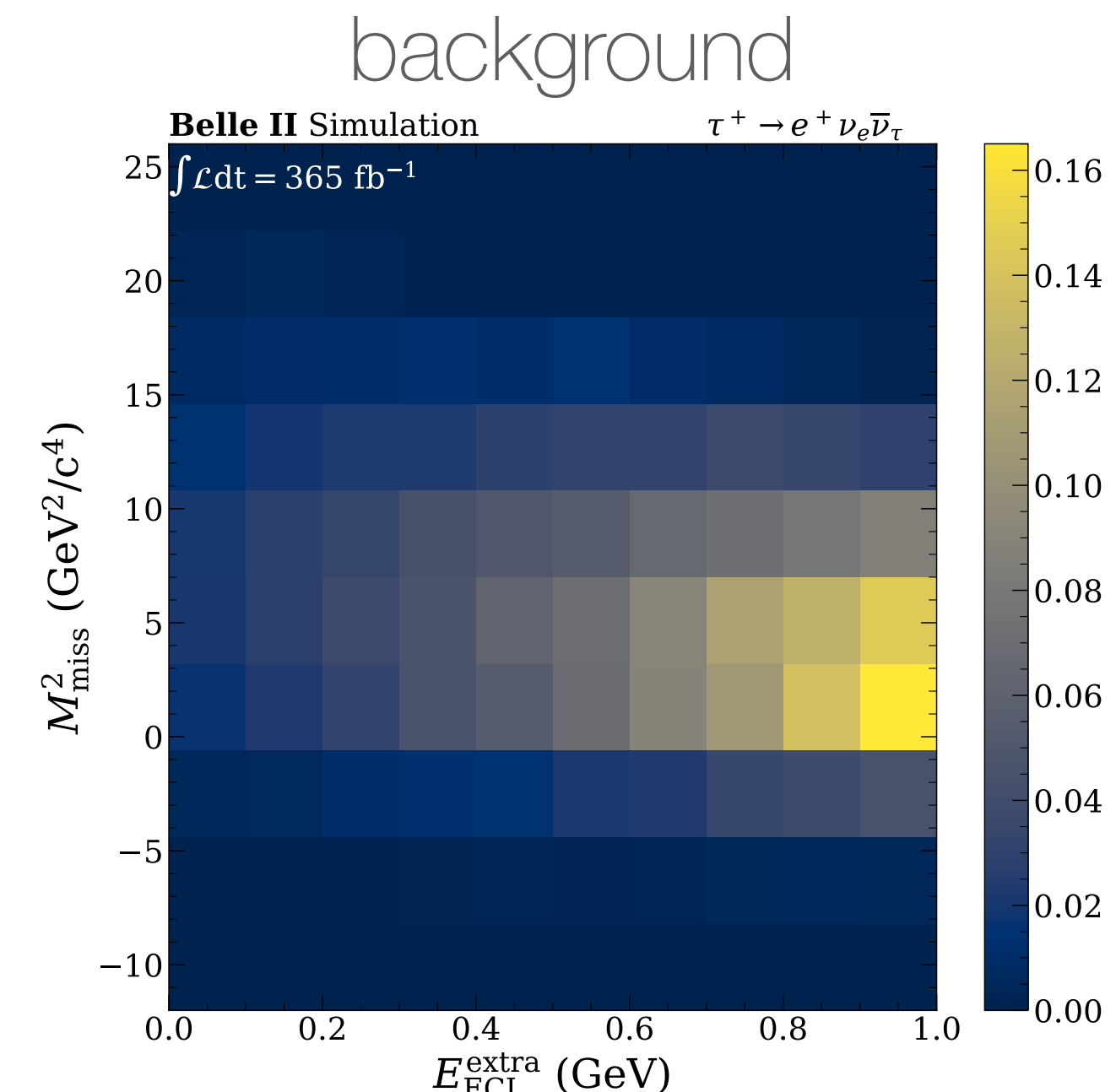
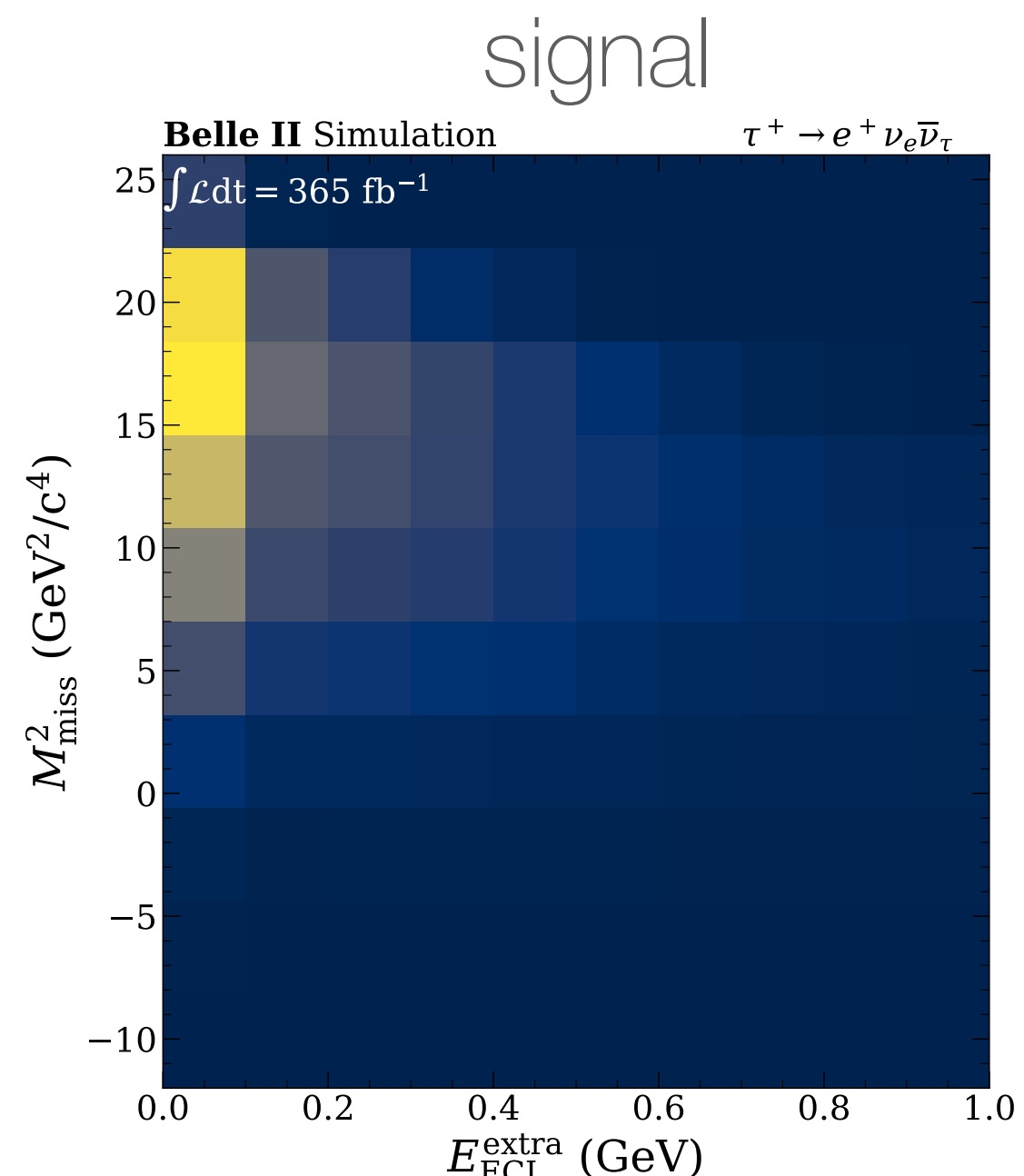
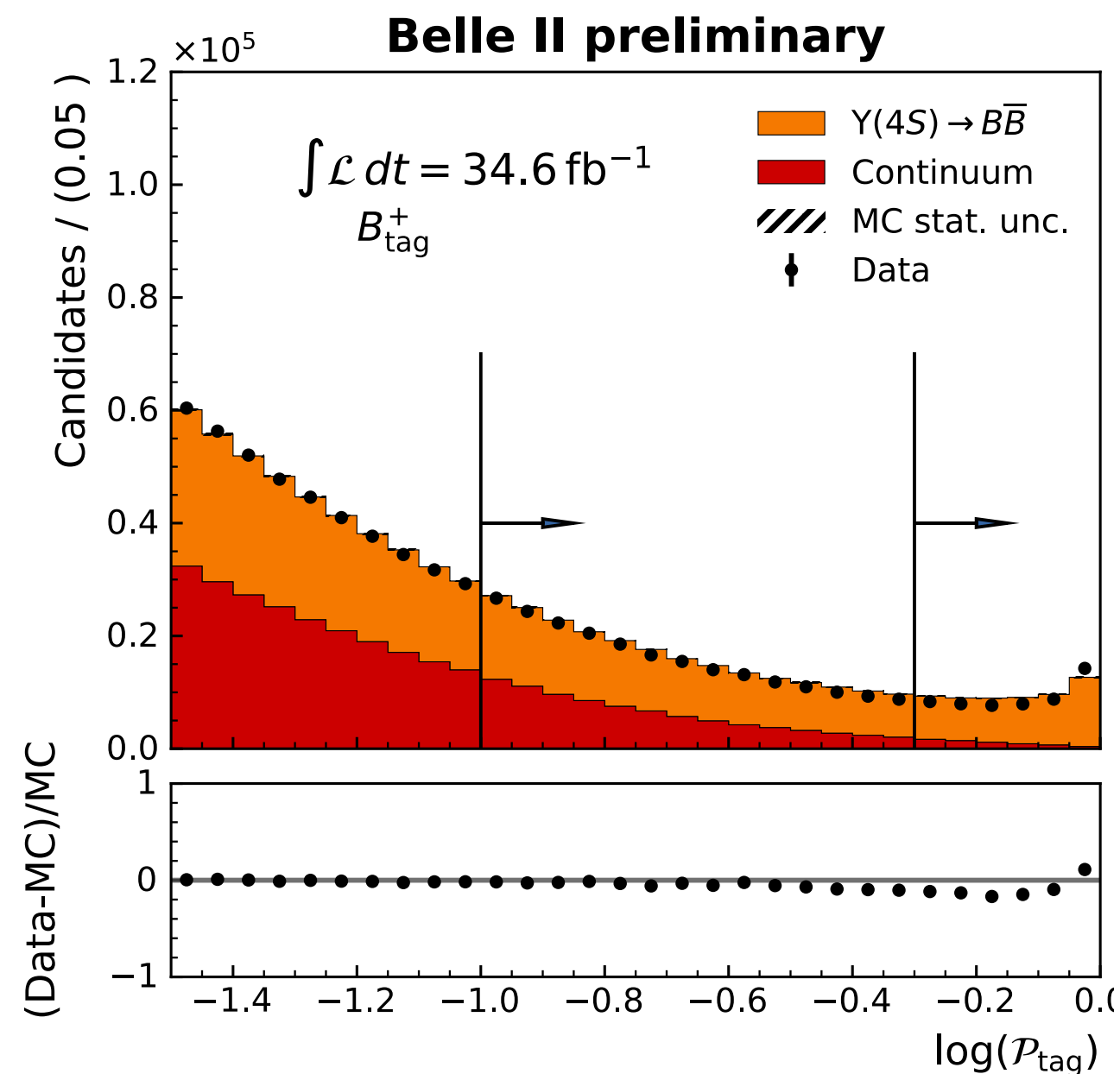
Source	\mathcal{B}	\mathcal{A}_{CP}
π^0 efficiency	8.1%	n/a
Continuum-suppression efficiency	1.9%	n/a
$B\bar{B}$ -background model	1.7%	0.01
Signal model	1.2%	0.02
Continuum-background model	0.9%	0.03
$\Upsilon(4S)$ branching fractions ($1 + f^{+-}/f^{00}$)	1.5 %	n/a
Sample size $N_{B\bar{B}}$	1.5%	n/a
$B^0\bar{B}^0$ -oscillation probability	n/a	< 0.01
Wrong-tag probability calibration	n/a	0.01
Total systematic uncertainty	8.9%	0.04
Statistical uncertainty	15.9%	0.30

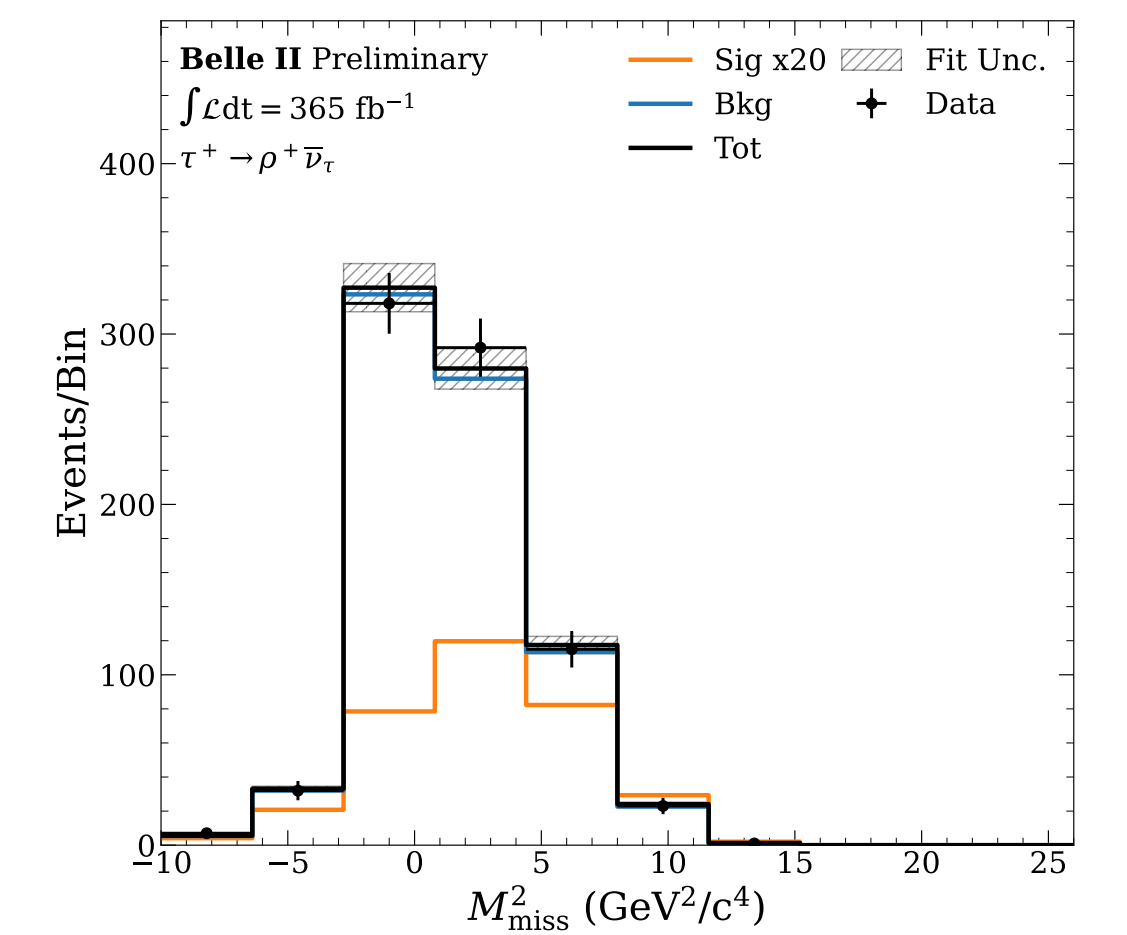
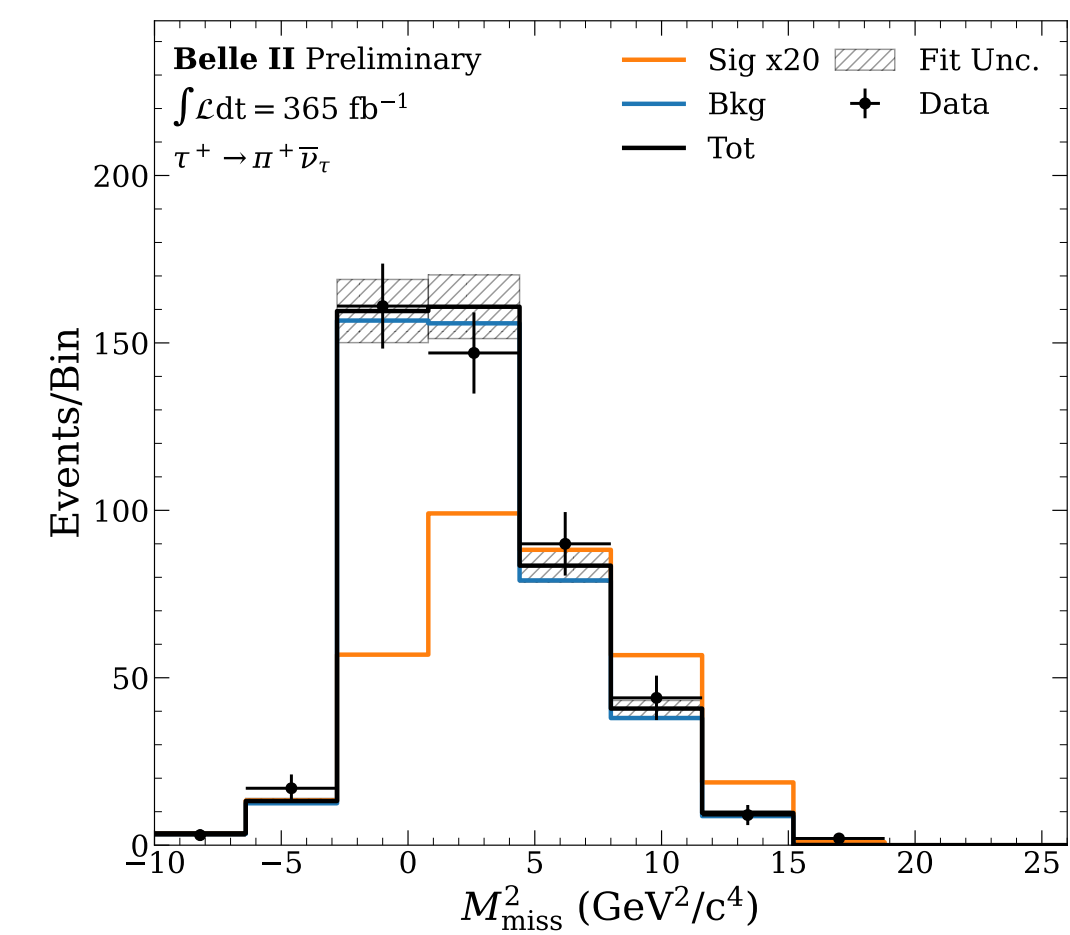
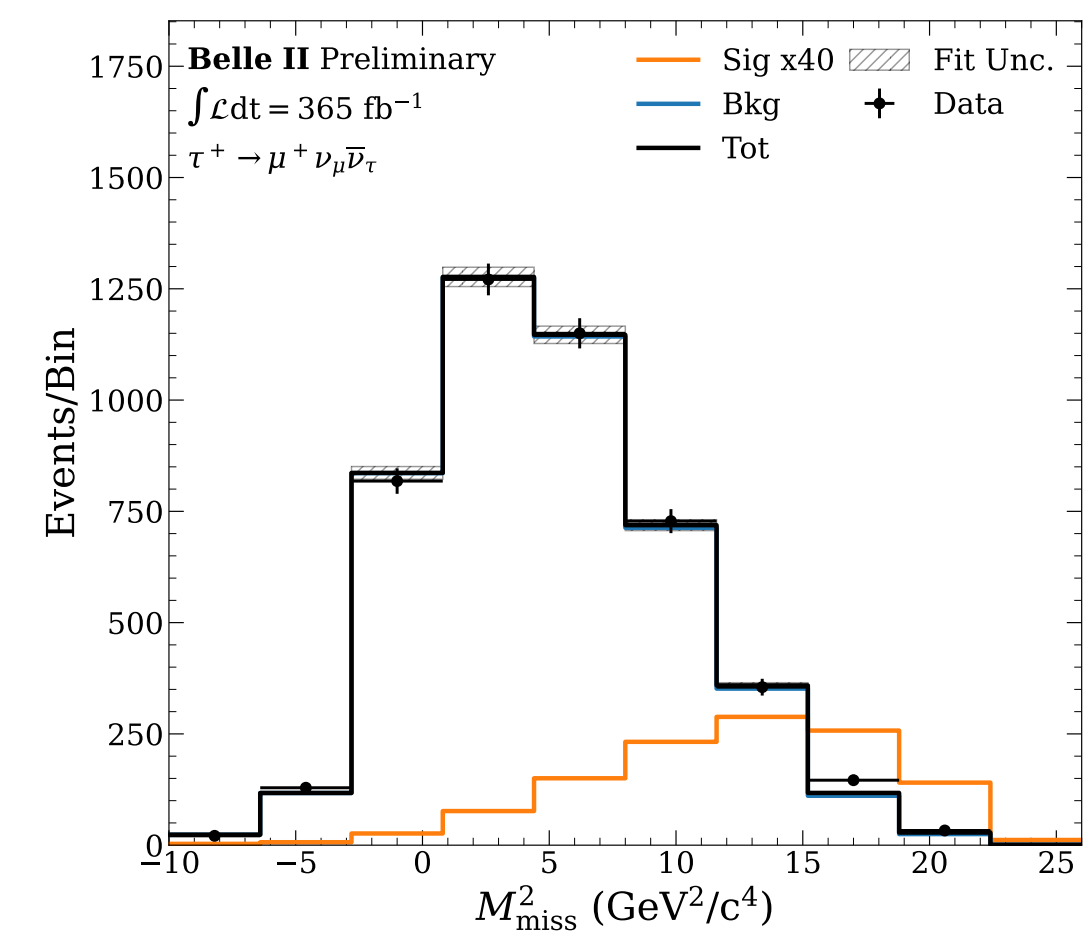
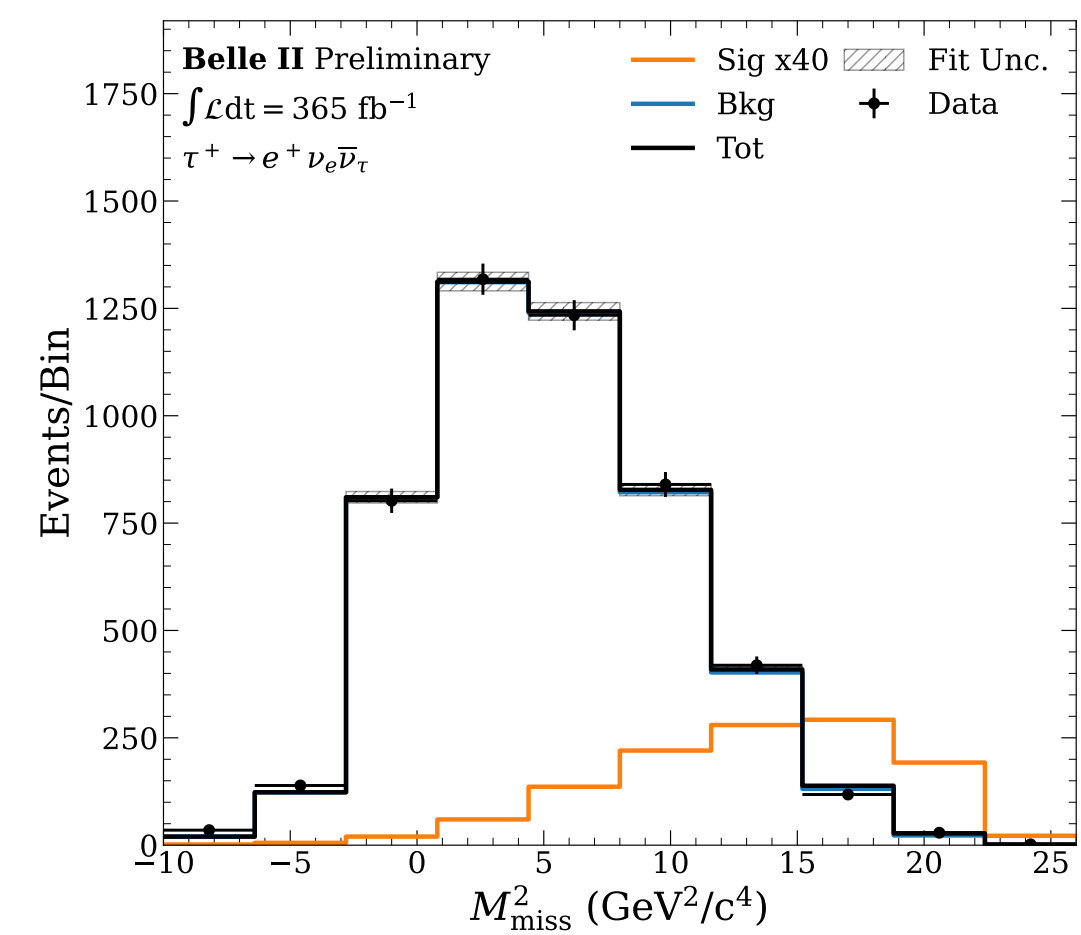
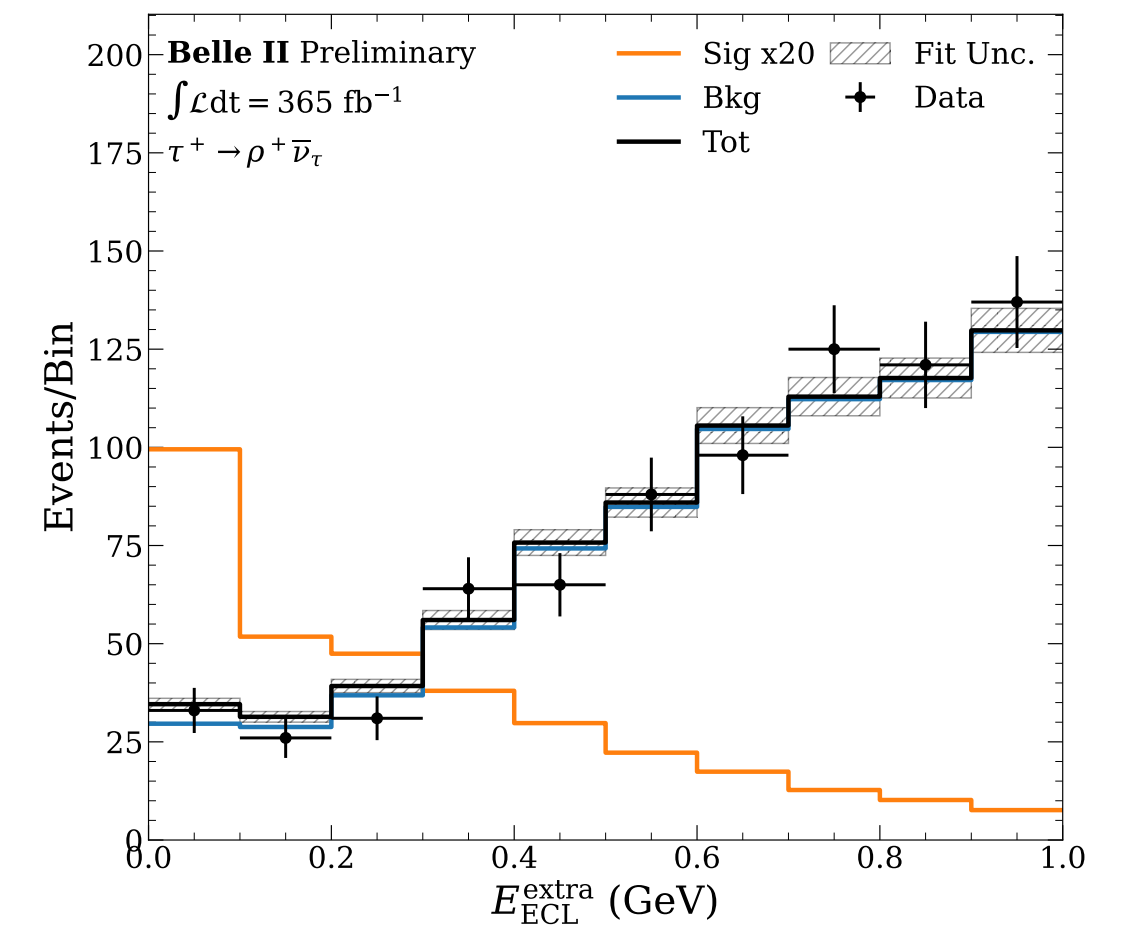
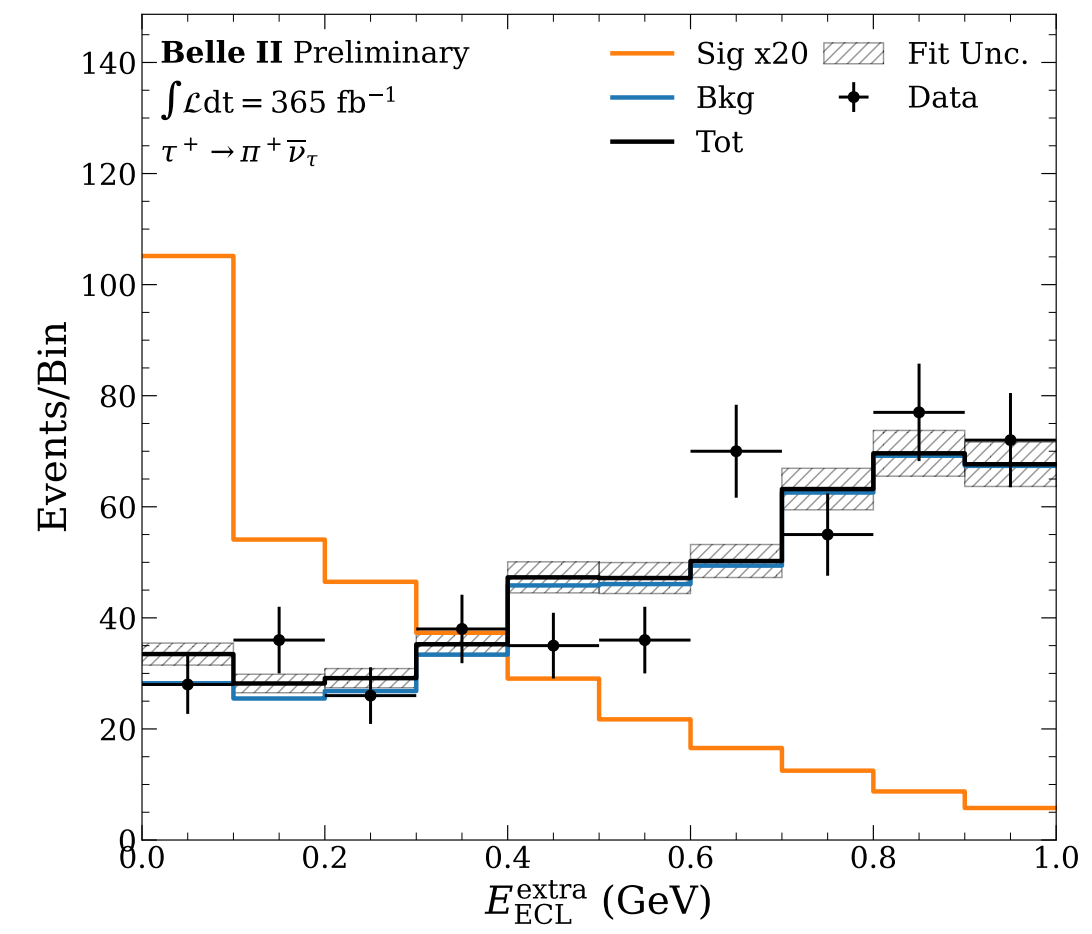
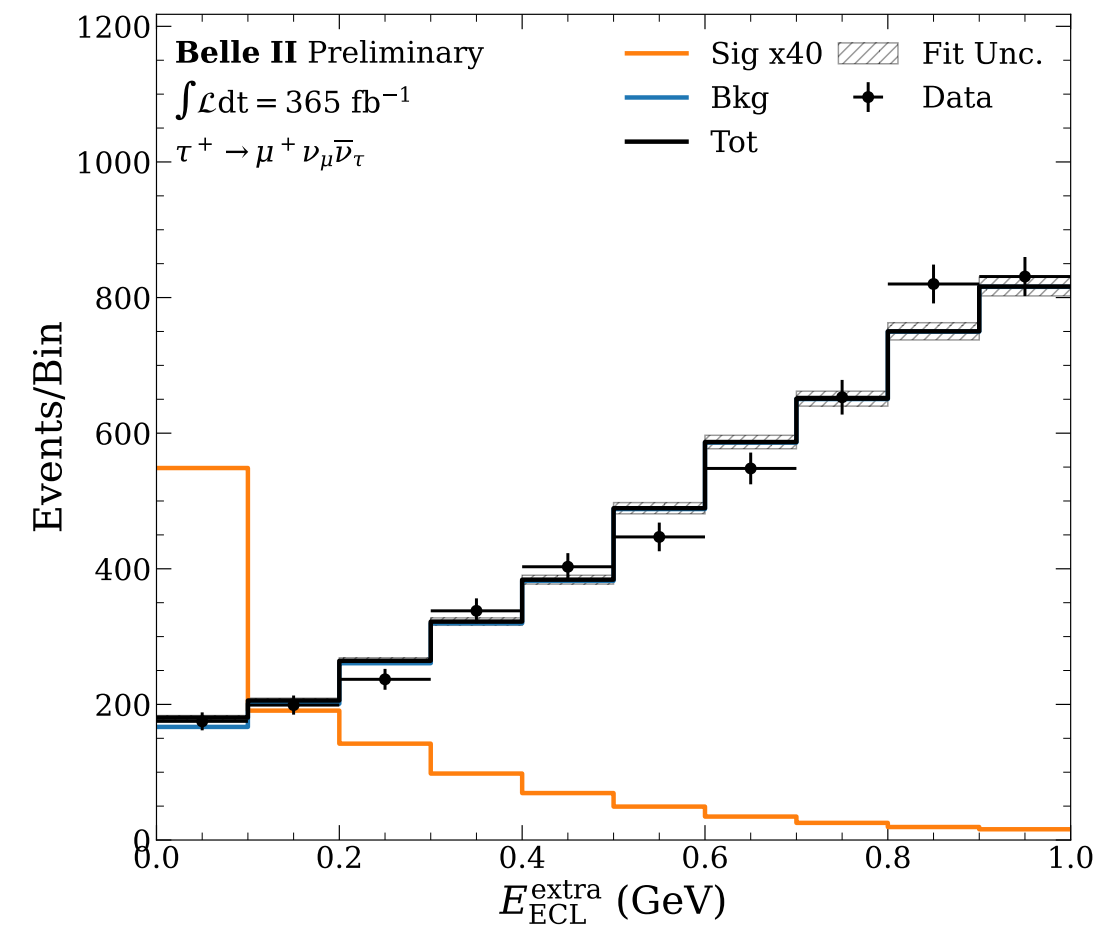
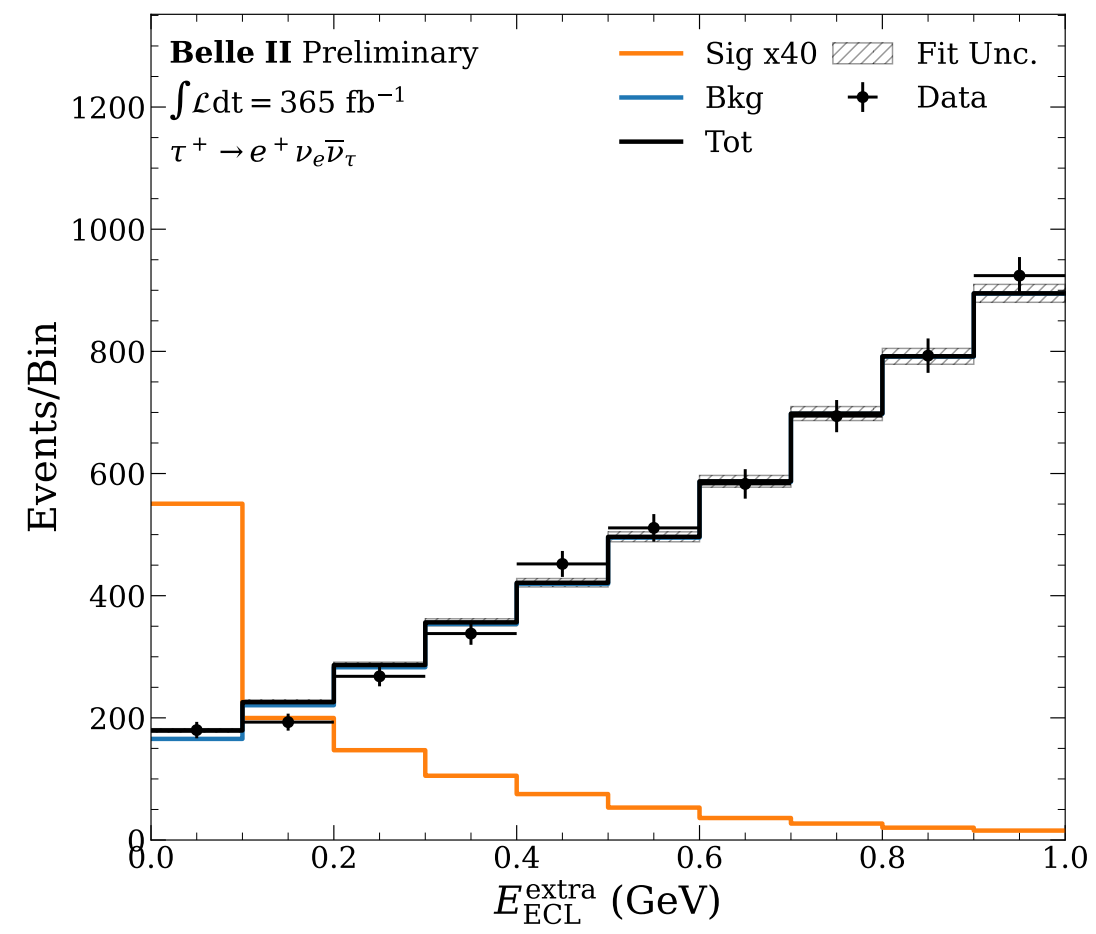

 Table VI. Systematic uncertainties for \mathcal{B} and f_L . Relative uncertainties are shown for \mathcal{B} .

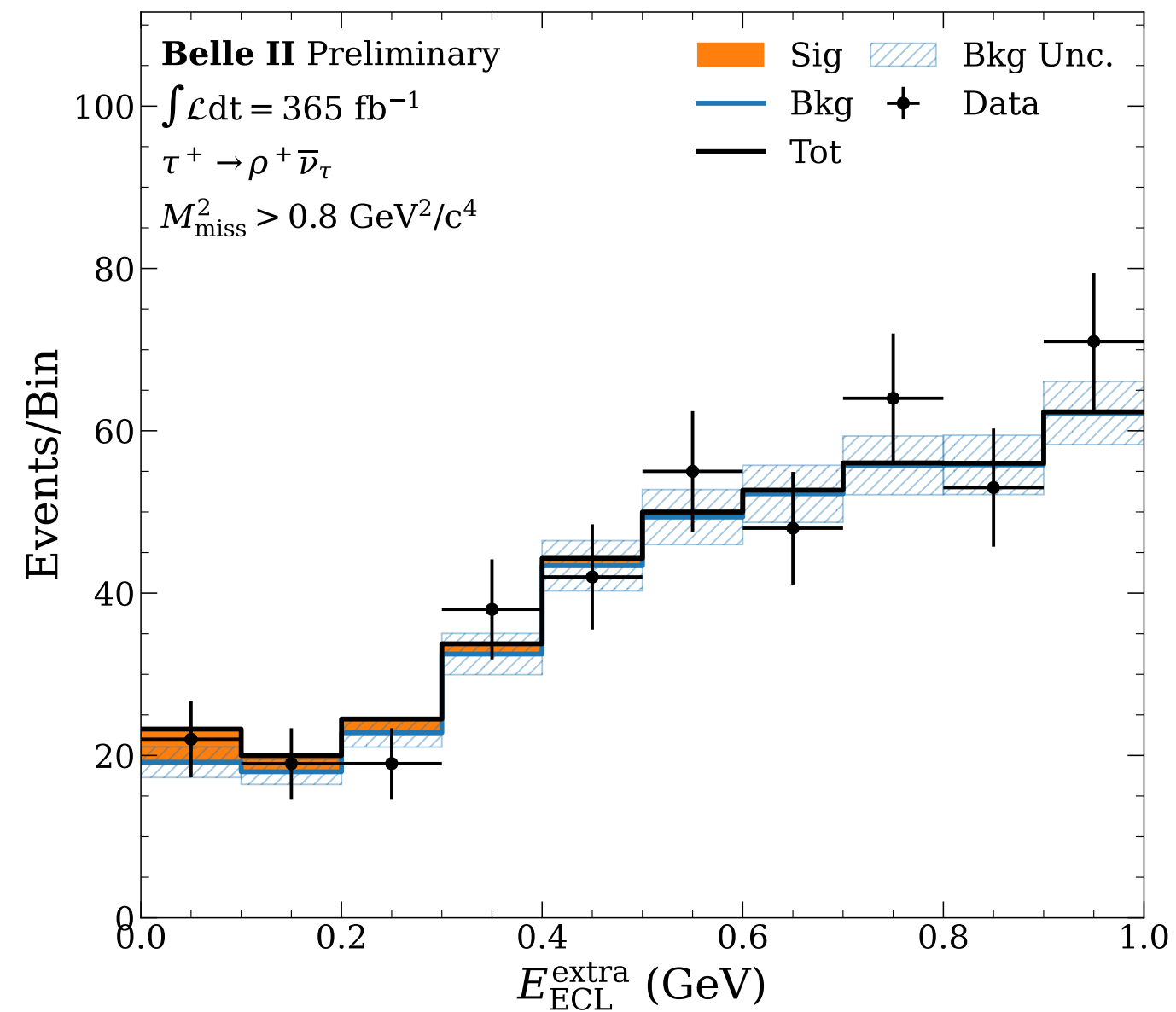
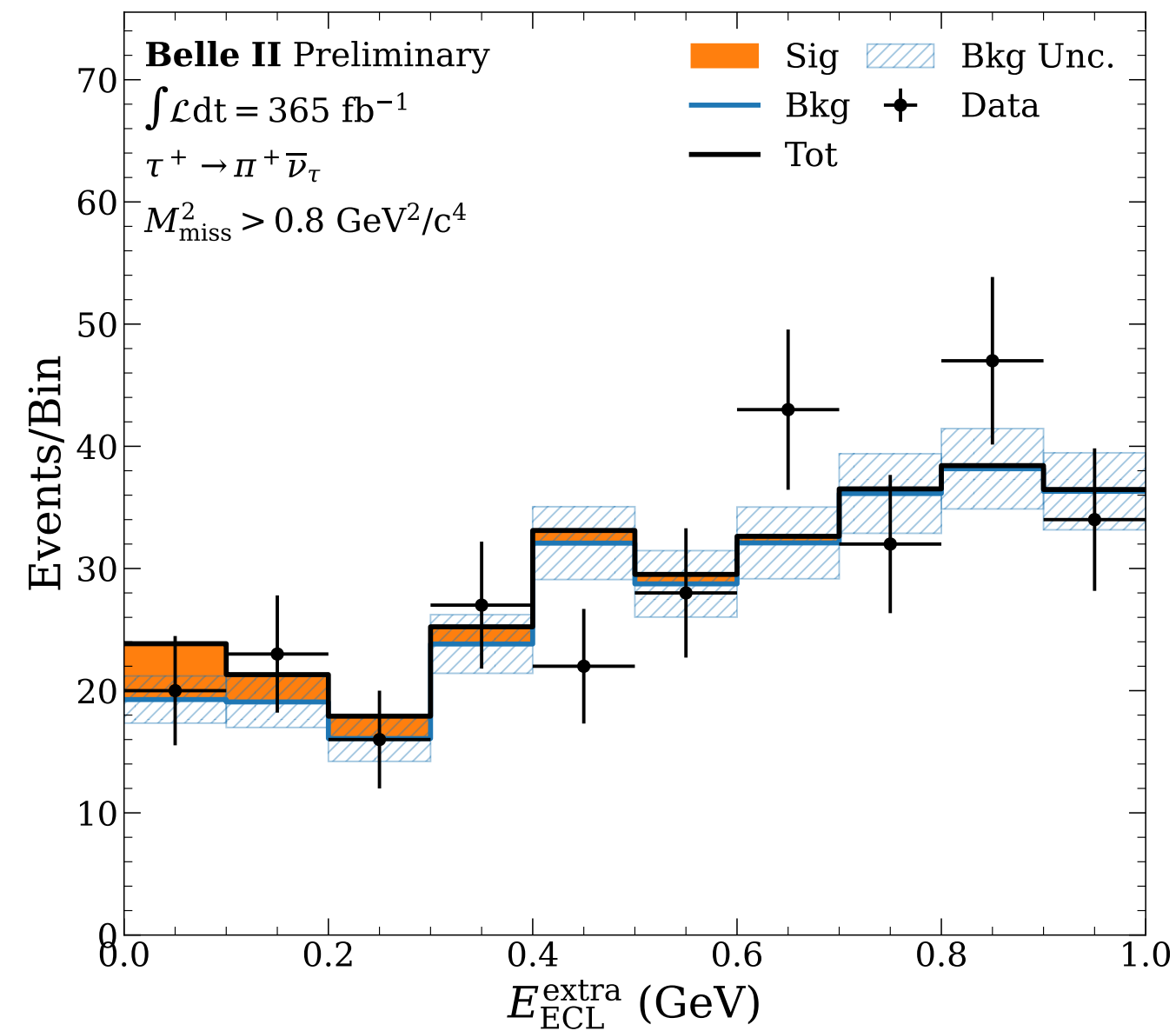
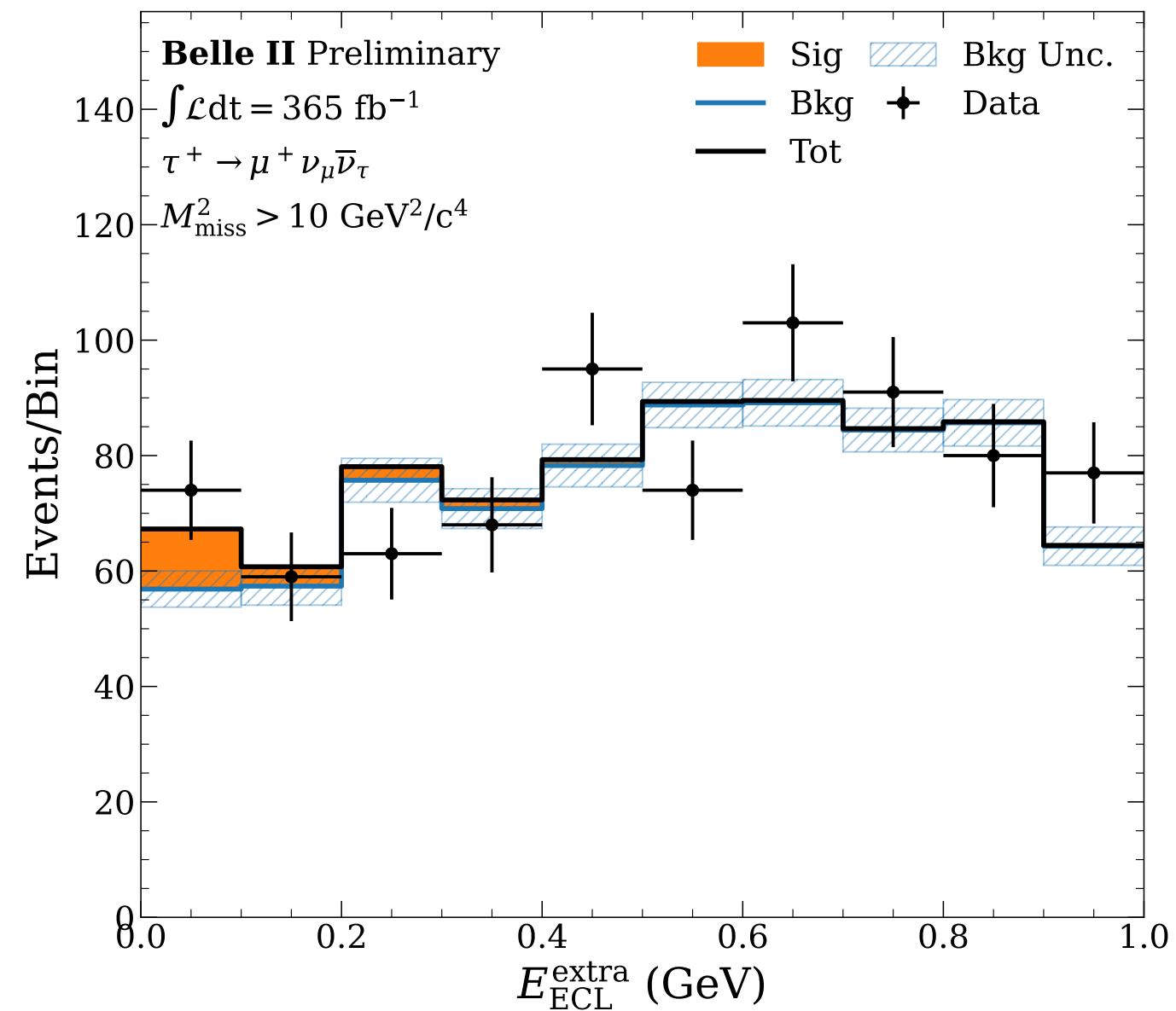
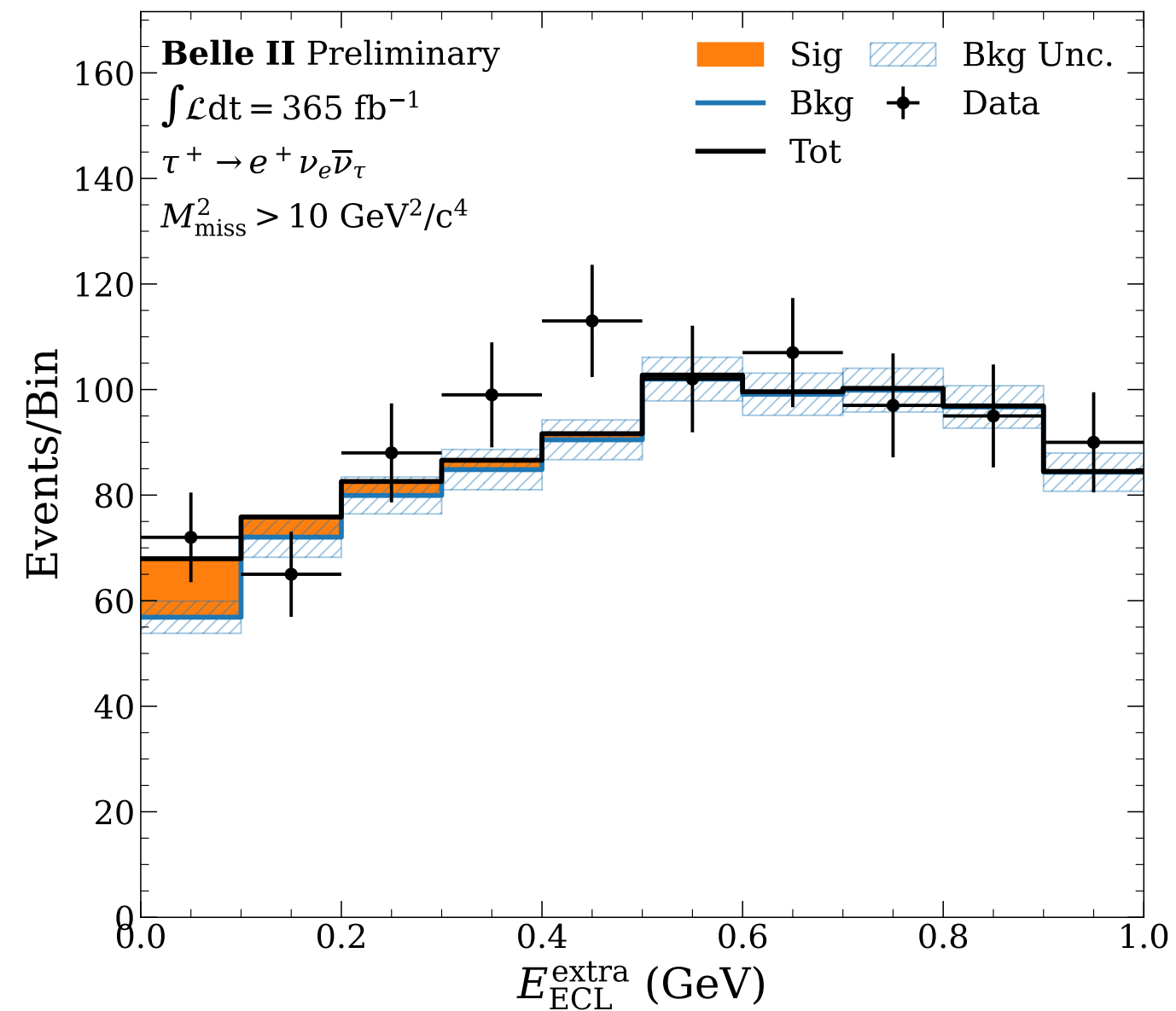
Source	\mathcal{B} [%]	$f_L [10^{-2}]$
Tracking	± 0.54	—
π^0 efficiency	± 7.67	—
PID	± 0.08	—
\mathcal{T}_C	± 2.87	—
MC sample size	± 0.24	± 0.2
Single candidate selection	± 0.55	± 0.3
SCF ratio	+2.97 -2.45	+0.2 -0.3
\mathcal{B} 's of peaking backgrounds	+0.94 -0.98	± 0.1
$\tau^+\tau^-$ background yield	+0.65 -0.69	± 0.0
Signal model	+1.14 -2.02	± 0.2
$q\bar{q}$ model	+0.49 -0.51	+0.1 -0.2
$B\bar{B}$ model	+1.00 -0.40	+0.3 -0.1
$\tau^+\tau^-$ model	+0.17 -0.26	+0.0 -0.1
Peaking model	+1.37 -1.01	+0.3 -0.5
Interference	± 1.20	± 0.5
Data-MC mis-modeling	+3.51 -1.70	+0.8 -0.3
Fit bias	± 1.03	± 1.2
f_{+-}/f_{00}	± 1.51	—
N_{BB}	± 1.45	—
Total systematic uncertainty	+10.07 -9.51	+1.7 -1.5
Statistical uncertainty	+7.93 -7.58	+2.4 -2.5


 Table VII. Systematic uncertainties for S and C .

Source	$S[10^{-2}]$	$C[10^{-2}]$
\mathcal{B} 's of peaking backgrounds	+0.6 -0.5	± 0.1
$\tau\tau$ background yield	± 0.9	+0.0 -0.1
Data-MC mis-modeling	+0.6 -1.1	+1.5 -0.6
Single candidate selection	± 1.3	± 1.9
SCF ratio	+0.5 -0.4	+0.7 -0.0
Signal model	+1.1 -1.4	+0.3 -0.4
$q\bar{q}$ model	+2.2 -1.0	± 0.2
$B\bar{B}$ model	± 0.9	+0.7 -0.5
$\tau^+\tau^-$ model	± 0.1	± 0.0
Peaking model	+0.8 -0.4	+0.2 -0.4
Fit bias	± 2.0	± 0.6
Interference	± 2.8	± 1.7
Resolution	+3.4 -4.4	+1.9 -1.4
Δt PDF for $q\bar{q}$ and $B\bar{B}$	+3.8 -1.8	+0.7 -0.1
Tag side interference	± 0.5	± 2.1
Wrong tag fraction	+0.2 -0.3	± 0.5
Background CP violation	+3.8 -3.6	+4.2 -3.7
CP violation in TP signal	+0.8 -0.2	+0.2 -0.4
Tracking detector misalignment	± 1.4	± 0.5
τ_{B^0} and Δm_d	+1.4 -1.6	± 0.3
Total systematic uncertainty	+8.2 -7.8	+6.1 -5.3
Statistical uncertainty	± 18.8	± 12.1





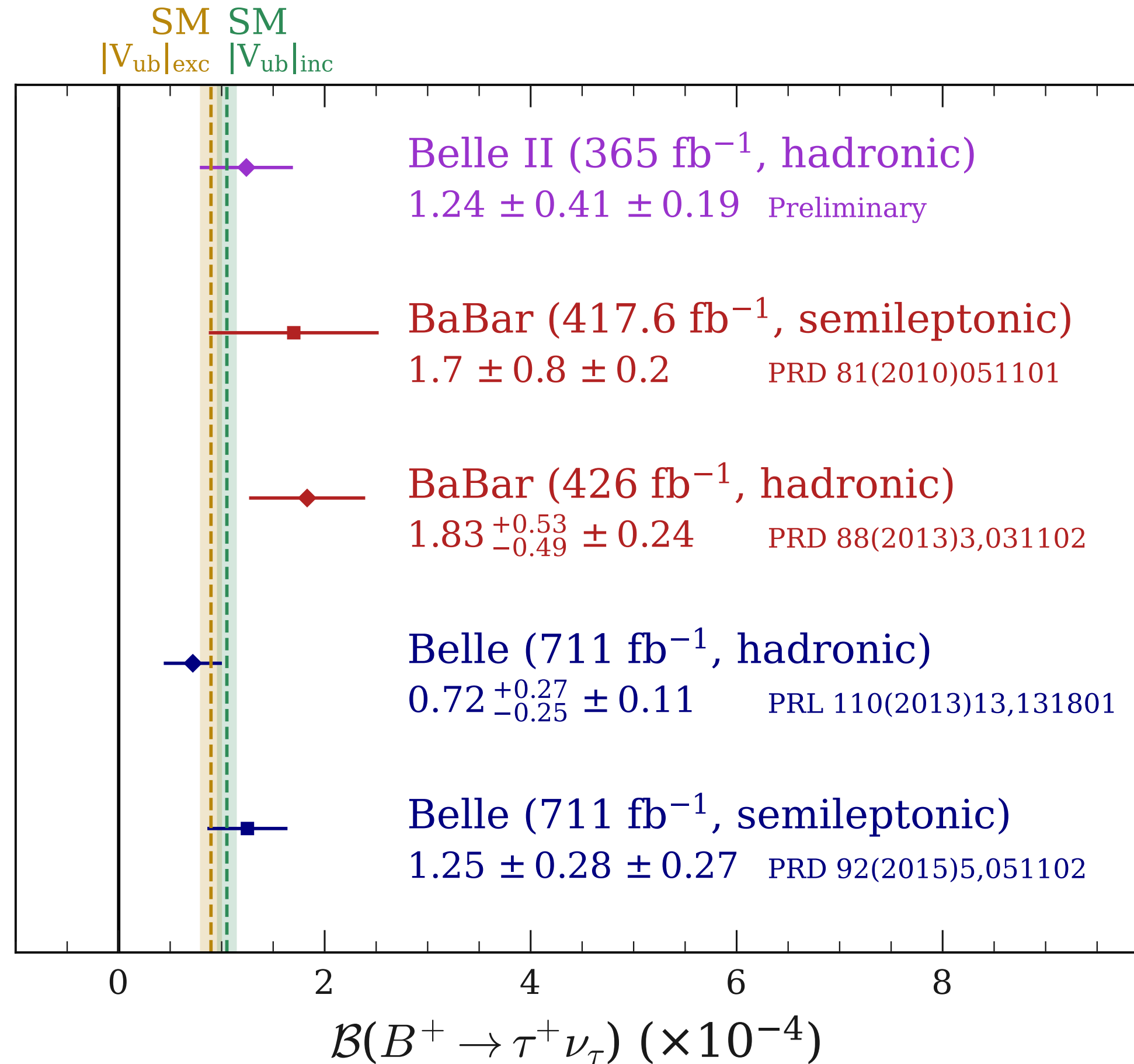


TAB. IV. Observed and expected values of the background yields in the fit. The expected values are estimated from a simulation corresponding to an integrated luminosity of 365 fb^{-1} .

Parameter	Observed value	Expected value
n_{b,e^+}	4907 ± 71	4846 ± 24
n_{b,μ^+}	4620 ± 69	4493 ± 24
n_{b,π^+}	454 ± 22	461 ± 9
n_{b,ρ^+}	772 ± 28	811 ± 11

TAB. V. Observed values of the signal yields and branching fractions, obtained from single fits for each τ^+ decay mode and the simultaneous fit.

Decay mode	n_s	$\mathcal{B}(10^{-4})$
Simultaneous	94 ± 31	1.24 ± 0.41
$e^+ \nu_e \bar{\nu}_\tau$	13 ± 16	0.51 ± 0.63
$\mu^+ \nu_\mu \bar{\nu}_\tau$	40 ± 20	1.67 ± 0.83
$\pi^+ \bar{\nu}_\tau$	31 ± 13	2.28 ± 0.93
$\rho^+ \bar{\nu}_\tau$	6 ± 25	0.42 ± 1.82



TAB. VI. Summary of systematic uncertainties (syst.) on the fitted branching fraction presented as relative uncertainties. The effect of each source is evaluated in the simultaneous fit of the four signal modes. The last three sources do not affect the signal yields.

Source	Syst.
Simulation statistics	13.3%
Fit variables PDF corrections	5.5%
Decays branching fractions in MC	4.1%
Tag B^- reconstruction efficiency	2.2%
Continuum reweighting	1.9%
π^0 reconstruction efficiency	0.9%
Continuum normalization	0.7%
Particle identification	0.6%
Number of produced $\Upsilon(4S)$	1.5%
Fraction of $B^+ B^-$ pairs	2.1%
Tracking efficiency	0.2%
Total	15.5%

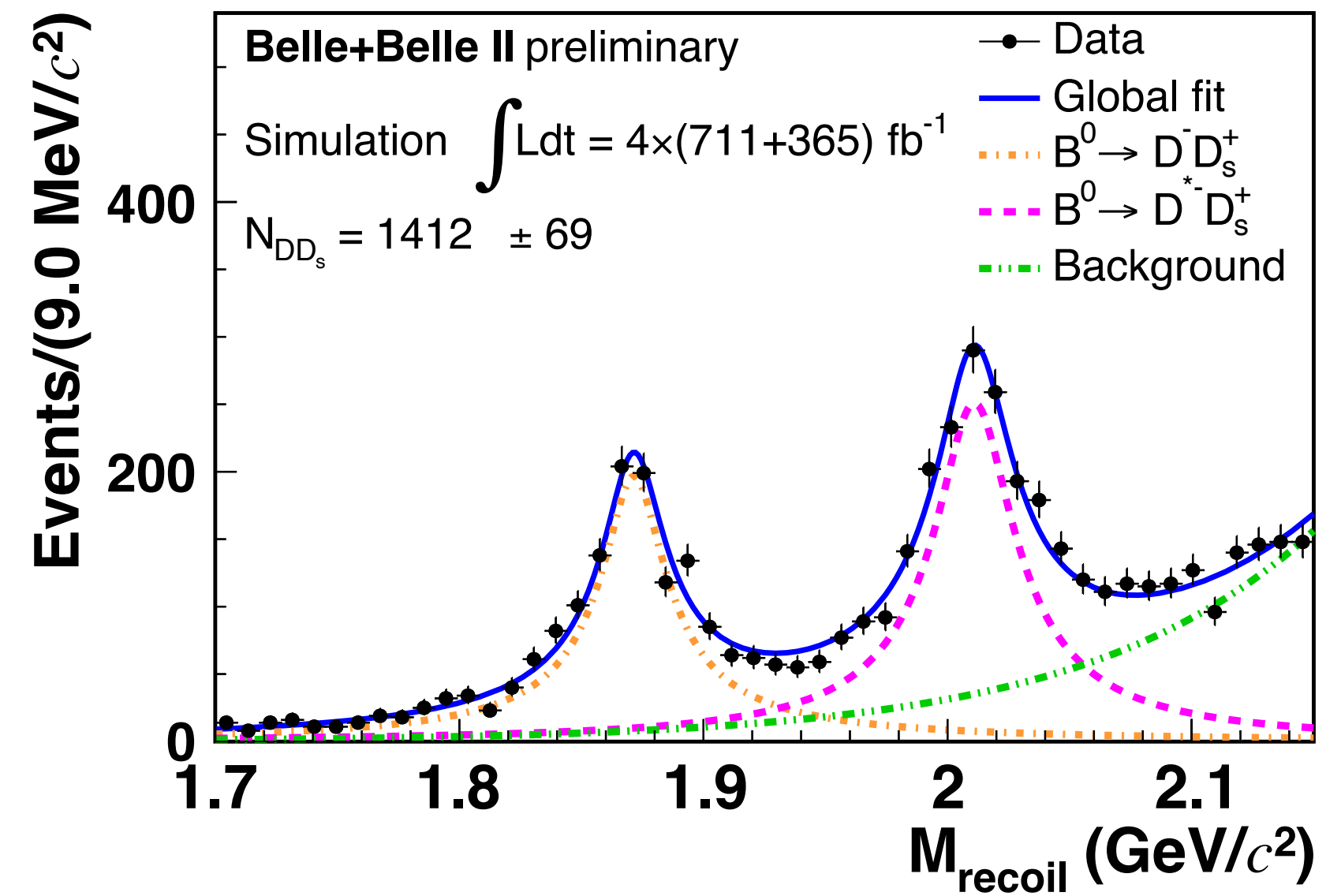
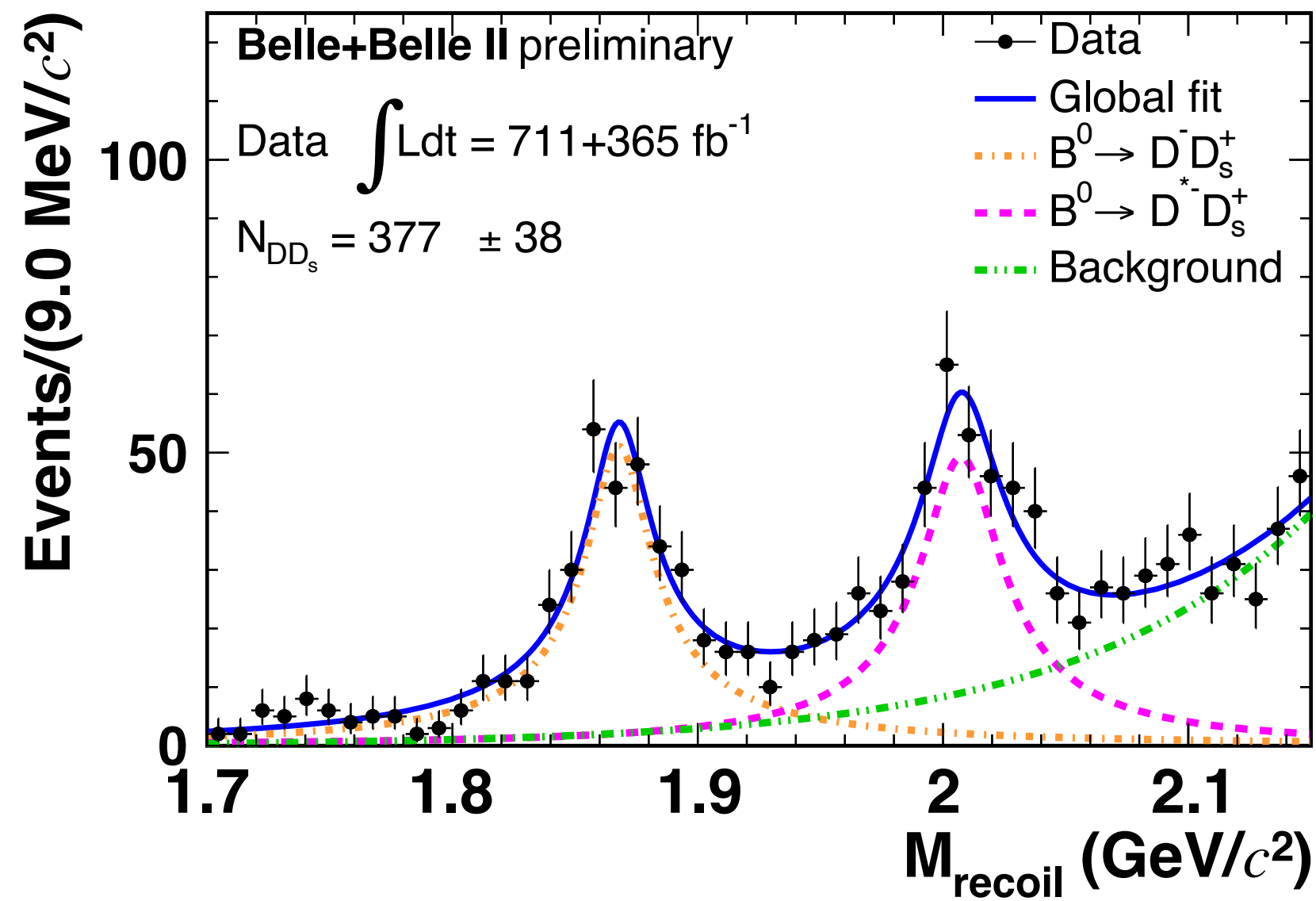


TABLE I. Efficiencies (ϵ), signal yields (N_{sig}) of the data fit, central value of the branching fractions and the observed \mathcal{B}^{UL} at 90% CL. The first uncertainty of the central value is statistical and the second is systematic.

Channels	$\epsilon(10^{-4})$	N_{sig}	$\mathcal{B}(10^{-5})$	
			Central value	UL
$B^0 \rightarrow K_S^0 \tau^+ \mu^-$	1.7	-1.8 ± 3.0	$-1.0 \pm 1.6 \pm 0.2$	1.1
$B^0 \rightarrow K_S^0 \tau^- \mu^+$	2.1	2.6 ± 3.5	$1.1 \pm 1.6 \pm 0.3$	3.6
$B^0 \rightarrow K_S^0 \tau^+ e^-$	2.0	-1.2 ± 2.4	$-0.5 \pm 1.1 \pm 0.1$	1.5
$B^0 \rightarrow K_S^0 \tau^- e^+$	2.1	-2.9 ± 2.0	$-1.2 \pm 0.9 \pm 0.3$	0.8

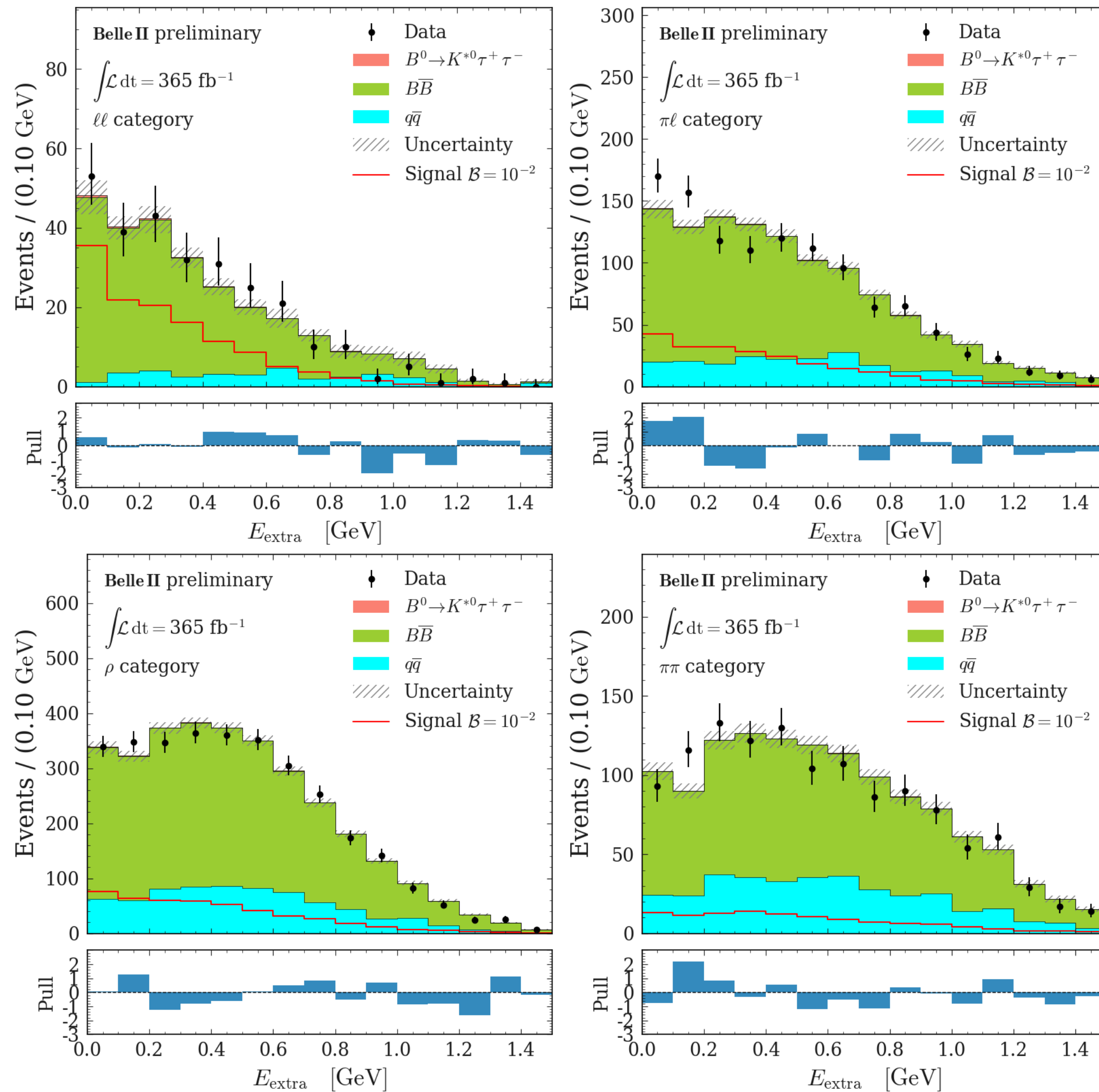


Table I: Signal efficiencies (ε) and expected background yields, for $\eta(\text{BDT}) > 0.4$. The signal categories are ordered according to the expected sensitivity.

Signal category	$\varepsilon \times 10^5$	$B\bar{B}$	$q\bar{q}$
ll	4.0	275	39
$\pi\ell$	7.6	1058	230
ρ	15.5	3279	845
$\pi\pi$	4.0	1077	424

Table II: The systematic uncertainties for the branching fraction of $B^0 \rightarrow K^{*0} \tau^+ \tau^-$, which were computed following the procedure in Ref. [38].

Source	Impact on $\mathcal{B} \times 10^{-3}$
$B \rightarrow D^{**} \ell / \tau \nu$ branching fractions	0.29
Simulated sample size	0.27
$q\bar{q}$ normalization	0.18
ROE cluster multiplicity	0.17
π and K ID	0.14
B decay branching fraction	0.11
Combinatorial $B\bar{B}$ normalization	0.09
Signal and peaking $B^0 \bar{B}^0$ normalization	0.07
Lepton ID	0.04
π^0 efficiency	0.03
f_{00}	0.01
$N_{\Upsilon(4S)}$	0.01
$D \rightarrow K_L$ decays	0.01
Signal form factors	0.01
Luminosity	< 0.01
Total systematics	0.52
Statistics	0.86